NASA CR-134842

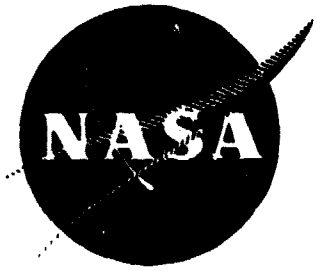

QUIET CLEAN SHORT-HAUL EXPERIMENTAL ENGINE

(QCSEE)

UTW Fan Preliminary Design

February 1975

by

Advancement Engineering & Technology Programs Department
General Electric Company

Prepared For

National Aeronautics and Space Administration

NASA Lewis Research Center
Contract NAS3-18021

1. Report No.	2. Government Accession No.	3. Recipient's Catalog No.
NASA CR-134842		

4. Title and Subtitle	5. Report Date
QUIET CLEAN SHORT-HAUL EXPERIMENTAL ENGINE (QCSEE) UTW FAN PRELIMINARY DESIGN	February 1975
	6. Performing Organization Code
7. Author(s)	8. Performing Organization Report No.
Advanced Engineering & Technology Programs Department Group Engineering Division	R75AEG213
	10. Work Unit No.
9. Performing Organization Name and Address	
General Electric Company 1 Jimison Road Cincinnati, Ohio 45215	11. Contract or Grant No. NAS3-18021
	13. Type of Report and Period Covered
12. Sponsoring Agency Name and Address	Contractor Report
National Aeronautics & Space Administration Washington, D.C. 20546	14. Sponsoring Agency Code

15. Supplementary Notes

Interim Report, Project Manager, C.C. Ciepluch, QCSEE Project Office, Technical Advisor, D. Reemsnyder, NASA Lewis Research Center, Cleveland, Ohio 44135

16. Abstract

The QCSEE Program provides for the design, fabrication, and testing of two experimental high bypass geared turbofan engines and propulsion systems for short-haul passenger aircraft. The overall objective of the program is to develop the propulsion technology required for future externally blown flap types of aircraft with engines located both under-the-wing and over-the-wing. This report covers the aerodynamic and mechanical preliminary design of the QCSEE under-the-wing 1.34 pressure ratio fan with variable blade pitch. Design information is given for two pitch change actuation systems which will provide reverse thrust.

17. Key Words (Suggested by Author(s))

Aerodynamics, Fan Mechanical Design
Composite Materials, Variable Pitch

19. Security Classif. (of this report)	20. [illegible]		
Unclassified	Unclassified	98	

* For sale by the National Technical Information Service, Springfield, Virginia 22151

TABLE OF CONTENTS

LIST OF ILLUSTRATIONS

LIST OF ILLUSTRATIONS (Continued)

LIST OF ILLUSTRATIONS (Concluded)

LIST OF TABLES

SECTION 1.0

FAN AERODYNAMIC DESIGN

1.1 SUMMARY

An under-the-wing (UTW) and an over-the-wing (OTW) fan rotor will be built and tested as part of the NASA QCSEE Program. The UTW fan is a geared variable-pitch design with 18 composite fan blades. This concept, which includes full reverse thrust capability, is expected to offer significant advantages to a high-bypass fan system including:

- Lighter weight through the use of composite fan blades and by eliminating the heavy, large diameter thrust reverser
- Faster thrust response
- Improved off-design SFC
- Reduced off-design noise generation

At the major operating conditions of takeoff and maximum cruise, a corrected flow of 405.5 kg/sec (894 lbm/sec) was selected for both fans which enables common inlet hardware to yield the desired 0.79 average throat Mach number at the critical takeoff noise measurement condition. The aerodynamic design bypass pressure ratio is 1.34 for the UTW and 1.36 for the OTW which is intermediate between the takeoff and maximum cruise power settings. The takeoff pressure ratios are 1.27 for the UTW and 1.34 for the OTW. The takeoff corrected tip speeds are 289 m/sec (950 ft/sec) for the UTW and 354 m/sec (1162 ft/sec) for the OTW. These pressure ratios and speeds were selected on the basis of minimum noise within the constraints of adequate stall margin and core engine supercharging.

The UTW fan was designed to permit rotation of the blades into the reverse thrust mode of operation through both flat pitch (like a propellor) and the stall pitch directions. The flowpath has been contoured to maintain tight blade tip and hub clearances throughout the blade actuation range.

The vane-frame, which is common to both engines, performs the dual function of an outlet guide vane for the bypass flow and a frame support for the engine components and nacelle. The UTW island configuration was selected specifically for the reverse thrust mode of operation.

Design practices and rotor material selections will be consistent with flight-designed fan rotors for both the UTW and the OTW. This includes consideration for fan LCF life and for such FAA flight requirements as burst speed margin and bird strike capability. All rotor components for the UTW fan rotor will be of a flight weight design.

1.2 UTW FAN AERODYNAMIC DESIGN

1.2.1 Operating Requirements

The major operating requirements for the under-the-wing (UTW) fan (Figure 1) are takeoff, where noise and thrust are of primary importance, and maximum cruise, where economy and thrust are of primary importance. At takeoff a low fan pressure ratio of 1.27 was selected to minimize the velocity of the bypass stream at nozzle exit. A corrected flow of 405.5 kg/sec (894 lbm/sec) at this pressure ratio yields the required engine thrust. The inlet throat is sized at this condition for an average Mach number of 0.79 to minimize the forward propagation of fan noise. This sizing of the inlet throat prohibits higher corrected flow at altitude cruise. The required maximum cruise thrust is obtained by raising the fan pressure ratio to 1.39. The aerodynamic design point was selected at an intermediate condition which is a pressure ratio of 1.34 and a corrected flow of 408 kg/sec (900 lb/sec). Table I summarizes the key parameters for these three conditions.

Table I. QCSEE UTW Variable-Pitch Fan.

Parameter	Design Point	Takeoff	Maximum Cruise
Total fan flow	408 kg/sec (900 lb/sec)	405.5 kg/sec (894 lb/sec)	405.5 kg/sec (894 lb/sec)
Pressure ratio - bypass flow	1.34	1.27	1.39
Pressure ratio - core flow	1.23	1.20	1.21
Bypass ratio	11.3	11.8	11.4
Pitch setting	Nominal	Open 2°	Closed 2°
Corrected tip speed	306 m/sec (1005 ft/sec)	289 m/sec (950 ft/sec)	324 m/sec (1063 ft/sec)

1.2.2. Basic Design Features

A cross section of the selected UTW fan configuration is shown in Figure 2. There are 18 variable-pitch composite rotor blades. The solidity of the blades is 0.95 at the OD and 0.98 at the ID. The chord is linear with radius. This permits rotation of the blades into the reverse thrust mode of operation through both the flat pitch and the stall pitch directions. The spherical casing radius over the rotor tip provides good blade tip clearances throughout the range of blade pitch angle settings. Circumferential grooved casing treatment is incorporated over the rotor tip to improve stall margin. Stall margins are significant because a minimum fan tip speed was selected to minimize noise generation. The circumferential grooved casing treatment type was selected since this type of treatment improves stall margin and has shown negligible adverse impact on overall fan efficiency. An additional benefit of

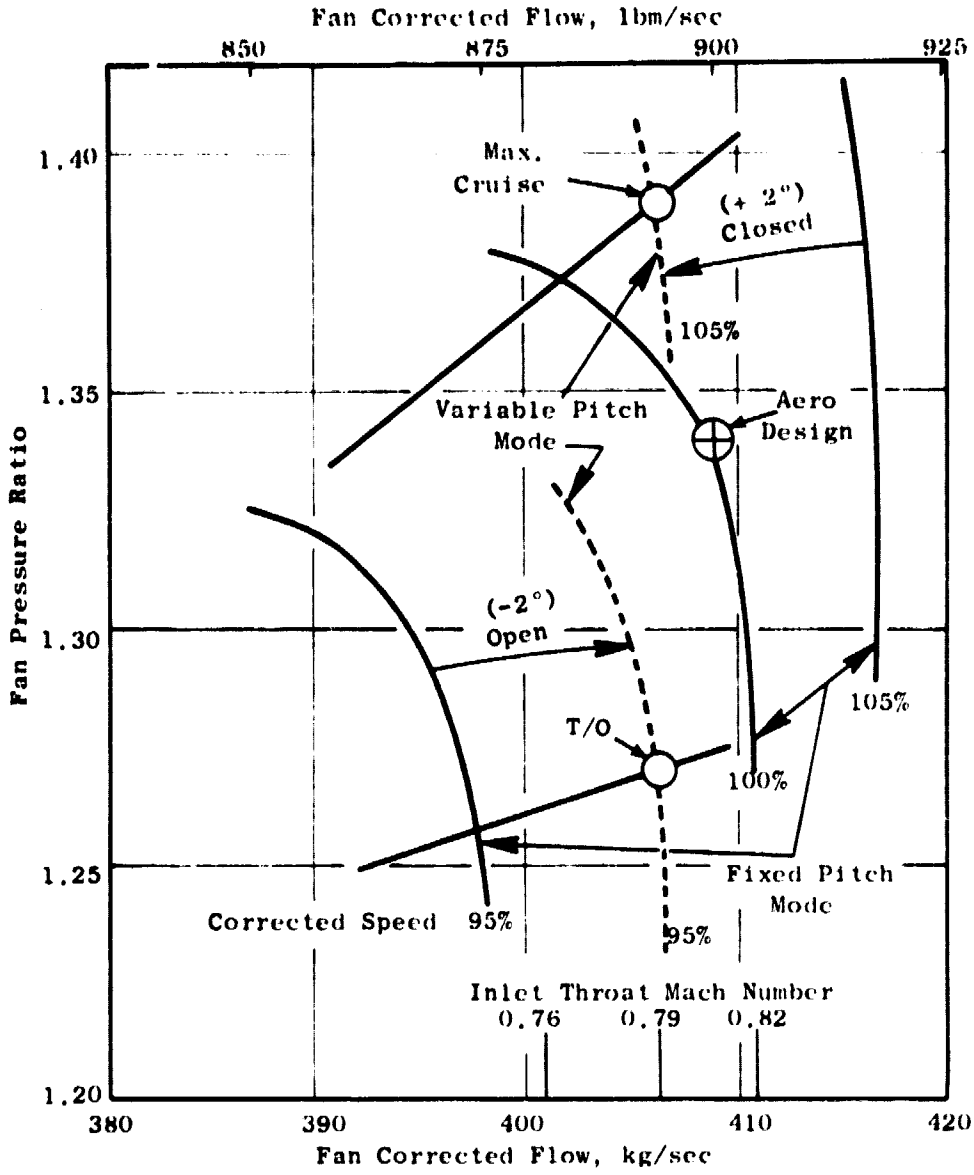

Figure 1. UTW Variable-Pitch Fan.

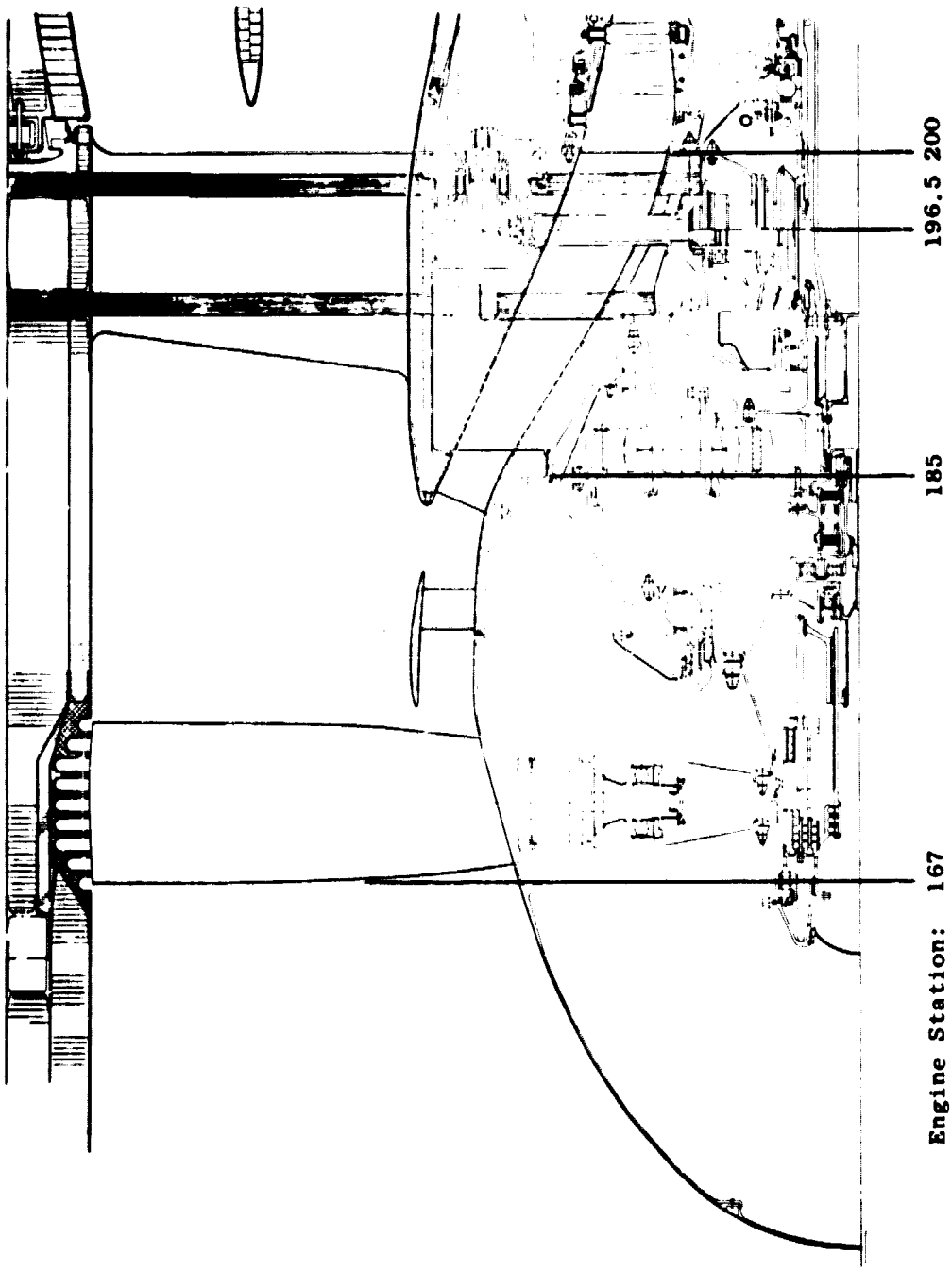

Figure 2. Cross Section of UTW Variable Pitch Fan.

the casing treatment is to reduce the material bulk over the blade tip, for a given clearance, which will reduce the severity of an inadvertent blade rub as might be encountered during a bird strike.

The vane-frame is positioned at an axial distance downstream of the rotor trailing edge equal to 1.5 true rotor tip chords. The vanes are nonaxisymmetric in that five vane geometries, each with a different camber and stagger, are employed around the annulus. This nonaxisymmetric geometry is required to conform the vane-frame downstream flow field to the geometry of the pylon, which protrudes forward into the vane-frame, and simultaneously maintain a condition of minimum circumferential static pressure distortion upstream of the vane-frame. There are 33 vanes in the vane-frame which yields a vane-blade ratio of 1.83. Immediately following the rotor, in the hub region, is an annular ring or island. The 96 OGV's for the fan hub, or core portion flow, are in the annular space between the under side of the island and the hub. A full circumference axial gap separates the island trailing edge from the splitter leading edge. The splitter divides the flow into the bypass portion and core portion. There are six struts in the gooseneck which guide the fan hub flow into the core compressor.

The island configuration was selected specifically to permit the attainment of a high hub supercharging pressure ratio for forward pitch operation without causing a large core flow induction pressure drop during reverse pitch operation, see Section 5.2.3. In the forward mode of operation, a vortex sheet is shed from the trailing edge of the island in the form of a swirl angle discontinuity since most of the swirl in the flow under the island is removed by the OGV. The total pressure on top of the island differs from that under the island only by the losses in the core OGV, hence the Mach numbers of the two streams are nearly the same. The General Electric CF6-6 fan incorporates a similar island configuration, except that the bypass OGV's are on top of the island and there is no swirl in the bypass flow at the island trailing edge. A vortex sheet is shed from the trailing edge of this island configuration also. This vortex sheet is in the form of a velocity magnitude discontinuity. The swirl angle is zero both on top of and under the island but the total pressures differ by the work input in the tip region of the 1/4 stage. Numerically, the strength of the QCSEE UTW island shed vortex is approximately the same as the strength of the CF6-6 island shed vortex. The orientation of the vortex vectors are rotated approximately 70° however.

1.2.3 Reverse Flow

A major feature of the UTW fan is its ability to change the direction of fan thrust by reversing the direction of flow through the fan. This flow reversal affects the pressure level into the core engine (and, hence, the core engine's ability to produce power) in two ways. First, there is the direct loss of the fan hub supercharging pressure; and second, there is the loss associated with inducting the flow into the core engine such as the recoveries of the exlet, vane frame, turn around the splitter leading edge, core OGV's, and gooseneck struts. The first loss is obviously related to the magnitude of

the design (forward mode) fan hub pressure ratio, but the second loss is also related to this magnitude. This is so because, when operating in the reverse thrust mode, camber on the core portion OGV's is in the wrong direction and high hub supercharging in forward operation increases the camber of both bypass and core OGV's. Concern over this matter because of relatively high hub pressure ratio of the UTW fan was the primary reason for selecting the island approach. The major advantage to this configuration is that flow can enter the core compressor through the axial gap between the island and splitter and thereby avoid the problem of adversely oriented camber on the core OGV's. The swirling flow must still, of course, pass through the axially oriented struts in the core inlet gooseneck. Relatively, this path for the flow is much less restrictive. A second benefit is that the bluntness of the splitter leading edge, compared to the island leading edge (which would be the splitter leading edge if the axial gap were filled), is conducive to minimizing losses associated with reversing the axial component of the core portion flow from its forward direction in the bypass duct to its aft direction in the core transition duct.

Reverse fan thrust can be achieved by rotating the blades through the flat pitch (like a propeller) or the stall pitch directions. Rotation of the blades into the reverse thrust condition puts a constraint on selection of blade solidity. This depends primarily on the direction in which the blades are rotated and the blade twist. The constraint is on those blade sections which pass through a tangential orientation, e.g., the leading edge of each blade must be able to pass the trailing edge of the adjacent blade, or physical interference will result. Therefore, those sections must have a solidity less than unity.

Figure 3 shows a tip and hub section of two adjacent blades in nominal, reverse through flat, and reverse through stall orientations. The 45° tip stagger for both reverse through flat and reverse through stall was selected based on experimental reverse thrust performance. For blade rotation through the flat pitch direction, the entire blade span is constrained to a solidity less than one. For rotation through the stall pitch direction, the outer portion of the blade is not constrained. However, because of the 40° twist in the blade, the chord of the hub region cannot be increased significantly without interference. The assumed orientation of the tip section would have to be in error on the order of 5° before significant hub region chord increase could be accommodated. Even if a hub region chord increase could be accommodated, a significant increase in supercharging potential is probably not available because the implied increase in blade twist would probably cause a physical interference.

It was therefore concluded that a hub solidity less than unity was a design requirement for reverse through stall pitch rather than a compromise to permit reverse through flat pitch.

1.2.4 Performance Representation with Variable Pitch

The variable pitch feature of the UTW fan adds a third independent variable to the representation of fan performance in that, in addition to normal independent variables of speed and operating line, the blade pitch

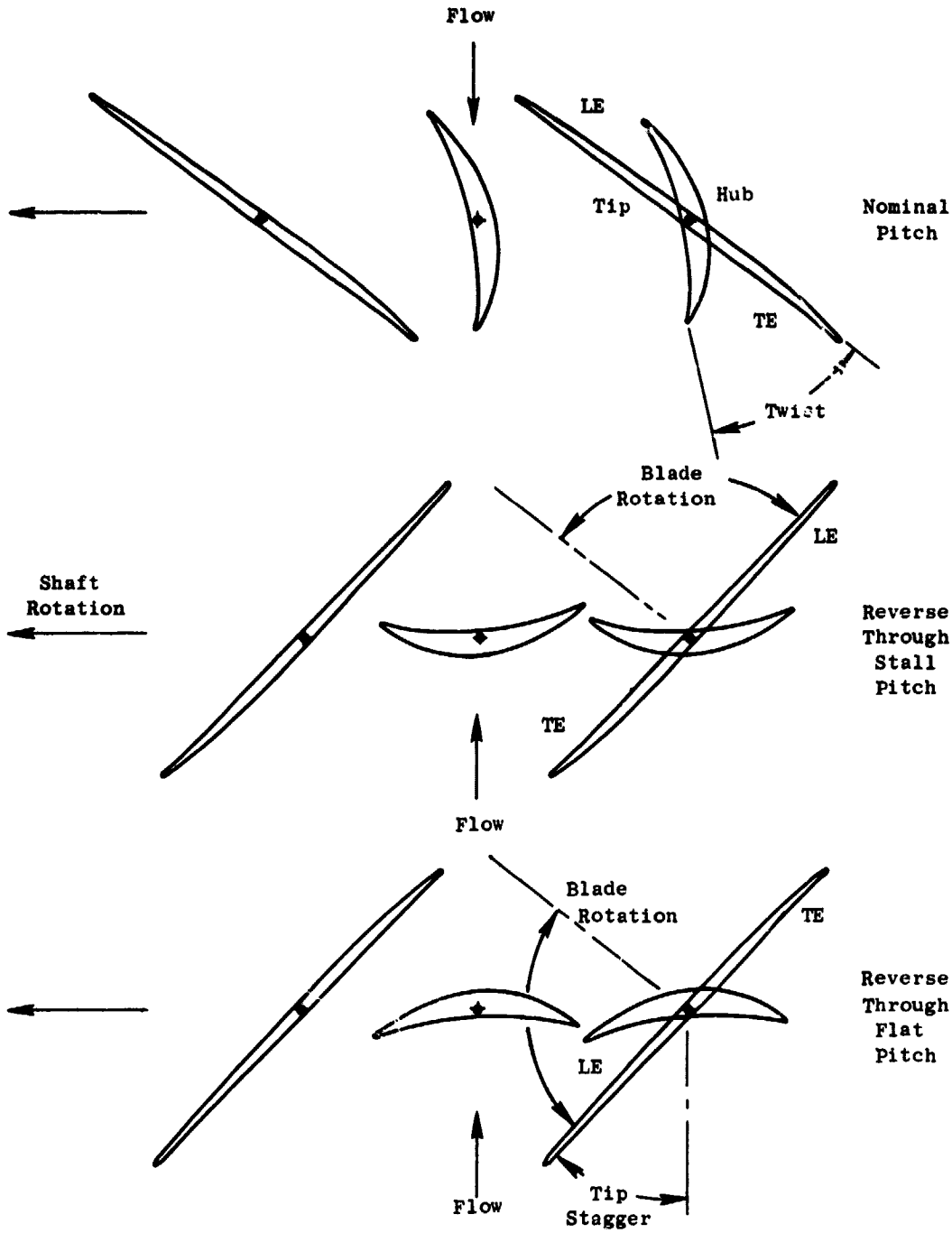

Figure 3. UTW Fan Blade Geometry at Different Pitch Angle Settings.

angle is also required. It has been found, however, that experimental stage characteristics at different rotor pitch angle settings can be collapsed into a nearly universal characteristic applicable for all blade angle settings. The method used to collapse the characteristics was to deduce the rotor incidence and deviation angle from the test data and then calculate the performance of the stage at nominal blade angle with the rotor operating at this incidence and deviation angle and the test efficiency. A separate correlation of aerodynamic loading is used to identify a stall limit, as the collapsing technique breaks down due to the change in aerodynamic loading inherent in the transformation. Figure 4 shows the stage characteristics assumed for the UTW fan at 100% corrected speed for a range of pitch angles. In the reverse flow mode of operation a similar, but simplified, form of the universal characteristic approach is used to represent fan performance. The same collapsing technique is incorporated to include the effect of blade angle setting.

1.2.5 Detailed Configuration Design

The corrected tip speed at the aerodynamic design point was selected at 306 m/sec (1005 ft/sec). This selection is a compromise for design purposes between 289 m/sec (950 ft/sec) at takeoff and the 324 m/sec (1063 ft/sec) at maximum cruise. The objective design point adiabatic efficiency is 88% for the bypass portion and 78% for the core portion. A stall margin of 16% is projected at takeoff. This stall margin is provided at minimum tip speed by incorporating circumferential grooved casing treatment over the rotor tip. Minimum tip speed is important because of the favorable impact of low tip speed on fan generated noise, fan efficiency in the transonic region, and the mechanical design of the variable pitch system. An inlet radius ratio of 0.44 balances the desire to minimize fan diameter within the physical constraints of the variable-pitch mechanism and gear box and good fan hub supercharging for the core engine. A fan inlet flow per annulus area of 199 $kg/sec\text{-}m^2$ (40.8 $lb/sec\text{-}ft^2$) at the design point results in a tip diameter of 1.803 m (71.0 in.).

The standard General Electric axisymmetric flow computation procedure was employed in calculating the velocity diagrams. Several calculation stations were included internal to the rotor blade to improve the overall accuracy of the solution in this region. The physical island geometry is represented in the calculations. Forward of the island and in the axial space between the island and the splitter, calculation stations span the radial distance from OD to ID. Within the axial space of the island, calculation stations span the radial distance between the OD and the topside of the island and between the underside of the island and the hub contour. In the bypass and core inlet ducts, calculation stations are also included. At each calculation station effective area coefficients consistent with established design practice were assumed.

A special constraint is necessary in the aerodynamic design of the island geometry in that a smooth flow or Kutta condition must be satisfied at the trailing edge of the island. The technique employed in this design was to

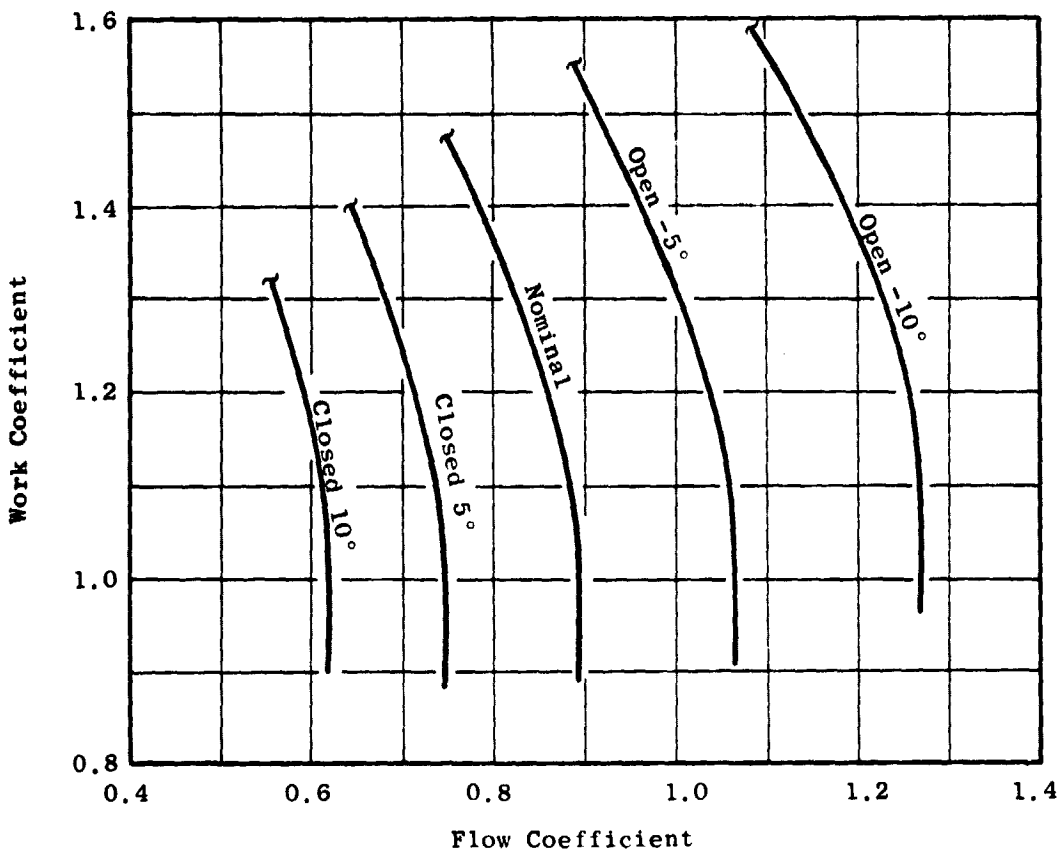

Figure 4. UTW Fan Stage Characteristics at 100% Speed for Various Pitch Settings.

specify a calculation station at the axial location of the island trailing edge which spanned the total flowpath height from OD to ID. Using this technique, a continuous radial distribution of static pressure results which was assumed to be consistent with matching the Kutta condition. The radial location of the island stream function at this calculation station was determined and the upstream geometry of the island was then adjusted to provide a smooth continuous contour blending into this point. Iteration was obviously necessary because of the interaction of the assumed geometry with the calculated radial location of the island stream function. Convergence was found to be quite rapid. An artificial radial displacement was incorporated between the island upper surface streamline and the island lower surface streamline in order to avoid problems in calculating the streamline curvatures. This displacement was assumed equal to the island thickness at the trailing edge and was smoothly blended to zero at an axial distance of approximately 10 edge thicknesses downstream.

The design radial distribution of rotor total pressure ratio is shown in Figure 5. This distribution is consistent with a stage average pressure ratio of 1.34 in the bypass region. Despite the lower than average pressure ratio in the hub region, it has been maximized to the extent possible subject to the constraint of acceptable rotor diffusion factors so as to provide maximum core engine supercharging. A stage average pressure ratio of 1.23 results at the core OGV exit. The radial distribution of rotor efficiency assumed for the design is shown in Figure 6. The assumption of effiency, rather than total pressure loss coefficient, is a General Electric design practice for rotors of this type. This distribution was based on the measured results from similar configurations with adjustments to account for recognized differences. The radial distribution of rotor diffusion factor which results from these assumptions is shown in Figure 7. The moderately high diffusion factor in the tip region of the blade, where stall generally initiates, confirm the need for casing treatment to obtain adequate margin. The radial distributions of rotor relative Mach number and air angle are shown in Figures 8 and 9, respectively.

The assumed radial distribution of total-pressure-loss coefficient for the core portion OGV is shown in Figure 10. The relatively high level, ($\sim$0.2) particularly in the ID region, is in recognition of the very high bypass ratio of the UTW engine and accordingly the small size of the core OGV compared to the rotor. The annulus height of the core OGV is approximately one-half of the rotor staggered spacing, a significant dimension when analyzing secondary flow phenomena. It is anticipated that the core OGV will be influenced by the rotor secondary flow over the entire annulus height. The diffusion factor, Mach number and air angle radial distributions which result from the design assumptions are also shown in Figure 10. An average swirl of 0.104 radian (6°) is retained in the fluid at exit from the core OGV. This was done to lower its aerodynamic loading and the magnitude of the vortex sheet shed from the island. The transition duct (core inlet) struts (6) are cambered to accept this swirl and remove it prior to entrance into the core engine.

A tabulation of significant blade element parameters for the UTW design is presented in Table II.

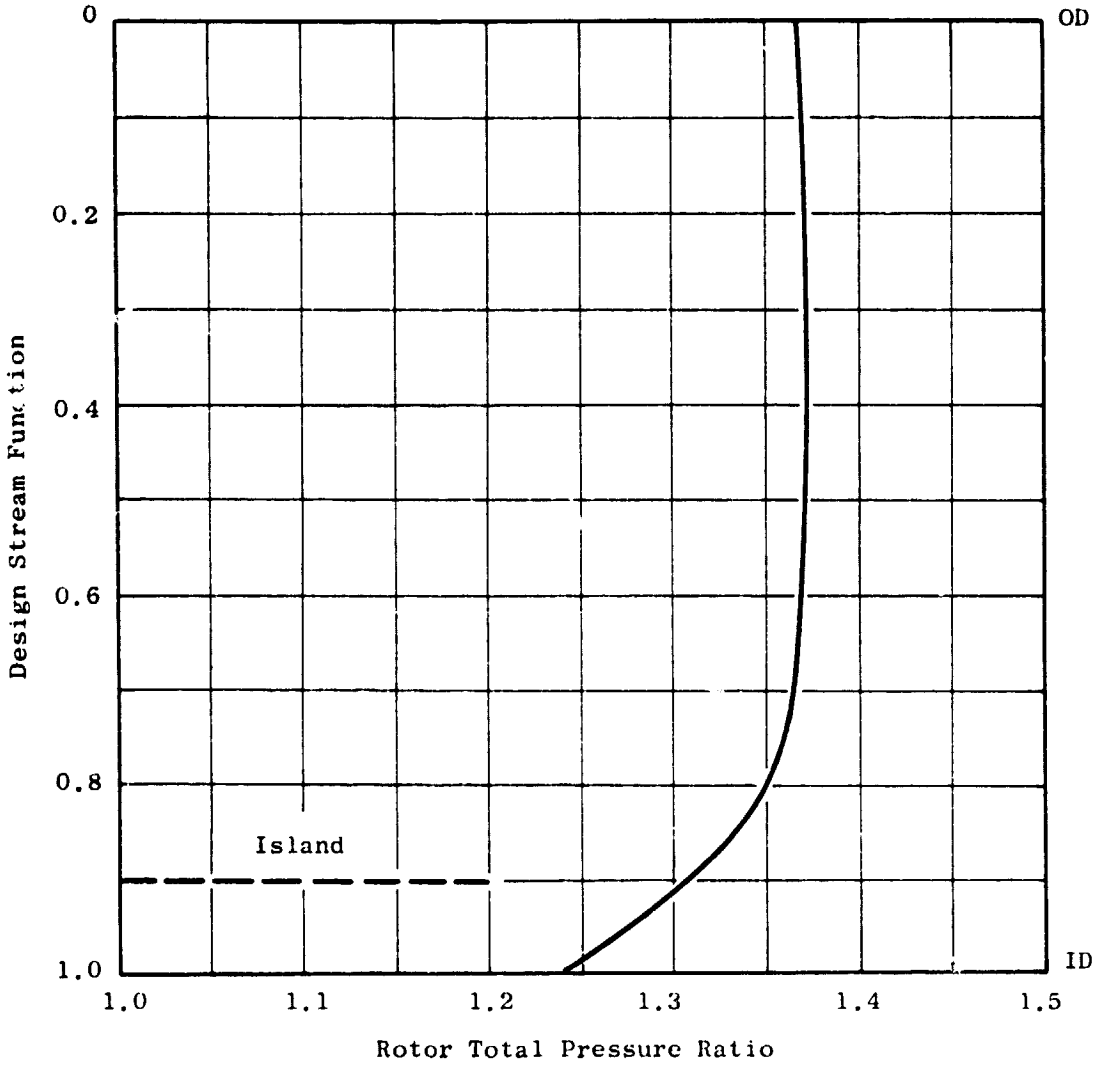

Figure 5. UTW Fan, Radial Distribution of Rotor Total Pressure Ratio.

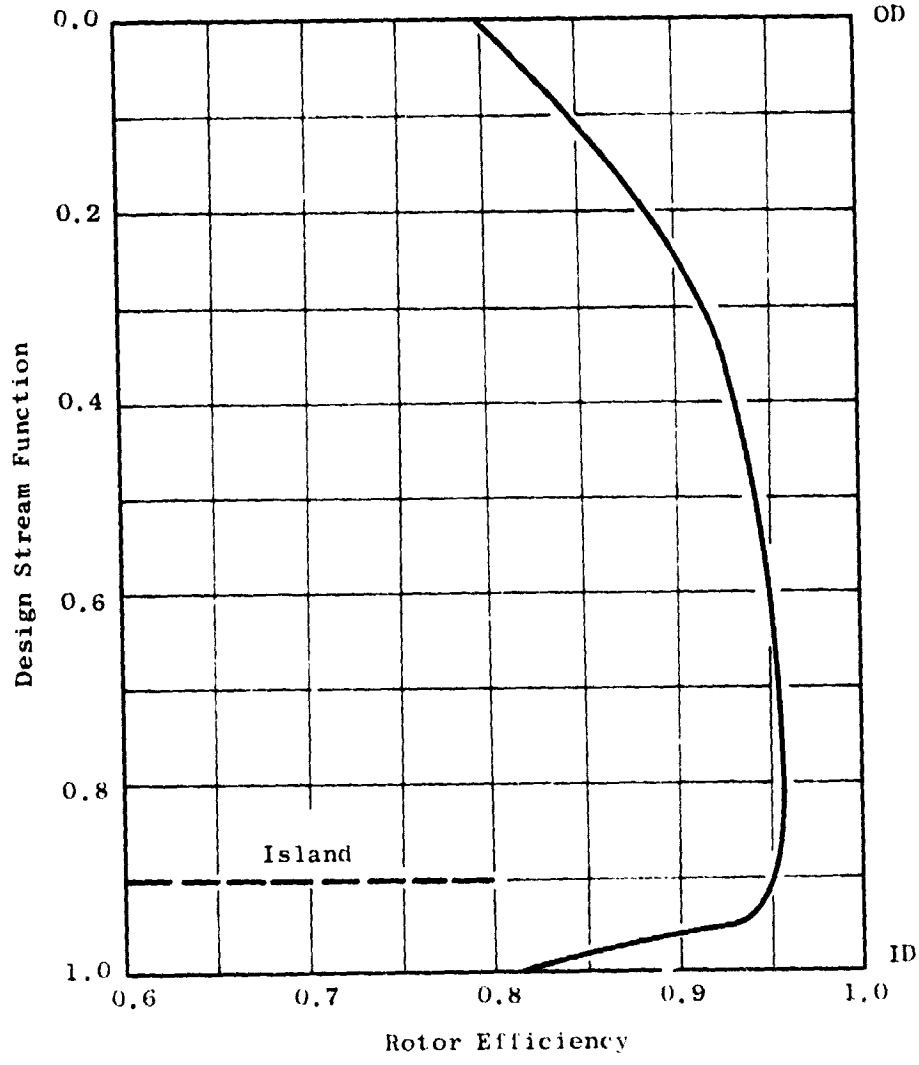

Figure 6. UTW Fan, Radial Distribution of Rotor Efficiency.

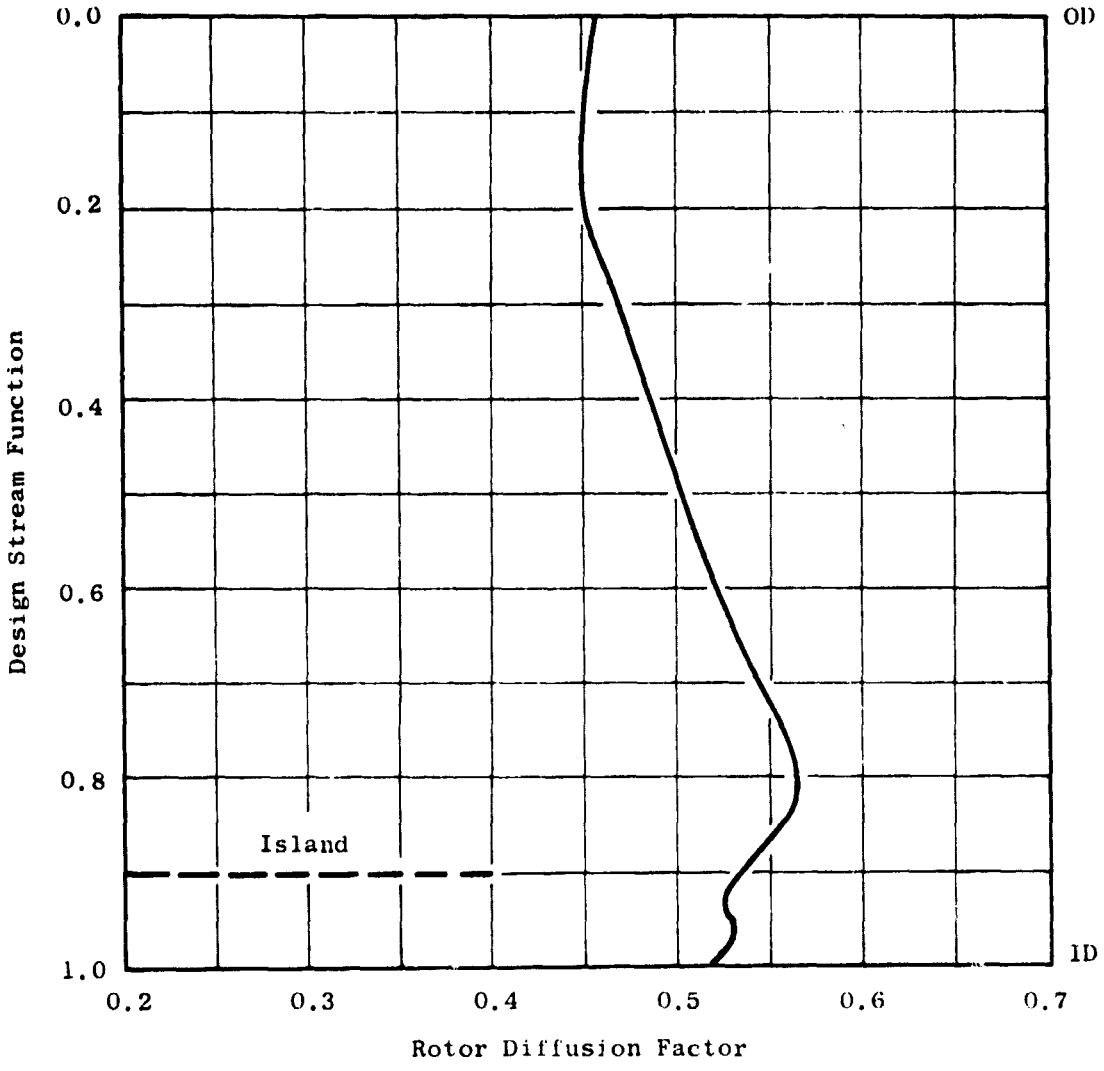

Figure 7. UTW Fan, Radial Distribution of Rotor Diffusion Factor.

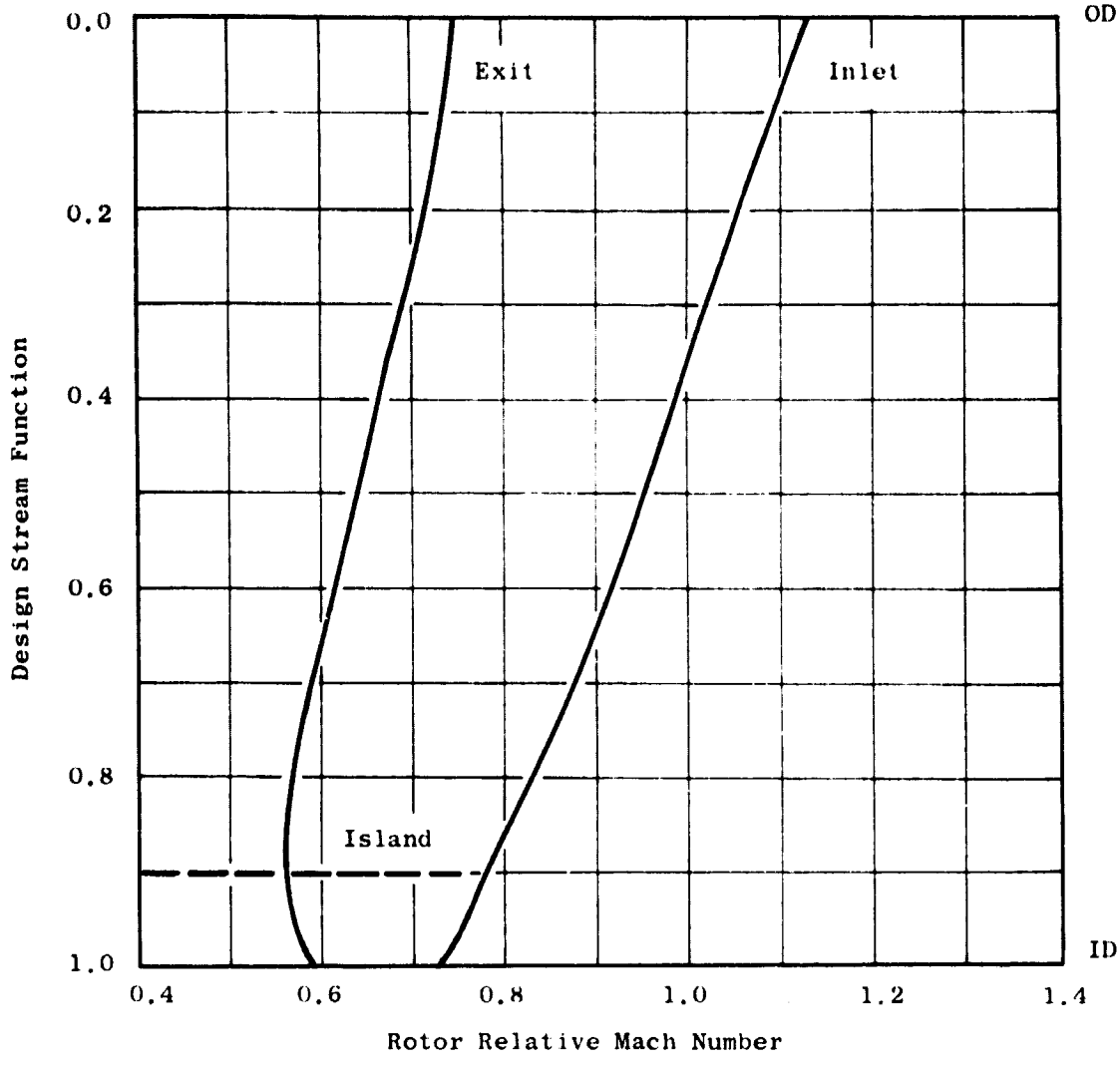

Figure 8. UTW Fan, Radial Distribution of Rotor Relative Mach Number.

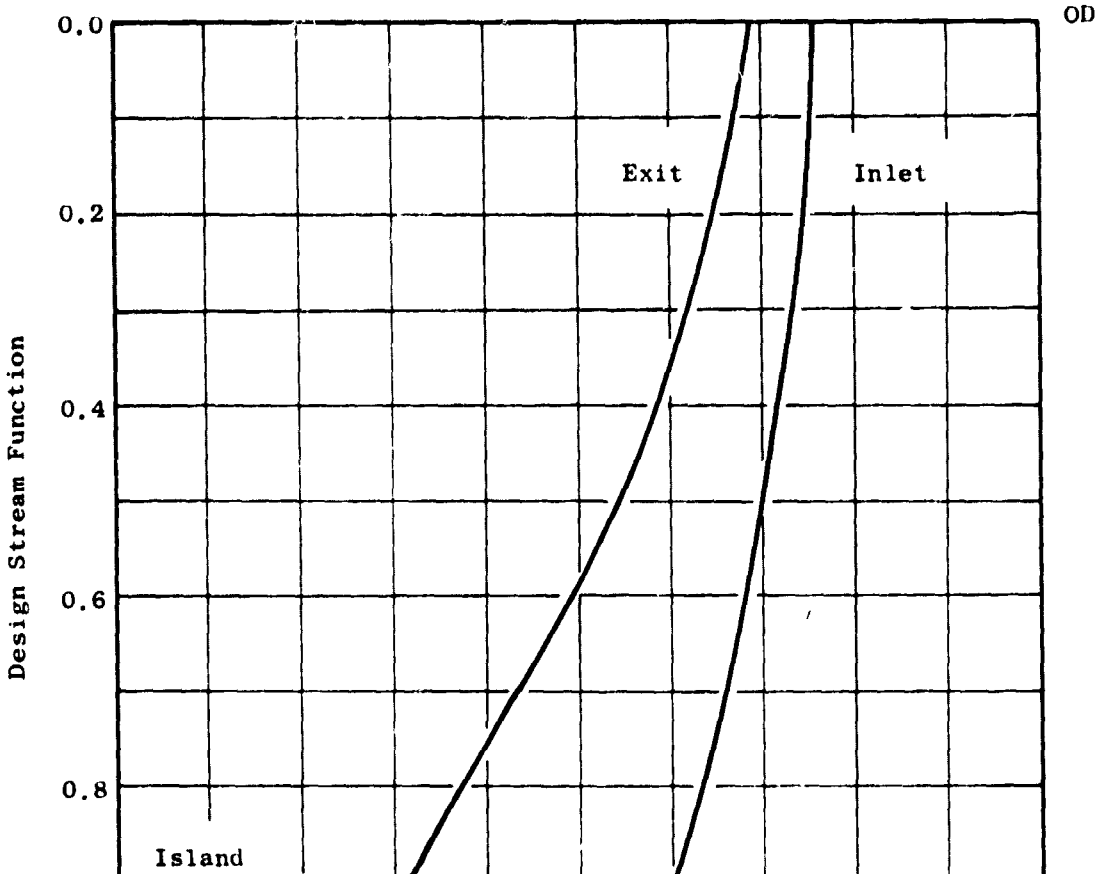

Figure 9. UTW Fan, Radial Distribution of Rotor Relative Air Angle.

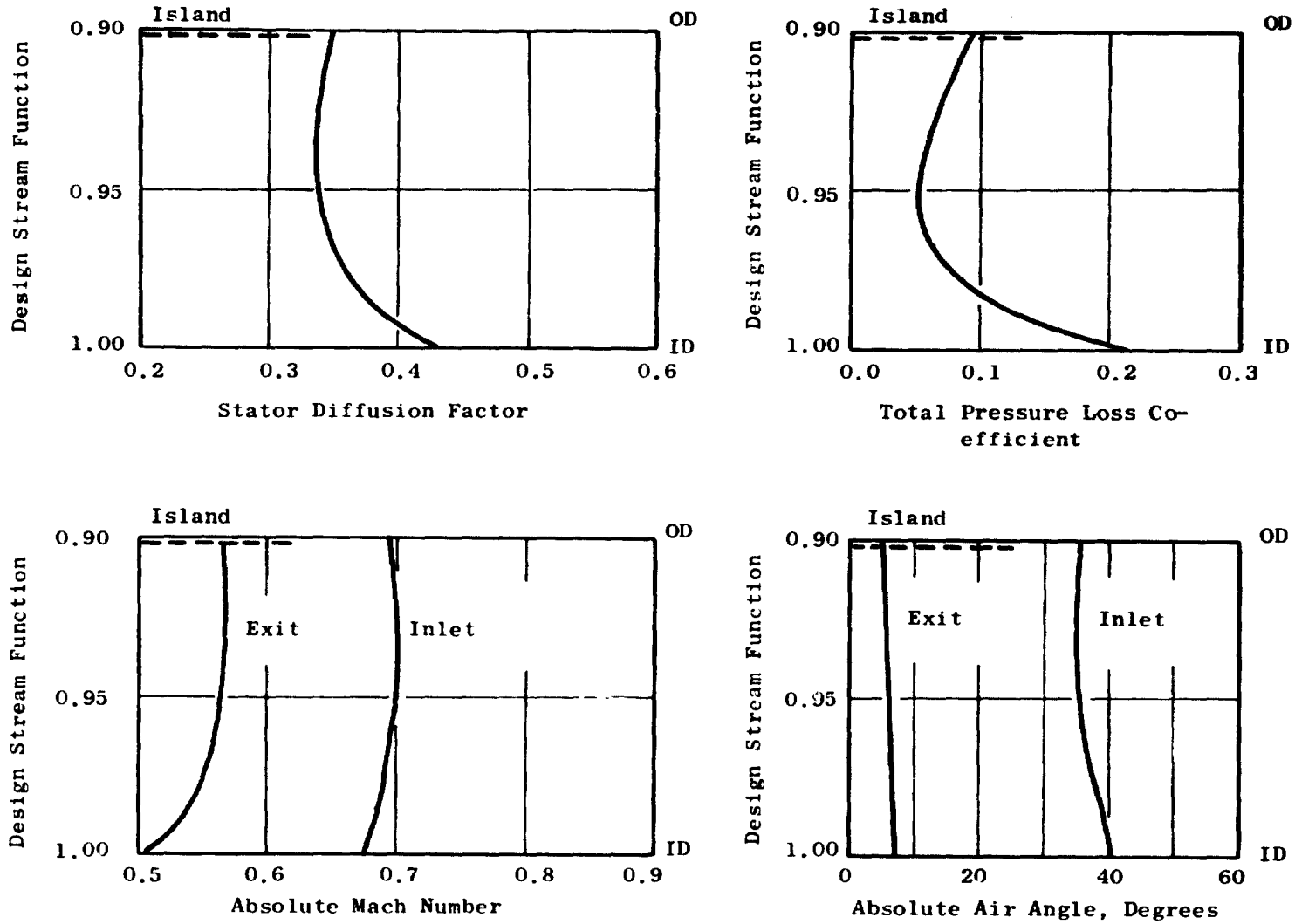

Figure 10. UTW Fan, Radial Distribution of Design Parameters for Core OGV.

Table II. Design Blade Element Parameters for QCSEE UTW Fan.

NOMENCLATURE FOR TABULATION

HEADING	IDENTIFICATION	METRIC UNITS
GENERAL		
SL	STREAMLINE NUMBER	-
PSI	STREAM FUNCTION	-
RADIUS	STREAMLINE RADIUS	CM.
% IMM	PERCENT IMMERSION FROM OUTER WALL	%
Z	AXIAL DIMENSION	CM.
BLKAGE	ANNULUS BLOCKAGE FACTOR	-
FLOW	WEIGHT FLOW	KG/SEC
ANGLES AND MACH NUMBERS		
PHI	MERIDIONAL FLOW ANGLE	DEG.
ALPHA	ABSOLUTE FLOW ANGLE =ARCTAN (CU/CZ)	DEG.
BETA	RELATIVE FLOW ANGLE =ARCTAN (-WU/CZ)	DEG.
M-ABS	ABSOLUTE MACH NUMBER	-
M-REL	RELATIVE MACH NUMBER	-
VELOCITIES		
C	ABSOLUTE VELOCITY	M/SEC
W	RELATIVE VELOCITY	M/SEC
CZ	AXIAL VELOCITY	M/SEC
U	BLADE SPEED	M/SEC
CU	TANGENTIAL COMPONENT OF C	M/SEC
WU	TANGENTIAL COMPONENT OF W	M/SEC
FLUID PROPERTIES		
PT	ABSOLUTE TOTAL PRESSURE	N/SQ.CM.
TT	ABSOLUTE TOTAL TEMPERATURE	DEG-K
TT-REL	RELATIVE TOTAL TEMPERATURE	DEG-K
PS	STATIC PRESSURE	N/SQ.CM.
TS	STATIC TEMPERATURE	DEG-K
RHO	STATIC DENSITY	KG/CU.METER
EFF	CUMULATIVE ADIABATIC EFFICIENCY REFERENCED TO PTI, TTI	-
PTI	INLET ABSOLUTE TOTAL PRESSURE	N/SQ.CM.
TTI	INLET ABSOLUTE TOTAL TEMPERATURE	DEG-K
AERODYNAMIC BLADING PARAMETERS		
TPLC	TOTAL PRESSURE LOSS COEFFICIENT	-
PR-ROW	TOTAL PRESSURE RATIO ACROSS BLADE ROW	-
DEL-T	TOTAL TEMPERATURE RISE ACROSS ROTOR	DEG-K
D	DIFFUSION FACTOR	-
DP/Q	STATIC PRESSURE RISE COEFFICIENT	-
CZ/CZ	AXIAL VELOCITY RATIO ACROSS BLADE ROW	-
SOLDTY	SOLIDITY	-
R-AVG	AVERAGE STREAMLINE RADIUS ACROSS BLADE ROW	CM.
F-TAN	TANGENTIAL BLADE FORCE PER UNIT BLADE LENGTH	N/CM
F-AXL	AXIAL BLADE FORCE PER UNIT BLADE LENGTH	N/CM
F-COEF	FLOW COEFFICIENT =CZ1/U1	-
T-COEF	WORK COEFFICIENT =(2*GAJ*CP*DEL-T)/(U2*U2)	-

Table II. Design Blade Element Parameters for QCSEE UTW Fan (Continued).

STATION 1.00000 Z 423.926830 ROTOR INLET METRIC UNITS

SL	PSI	RADIUS	% SPN	PHI	ALPHA	BETA	M-ABS	M-REL	L	R	CZ	U	CU	RU	SL
1	0.	90.1702	0.	0.	0.	56.03	0.630	1.120	206.4	369.4	206.4	306.3	0.	-306.3	1
2	0.1000	86.5671	7.2	2.31	0.	55.35	0.620	1.091	203.5	357.6	203.5	298.1	0.	-298.1	2
3	0.2500	80.7672	18.7	3.55	0.	53.97	0.609	1.054	199.9	339.5	199.5	274.4	0.	-274.4	3
4	0.4000	74.5029	31.2	5.45	0.	51.68	0.612	0.985	201.0	323.2	200.1	253.1	0.	-253.1	4
5	0.6900	60.5384	59.1	10.26	0.	46.06	0.614	0.877	201.4	287.8	198.2	205.7	0.	-205.7	5
6	0.8000	54.2263	71.7	12.60	0.	43.31	0.610	0.829	200.3	272.1	195.4	184.2	0.	-184.2	6
7	0.9420	44.6160	90.8	15.73	0.	38.32	0.607	0.762	199.3	250.3	191.8	151.6	0.	-151.6	7
8	0.9810	43.1564	93.7	15.97	0.	37.39	0.608	0.750	199.5	247.6	191.8	146.6	0.	-146.6	8
9	0.9810	41.5660	96.9	16.09	0.	36.24	0.611	0.747	200.5	245.2	192.7	141.2	0.	-141.2	9
10	1.0000	40.0051	100.0	15.80	0.	34.85	0.619	0.745	202.9	244.2	195.2	135.9	0.	-135.9	10

SL	PSI	RADIUS	PT	TT	TT-REL	PS	TS	RHO	PT/PTI	TT/TTI	EFF	HLRAGF	SL
1	0.	90.1702	10.132	288.16	334.86	7.755	266.97	1.01199	1.0000	1.00000		0.98000	1
2	0.1000	86.5671	10.132	288.16	331.20	7.816	267.56	1.01763	1.0000	1.00000		0.98000	2
3	0.2500	80.7672	10.132	288.16	325.63	7.888	268.27	1.02437	1.0000	1.00000		0.98000	3
4	0.4000	74.5029	10.132	288.16	320.04	7.867	268.06	1.02239	1.0000	1.00000		0.98000	4
5	0.6900	60.5384	10.132	288.16	309.21	7.858	267.97	1.02157	1.0000	1.00000		0.98000	5
6	0.8000	54.2263	10.132	288.16	305.05	7.881	268.20	1.02374	1.0000	1.00000		0.98000	6
7	0.9420	44.6160	10.132	288.16	299.59	7.902	268.40	1.02565	1.0000	1.00000		0.98000	7
8	0.9810	43.1564	10.132	288.16	298.86	7.897	268.35	1.02517	1.0000	1.00000		0.98000	8
9	0.9810	41.5660	10.132	288.16	298.08	7.876	268.15	1.02326	1.0000	1.00000		0.98000	9
10	1.0000	40.0051	10.132	288.16	297.35	7.828	267.68	1.01876	1.0000	1.00000		0.98000	10

MASS AVERAGED VALUES

PI/PTI 1.0000 EFF PT 10.132 TT 288.16 TT/TTI 1.00000 CZ 198.76
CORR. FLOW 408.233 CORR. RPM 3244.1 CORR. U-TIP 306.3

PTI 10.132
TTI 288.161
GAMMA 1.4000

Table II. Design Blade Element Parameters for QCSEE UTW Fan (Continued).

STATION 1.50000 Z 442.722866 ROTOR EXIT ENGLISH UNITS

SL	PSI	RADIUS	% SPN	PHI	ALPHA	BETA	M-ABS	M-REL	C	W	CZ	U	CU	RU	SL
1	0.	90.1702	0.	-4.54	33.17	49.81	0.584	0.745	203.3	259.2	169.8	306.3	111.0	-195.3	1
2	0.1000	86.6954	7.7	-0.84	32.05	46.75	0.593	0.734	205.1	254.5	174.4	298.5	109.2	-185.3	2
3	0.2500	81.2467	19.8	0.37	32.12	45.62	0.597	0.698	206.2	241.2	174.8	276.0	109.6	-166.4	3
4	0.4000	75.4725	32.0	1.42	32.90	38.71	0.612	0.659	210.9	226.9	177.0	256.4	114.5	-141.9	4
5	0.6900	62.8425	60.0	4.66	35.64	24.96	0.663	0.590	228.7	201.7	185.8	213.5	131.8	-81.7	5
6	0.8000	57.3360	72.8	7.83	37.25	16.97	0.678	0.586	231.0	192.8	182.8	194.8	139.0	-55.8	6
7	0.9420	48.9809	91.4	8.21	35.96	8.89	0.695	0.572	234.7	192.9	188.7	188.4	136.9	-29.5	7
8	0.9610	47.7528	94.1	8.14	36.80	8.56	0.703	0.570	237.0	192.2	189.0	182.2	140.4	-21.8	8
9	0.9810	46.4111	97.1	8.34	36.88	4.04	0.719	0.579	241.8	194.6	192.1	157.7	144.1	-13.6	9
10	1.0000	45.0952	100.0	8.74	37.02	1.53	0.738	0.592	247.6	198.6	196.2	153.2	148.0	-5.2	10

SL	PSI	RADIUS	PT	TT	TT-REL	PS	TS	RHO	PT/PTI	TT/TTI	EFF	BLKAGE	SL
1	0.	90.1702	[illegible]	322.00	358.86	11.002	301.44	1.27154	1.3680	1.11743	0.7975	0.98000	1
2	0.1000	86.6954	15.871	320.17	331.53	10.931	299.10	1.27319	1.3690	1.11107	0.8455	0.98000	2
3	0.2500	81.2467	15.691	317.28	326.08	10.919	297.12	1.26826	1.3710	1.10451	0.9027	0.98000	3
4	0.4000	75.4725	15.902	317.39	320.88	10.794	295.25	1.27358	1.3720	1.10143	0.9324	0.98000	4
5	0.6900	62.8425	15.820	316.17	310.84	10.287	290.59	1.23329	1.3640	1.09719	0.9542	0.98000	5
6	0.8000	57.3360	15.678	315.11	307.04	10.050	288.55	1.21340	1.3500	1.09352	0.9572	0.98000	6
7	0.9420	48.9809	13.000	310.83	301.94	9.411	283.83	1.15674	1.2830	1.07888	0.9379	0.98000	7
8	0.9610	47.7528	12.848	310.85	301.26	9.237	282.87	1.13762	1.2680	1.07888	0.8921	0.98000	8
9	0.9810	46.4111	12.706	310.78	300.55	9.007	281.68	1.11396	1.2540	1.07849	0.8512	0.98000	9
10	1.0000	45.0952	12.564	310.72	299.84	8.751	280.22	1.08799	1.2400	1.07829	0.8096	0.98000	10

SL	PSI	TPLC	PR-ROW	DEL-T	D	DP/Q	CZ/CZ	SOLDTY	M-AVG	P-TAN	P-AXL	P-CORR	T-CORR	SL
1	0.	0.13242	1.3660	35.84	0.456	0.346	0.823	0.9500	90.1702	1294.99	1412.76	0.674	0.765	1
2	0.1000	0.10102	1.3690	32.01	0.449	0.359	0.858	0.9506	86.6515	1235.64	1369.50	0.691	0.741	2
3	0.2500	0.06502	1.3710	30.12	0.460	0.396	0.875	0.9522	81.0070	1157.65	1281.33	0.727	0.794	3
4	0.4000	0.04720	1.3720	29.23	0.485	0.433	0.885	0.9541	74.9877	1124.64	1154.99	0.790	0.893	4
5	0.6900	0.03651	1.3640	28.01	0.542	0.475	0.928	0.9595	61.6904	1062.73	827.95	0.964	1.235	5
6	0.8000	0.03600	1.3500	26.95	0.564	0.483	0.935	0.9628	55.7812	996.37	670.88	1.061	1.427	6
7	0.9420	0.05069	1.2830	22.67	0.524	0.407	0.984	0.9701	46.7985	809.62	425.88	1.265	1.645	7
8	0.9610	0.08958	1.2680	22.67	0.550	0.471	0.986	0.9716	45.4544	800.34	367.47	1.308	1.731	8
9	0.9810	0.12430	1.2540	22.62	0.525	0.320	0.997	0.9735	43.9885	795.93	309.81	1.364	1.828	9
10	1.0000	0.15903	1.2400	22.56	0.510	0.265	1.005	0.9757	42.5502	790.72	252.33	1.436	1.932	10

MASS AVERAGED VALUES

PT/PTI 1.3539 EFF 0.9123 PT 13.718 TT 316.72 TT/TTI 1.09911 CZ 179.20 ROW PT2/PT1 1.3539
CORR. FLOW 316.116 CORR. RPM 3094.3

Table II. Design Blade Element Parameters for QCSEE UTW Fan (Continued).

STATION 1.70000 Z 453.263893 CORE OGV INLET

METRIC UNITS

SL	PSI	RADIUS	% IMP	RMI	ALPHA	BETA	M-ABS	M-REL	C	W	CZ	U	CU	MU	SL
1	0.9021	51.5672	0.	-3.00	35.39	11.23	0.700	0.582	236.6	196.7	192.7	175.2	136.9	-38.3	1
2	0.9420	49.1659	37.8	-2.42	35.31	9.04	0.700	0.579	236.1	195.2	192.8	167.0	136.4	-30.7	2
3	0.9610	47.9548	56.9	-2.21	36.64	7.00	0.694	0.562	234.4	189.5	188.0	162.9	139.8	-23.1	3
4	0.9810	46.5999	78.2	-2.02	38.20	4.63	0.687	0.542	232.2	183.1	182.4	158.3	143.5	-14.8	4
5	1.0000	45.2146	100.0	-2.41	40.46	2.00	0.672	0.512	227.4	173.2	172.9	153.8	147.8	-8.0	5

SL	PST	RADIUS	PT	TT	TT-REL	PS	TS	RHO	PT/PTI	TT/TTI	EFF	BLKAGE	SL
1	0.9021	51.5672	13.186	512.04	303.43	9.506	284.17	1.16539	1.3018	1.082285	0.9440	0.98000	1
2	0.9420	49.1659	13.000	510.83	302.05	9.372	283.09	1.15334	1.2830	1.078868	0.9379	0.98000	2
3	0.9610	47.9548	12.846	510.85	301.37	9.308	283.84	1.14362	1.2690	1.078868	0.8921	0.98000	3
4	0.9810	46.5999	12.706	510.78	300.63	9.284	283.95	1.13657	1.2540	1.078849	0.8512	0.98000	4
5	1.0000	45.2146	12.564	510.72	299.90	9.283	284.98	1.13476	1.2400	1.078829	0.8096	0.98000	5

MASS AVERAGED VALUES

PT/PTI 1.2737 EFF 0.9009 PT 12.906 TT 511.06 TT/TTI 1.07945 CZ 187.83

CORR. FLOW 32.600 CORR. RPM 3122.4

Table II. Design Blade Element Parameters for QCSEE UTW Fan (Continued).

STATION 1.90000 Z 457.835899 CORE OGV EXIT METRIC UNITS

SL	PSI	RADIUS	% IMM	PHI	ALPHA	BETA	M-ABS	M-REL	C	W	CZ	U	CU	WU	SL
1	0.9021	51.3259	0.	-3.02	4.97	39.75	0.555	0.719	190.8	247.1	189.6	174.4	16.5	-157.8	1
2	0.9420	48.9771	37.9	-2.92	5.77	37.65	0.560	0.703	191.9	241.0	190.7	156.4	19.3	-147.1	2
3	0.9610	47.8116	56.8	-2.11	6.16	36.98	0.553	0.689	189.9	236.3	188.7	162.4	20.4	-142.1	3
4	0.9810	46.5110	77.8	-1.45	6.56	36.85	0.555	0.685	184.0	228.4	182.8	156.0	21.0	-137.0	4
5	1.0000	45.1359	100.0	-1.46	6.97	38.76	0.484	0.616	167.0	212.6	165.7	153.3	20.3	-133.1	5

SL	PSI	RADIUS	PI	TI	TI-REL	PS	TS	RHO	PI/PI1	TI/TI1	EFF	BLKAGE	SL
1	0.9021	51.3259	12.861	312.04	324.30	10.432	293.92	1.25643	1.2693	1.08265	0.8510	0.94000	1
2	0.9420	48.9771	12.809	310.83	321.42	10.355	292.51	1.23328	1.2641	1.07865	0.8803	0.94000	2
3	0.9610	47.8116	12.650	310.83	320.67	10.273	292.89	1.22192	1.2484	1.07868	0.8319	0.94000	3
4	0.9810	46.5110	12.570	310.78	319.90	10.177	293.92	1.20618	1.2208	1.07849	0.7475	0.94000	4
5	1.0000	45.1359	11.849	310.72	319.33	10.097	296.84	1.18504	1.1694	1.07829	0.5842	0.94000	5

SL	PSI	TPLC	PR-ROW	DEL-T	D	DP/C	CZ/CZ	SOLDTY	H-AVG	F-TAN	F-AXL	F-COEF	T-COEF	SL
1	0.9021	0.08864	0.9752		0.371	0.251	0.985	1.4411	51.4465	848.85	278.81			1
2	0.9420	0.05267	0.9853		0.352	0.271	0.990	1.5087	49.0715	783.90	290.48			2
3	0.9610	0.05590	0.9846		0.355	0.273	1.003	1.5436	47.8851	760.28	294.76			3
4	0.9810	0.09782	0.9735		0.374	0.265	1.002	1.5647	46.5555	727.85	269.55			4
5	1.0000	0.21766	0.9451		0.436	0.248	0.958	1.6445	45.1753	675.89	193.28			5

MASS AVERAGED VALUES

PI/PI1 1.2440 EFF 0.8101 PT 12.605 TT 311.06 TT/TI1 1.07945 CZ 185.95 ROW PI2/PI1 0.9766

CORR. FLOW 33.380 CORR. RPM 5122.4

Table II. Design Blade Element Parameters for QCSEE UTW Fan (Continued).

STATION 11.50000 Z 482.600948 BYPASS OGV INLET METRIC UNITS

SL	PSI	RADIUS	% IPM	PHI	ALPHA	BETA	M-ABS	M-REL	C	W	CZ	U	CU	MU	SL
1	0.	90.1702	0.	0.	51.07	46.68	0.620	0.775	215.1	268.5	184.2	306.5	111.0	-195.3	1
2	0.1000	86.8359	9.0	0.31	30.18	44.78	0.628	0.765	216.8	264.1	187.4	295.0	109.0	-186.0	2
3	0.2500	81.6850	22.8	0.76	29.72	41.41	0.640	0.741	220.0	254.7	191.0	277.5	109.0	-168.5	3
4	0.4000	76.2516	37.4	1.23	30.45	37.07	0.653	0.705	223.7	241.7	192.8	259.0	113.4	-145.7	4
5	0.6900	64.3910	69.5	2.05	33.51	24.89	0.684	0.629	233.1	214.3	194.3	218.7	128.6	-90.1	5
6	0.8000	59.2058	83.3	1.78	34.71	18.89	0.696	0.605	236.5	205.5	194.4	201.1	134.6	-66.5	6
7	0.9021	55.8026	97.8	0.25	34.67	15.20	0.681	0.580	230.7	196.6	189.7	182.6	131.2	-51.5	7
8	0.9022	55.7973	97.8	0.24	4.19	37.01	0.652	0.814	221.5	276.7	221.0	182.8	16.2	-166.6	8
9	0.9184	52.9921	100.0	0.	4.44	36.50	0.650	0.806	220.8	273.9	220.1	180.0	17.1	-162.9	9

SL	PSI	RADIUS	PT	TT	TT-REL	PS	TS	RHO	PT/PTI	TT/TTI	EFF	BLKAGE	SL
1	0.	90.1702	13.861	322.00	334.86	10.692	298.98	1.24581	1.3680	1.11745	0.7975	0.95000	1
2	0.1000	86.8359	13.871	320.17	331.47	10.656	296.77	1.24852	1.3690	1.11107	0.8453	0.95000	2
3	0.2500	81.6850	13.891	318.28	326.48	10.548	294.20	1.24903	1.3710	1.10451	0.9027	0.95000	3
4	0.4000	76.2516	13.902	317.39	321.56	10.443	292.48	1.24366	1.3720	1.10143	0.9324	0.95000	4
5	0.6900	64.3910	13.820	316.17	311.98	10.107	289.13	1.21781	1.3640	1.09719	0.9542	0.95000	5
6	0.8000	59.2058	13.676	315.11	308.29	9.895	287.27	1.20002	1.3500	1.09352	0.9572	0.95000	6
7	0.9021	55.8026	13.188	312.04	304.79	9.669	285.55	1.17957	1.3016	1.08285	0.9440	0.95000	7
8	0.9022	55.7973	12.861	312.04	325.72	9.669	287.61	1.17113	1.2693	1.08285	0.8510	0.95000	8
9	0.9184	52.9921	12.840	311.54	324.61	9.667	287.28	1.17232	1.2672	1.08115	0.8626	0.95000	9

MASS AVERAGED VALUES

PT/PTI 1.3610 EFF 0.9124 PT 13.791 TT 317.24 TT/TTI 1.10090 CZ 192.06

CORR. FLOW 289.029 CORR. RPM 5091.8

Table II. Design Blade Element Parameters for QCSEE UTW Fan (Continued).

STATION 11.90000 Z 508.000999 BYPASS OGV EXIT METRIC UNITS

SL	PSI	RADIUS	% IMM	PHI	ALPHA	BETA	M-ABS	M-REL	L	R	CZ	U	CU	RU	SL
1	0.	90.1702	0.	0.	0.	59.31	0.519	1.017	181.8	356.2	181.8	306.3	0.	-306.3	1
2	0.1000	86.8872	8.8	-0.25	0.	57.62	0.537	1.002	187.2	349.5	187.2	295.2	0.	-295.2	2
3	0.2500	81.8571	22.4	-0.21	0.	55.87	0.542	0.967	188.5	335.9	188.5	278.1	0.	-278.1	3
4	0.4000	76.5508	36.6	-0.07	0.	54.06	0.543	0.926	188.5	321.2	188.5	260.1	0.	-260.1	4
5	0.6900	64.9958	67.7	0.44	0.	49.98	0.535	0.832	185.4	288.3	185.4	220.8	0.	-220.8	5
6	0.8000	59.9231	81.4	0.93	0.	48.39	0.522	0.786	180.8	272.3	180.8	203.6	0.	-203.6	6
7	0.9021	54.2126	96.7	0.13	0.	50.58	0.436	0.686	151.4	238.4	151.4	184.2	0.	-184.2	7
8	0.9022	54.2056	96.7	0.13	0.	53.24	0.394	0.659	137.6	229.9	137.6	184.1	0.	-184.1	8
9	0.9184	52.9921	100.0	0.	0.	54.09	0.374	0.637	130.4	222.5	130.4	180.0	0.	-180.0	9

SL	PSI	RADIUS	PT	TT	TT-REL	PS	TS	RHO	PT/PTI	TT/TTI	EFF	BLKAGE	SL
1	0.	90.1702	15.515	322.00	368.70	11.248	305.55	1.28250	1.3338	1.11743	0.7304	0.94000	1
2	0.1000	86.8872	13.691	320.17	363.53	11.254	302.73	1.29509	1.3512	1.11107	0.8086	0.94000	2
3	0.2500	81.8571	13.766	318.28	356.76	11.271	300.60	1.30618	1.3586	1.10451	0.8756	0.94000	3
4	0.4000	76.5508	13.791	317.39	351.05	11.283	299.70	1.31152	1.3610	1.10143	0.9077	0.94000	4
5	0.6900	64.9958	13.696	316.17	340.43	11.272	299.05	1.31310	1.3517	1.09719	0.9252	0.94000	5
6	0.8000	59.9231	13.528	315.11	335.74	11.256	298.84	1.30990	1.3351	1.09352	0.9204	0.94000	6
7	0.9021	54.2126	12.766	312.04	328.92	11.206	300.63	1.29858	1.2599	1.08285	0.8236	0.94000	7
8	0.9022	54.2056	12.475	312.04	328.91	11.206	302.62	1.29005	1.2312	1.08285	0.7390	0.94000	8
9	0.9184	52.9921	12.339	311.54	327.67	11.206	303.09	1.28800	1.2178	1.08115	0.7156	0.94000	9

SL	PSI	TPLC	PR-ROW	DEL-T	C	DP/Q	CZ/CZ	SOLDTY	M-AVG	F-TAN	F-AXL	F-CURF	T-CURF	SL
1	0.	0.10933	0.9750		0.366	0.176	0.987	1.2233	90.1702	1374.50	285.46			1
2	0.1000	0.05574	0.9870		0.330	0.191	0.999	1.2974	86.8615	1339.12	334.45			2
3	0.2500	0.03710	0.9910		0.317	0.216	0.987	1.4236	81.7700	1283.06	341.47			3
4	0.4000	0.03216	0.9920		0.318	0.243	0.978	1.5750	76.4012	1252.39	355.51			4
5	0.6900	0.03350	0.9910		0.342	0.314	0.955	1.9934	64.6934	1185.91	392.18			5
6	0.8000	0.04978	0.9890		0.362	0.354	0.930	2.2278	59.5644	1119.04	389.13			6
7	0.9021	0.11991	0.9680		0.454	0.437	0.798	2.5745	54.0076	884.81	265.87			7
8	0.9022	0.12085	0.9700		0.393	0.482	0.623	2.5761	54.0015	113.20	-42.19			8
9	0.9184	0.15785	0.9610		0.423	0.485	0.592	2.8676	52.9921	114.76	-64.87			9

MASS AVERAGED VALUES

PT/PTI 1.3445 EFF 0.8748 PT 15.623 TT 317.24 TT/TTI 1.10090 CZ 183.37 ROW P12/P11 0.9879

CORR. FLOW 292.580 CORR. RPM 3091.8

Table II. Design Blade Element Parameters for QCSEE UTW Fan (Continued).

NOMENCLATURE FOR TABULATION

HEADING	IDENTIFICATION	ENGLISH UNITS
GENERAL		
SL	STREAMLINE NUMBER	-
PSI	STREAM FUNCTION	-
RADIUS	STREAMLINE RADIUS	IN.
% IMM	PERCENT IMMERSION FROM OUTER WALL	%
Z	AXIAL DIMENSION	IN.
BLKAGE	ANNULUS BLOCKAGE FACTOR	-
FLOW	WEIGHT FLOW	LBM/SEC
ANGLES AND MACH NUMBERS		
PHI	MERIDIONAL FLOW ANGLE	DEG.
ALPHA	ABSOLUTE FLOW ANGLE =ARCTAN (CU/CZ)	DEG.
BETA	RELATIVE FLOW ANGLE =ARCTAN (-WU/CZ)	DEG.
M-ABS	ABSOLUTE MACH NUMBER	-
M-REL	RELATIVE MACH NUMBER	-
VELOCITIES		
C	ABSOLUTE VELOCITY	FT/SEC
W	RELATIVE VELOCITY	FT/SEC
CZ	AXIAL VELOCITY	FT/SEC
U	BLADE SPEED	FT/SEC
CU	TANGENTIAL COMPONENT OF C	FT/SEC
WU	TANGENTIAL COMPONENT OF W	FT/SEC
FLUID PROPERTIES		
PT	ABSOLUTE TOTAL PRESSURE	LBF/SQ.IN.
TT	ABSOLUTE TOTAL TEMPERATURE	DEG-R
TT-REL	RELATIVE TOTAL TEMPERATURE	DEG-R
PS	STATIC PRESSURE	LBF/SQ.IN.
TS	STATIC TEMPERATURE	DEG-R
RHO	STATIC DENSITY	LBM/CU.FT.
EFF	CUMULATIVE ADIABATIC EFFICIENCY REFERENCED TO PTI, TTI	-
PTI	INLET ABSOLUTE TOTAL PRESSURE	LBF/SQ.IN.
TTI	INLET ABSOLUTE TOTAL TEMPERATURE	DEG-R
AERODYNAMIC BLADING PARAMETERS		
TPLC	TOTAL PRESSURE LOSS COEFFICIENT	-
PR-ROW	TOTAL PRESSURE RATIO ACROSS BLADE ROW	-
DEL-T	TOTAL TEMPERATURE RISE ACROSS ROTOR	DEG-R
D	DIFFUSION FACTOR	-
DP/Q	STATIC PRESSURE RISE COEFFICIENT	-
CZ/CZ	AXIAL VELOCITY RATIO ACROSS BLADE ROW	-
SOLDTY	SOLIDITY	-
R-AVG	AVERAGE STREAMLINE RADIUS ACROSS BLADE ROW	IN.
F-TAN	TANGENTIAL BLADE FORCE PER UNIT BLADE LENGTH	LBF/IN
F-AXL	AXIAL BLADE FORCE PER UNIT BLADE LENGTH	LBF/IN
F-COEF	FLOW COEFFICIENT =CZ1/U1	-
T-COEF	WORK COEFFICIENT =(2*G*J*CP*DEL-T)/(U2*U2)	-

Table II. Design Blade Element Parameters for QCSEE UTW Fan (Continued).

STATION 1.00000 Z 166.900000 ROTOR INLET ENGLISH UNITS

SL	PSI	RADIUS	% IMM	PHI	ALPHA	BETA	M-ABS	M-REL	C	W	CZ	U	CU	WU	SL
1	0.	35.5000	0.	0.	0.	56.03	0.630	1.128	677.1	1211.8	677.1	1005.0	0.	-1005.0	1
2	0.1000	34.0815	7.2	2.51	0.	55.35	0.620	1.091	667.5	1173.2	667.0	964.8	0.	-964.8	2
3	0.2500	31.7981	18.7	3.55	0.	53.97	0.609	1.034	655.9	1113.8	654.7	900.2	0.	-900.2	3
4	0.4000	29.3318	31.2	5.45	0.	51.68	0.612	0.985	659.4	1060.3	656.4	830.4	0.	-830.4	4
5	0.6900	25.8340	59.1	10.26	0.	46.06	0.614	0.877	660.8	944.4	650.2	674.7	0.	-674.7	5
6	0.8000	21.3489	71.7	12.60	0.	43.31	0.610	0.829	657.0	892.7	641.2	604.4	0.	-604.4	6
7	0.9420	17.5653	90.8	15.73	0.	38.32	0.607	0.762	653.7	821.4	629.2	497.3	0.	-497.3	7
8	0.9610	16.9907	93.7	15.97	0.	37.39	0.608	0.754	654.6	812.5	629.3	481.0	0.	-481.0	8
9	0.9810	16.3645	96.9	16.09	0.	36.24	0.611	0.747	657.8	804.6	632.1	463.5	0.	-463.5	9
10	1.0000	15.7500	100.0	15.80	0.	34.85	0.619	0.745	665.6	801.1	640.4	445.9	0.	-445.9	10

SL	PSI	RADIUS	PT	TT	TT-REL	PS	TS	RHO	PT/PTI	TT/TTI	EFF	BLKAGE	SL
1	0.	35.5000	14.696	518.69	602.75	11.248	480.54	0.06318	1.0000	1.00000		0.98000	1
2	0.1000	34.0815	14.696	518.69	596.17	11.356	481.61	0.06355	1.0000	1.00000		0.98000	2
3	0.2500	31.7981	14.696	518.69	586.13	11.441	482.88	0.06395	1.0000	1.00000		0.98000	3
4	0.4000	29.3318	14.696	518.69	576.08	11.410	482.51	0.06383	1.0000	1.00000		0.98000	4
5	0.6900	25.8340	14.696	518.69	556.58	11.397	482.35	0.06378	1.0000	1.00000		0.98000	5
6	0.8000	21.3489	14.696	518.69	549.09	11.451	482.76	0.06391	1.0000	1.00000		0.98000	6
7	0.9420	17.5653	14.696	518.69	539.27	11.461	483.12	0.06403	1.0000	1.00000		0.98000	7
8	0.9610	16.9907	14.696	518.69	537.95	11.453	483.03	0.06400	1.0000	1.00000		0.98000	8
9	0.9810	16.3645	14.696	518.69	536.55	11.424	482.67	0.06388	1.0000	1.00000		0.98000	9
10	1.0000	15.7500	14.696	518.69	535.24	11.353	481.82	0.06360	1.0000	1.00000		0.98000	10

MASS AVERAGED VALUES

PT/PTI 1.0000 EFF PT 14.696 TT 518.69 TT/TTI 1.00000 CZ 652.10

CORR. FLOW 900.000 CORR. RPM 5244.1 CORR. U-TIP 1005.0

PTI 14.696
TTI 518.690
GAMMA 1.4000

Table II. Design Blade Element Parameters for QCSEE UTW Fan (Continued).

STATION 1.50000 Z 174.299999 ROTOR EXIT ENGLISH UNITS

SL	PSI	RADIUS	% IMM	PHI	ALPHA	BETA	M-ABS	M-REL	C	W	CZ	U	CU	MU	SL
1	0.	35.5000	0.	-4.54	53.17	49.01	0.584	0.745	666.9	850.3	557.0	1005.0	364.1	-640.9	1
2	0.1000	34.1320	7.7	-0.84	52.05	46.75	0.593	0.734	675.0	834.9	572.0	966.3	358.2	-608.1	2
3	0.2500	31.9868	19.8	0.37	52.12	43.62	0.597	0.698	676.5	791.4	572.9	905.5	359.7	-545.9	3
4	0.4000	29.7135	32.6	1.42	52.90	38.71	0.612	0.659	691.9	744.5	580.8	841.2	375.1	-465.4	4
5	0.6900	24.7411	60.6	4.66	55.64	23.96	0.663	0.590	743.7	661.8	603.1	700.4	432.4	-268.0	5
6	0.8000	22.5752	72.8	7.83	57.25	16.97	0.678	0.566	758.0	632.5	599.8	639.0	456.1	-183.0	6
7	0.9420	19.2838	91.4	8.21	55.96	8.89	0.695	0.572	769.9	632.8	619.0	545.9	449.1	-96.8	7
8	0.9610	18.8001	94.1	8.14	56.60	6.58	0.703	0.570	777.6	630.6	620.2	532.2	460.7	-71.6	8
9	0.9810	18.2720	97.1	8.64	56.68	4.04	0.719	0.579	795.3	638.6	630.5	517.3	472.8	-44.5	9
10	1.0000	17.7540	100.0	8.74	57.02	1.53	0.738	0.592	812.2	651.4	643.6	502.6	485.4	-17.2	10

SL	PSI	RADIUS	PI	TT	TT-REL	PS	TS	RHO	PT/PTI	TT/TTI	EFF	BLKAGE	SL
1	0.	35.5000	20.104	579.60	602.75	15.958	542.58	0.07938	1.3680	1.11745	0.7975	0.96000	1
2	0.1000	34.1320	20.119	576.30	596.40	15.854	538.38	0.07949	1.3690	1.11107	0.8455	0.96000	2
3	0.2500	31.9868	20.148	572.90	586.94	15.837	534.85	0.07993	1.3710	1.10451	0.9027	0.96000	3
4	0.4000	29.7135	20.163	571.30	577.58	15.655	531.45	0.07951	1.3720	1.10143	0.9324	0.96000	4
5	0.6900	24.7411	20.045	569.10	559.52	14.921	523.06	0.07699	1.3640	1.09719	0.9542	0.96000	5
6	0.8000	22.5752	19.839	567.20	552.68	14.577	519.59	0.07575	1.3500	1.09352	0.9572	0.96000	6
7	0.9420	19.2838	18.855	559.50	543.49	13.649	510.17	0.07221	1.2830	1.07868	0.9379	0.96000	7
8	0.9610	18.8001	18.634	559.50	542.26	13.398	509.17	0.07102	1.2680	1.07868	0.8921	0.96000	8
9	0.9810	18.2720	18.429	559.40	540.96	13.064	507.02	0.06954	1.2540	1.07849	0.8512	0.96000	9
10	1.0000	17.7540	18.223	559.30	539.71	12.693	504.40	0.06792	1.2400	1.07829	0.8096	0.96000	10

SL	PSI	TPLC	PR-ROW	DEL-T	D	DP/Q	CZ/CZ	SOLDTY	R-AVG	F-TAN	F-AXL	F-COEF	T-COEF	SL
1	0.	0.13242	1.3680	60.91	0.456	0.346	0.823	0.9500	35.5000	759.46	606.71	0.674	0.765	1
2	0.1000	0.10102	1.3690	57.61	0.449	0.359	0.858	0.9506	34.1067	705.58	782.01	0.691	0.741	2
3	0.2500	0.06502	1.3710	54.21	0.460	0.396	0.875	0.9522	31.8924	661.03	731.66	0.727	0.794	3
4	0.4000	0.04720	1.3720	52.61	0.485	0.433	0.885	0.9541	29.5227	642.31	659.52	0.790	0.893	4
5	0.6900	0.03651	1.3640	50.41	0.542	0.475	0.928	0.9595	24.2875	606.84	472.77	0.964	1.235	5
6	0.8000	0.03600	1.3500	48.51	0.564	0.483	0.955	0.9628	21.9610	584.95	385.07	1.061	1.427	6
7	0.9420	0.05069	1.2830	40.81	0.524	0.407	0.984	0.9701	18.4246	462.31	243.18	1.265	1.645	7
8	0.9610	0.08958	1.2680	40.81	0.530	0.371	0.986	0.9716	17.8954	457.01	209.85	1.308	1.731	8
9	0.9810	0.12430	1.2540	40.71	0.525	0.320	0.997	0.9735	17.3183	453.55	176.91	1.364	1.828	9
10	1.0000	0.15904	1.2400	40.61	0.516	0.265	1.005	0.9757	16.7520	451.51	144.09	1.436	1.952	10

MASS AVERAGED VALUES

PT/PTI 1.3539 EFF 0.9123 PT 19.897 TT 570.10 TT/TTI 1.09911 CZ 587.93 ROW PT2/PTI 1.3539

CORR. FLOW 696.917 CORR. RPM 3094.3

Table II. Design Blade Element Parameters for QCSEE UTW Fan (Continued).

STATION 1.70000 Z 178.450001 CORE OGV INLET ENGLISH UNITS

SL	PSI	RADIUS	% SPF	PHI	ALPHA	BETA	M-ABS	M-REL	C	W	CZ	U	CU	RU	SL
1	0.9021	20.3020	0.	-3.00	55.39	11.25	0.700	0.582	776.3	645.4	632.2	574.7	449.2	-125.5	1
2	0.9420	19.3566	37.8	-2.42	55.31	9.04	0.700	0.579	774.6	640.3	631.7	548.0	447.4	-100.6	2
3	0.9610	18.8797	56.9	-2.21	56.64	7.00	0.694	0.562	769.0	621.9	616.8	534.5	456.7	-75.8	3
4	0.9810	18.3464	78.2	-2.02	58.20	4.63	0.687	0.542	761.7	600.7	598.3	519.4	470.9	-48.5	4
5	1.0000	17.8010	100.0	-2.41	60.48	2.00	0.672	0.512	746.2	568.2	567.3	505.9	484.1	-19.8	5

SL	PSI	RADIUS	PT	TT	TT-REL	PS	TS	RHO	PT/PTI	TT/TTI	EFF	BLKAGE	SL
1	0.9021	20.3020	19.128	561.66	546.18	15.788	511.51	0.07276	1.5016	1.08285	0.9480	0.96000	1
2	0.9420	19.3566	18.855	559.50	543.68	15.593	509.56	0.07200	1.2830	1.07868	0.9379	0.96000	2
3	0.9610	18.8797	18.634	559.50	542.47	15.500	510.28	0.07141	1.2680	1.07868	0.8921	0.96000	3
4	0.9810	18.3464	18.429	559.40	541.14	15.436	511.11	0.07096	1.2540	1.07849	0.8512	0.96000	4
5	1.0000	17.8010	18.223	559.30	539.83	15.463	512.96	0.07084	1.2400	1.07829	0.8096	0.96000	5

MASS AVERAGED VALUES

PT/PTI 1.2757 EFF 0.9009 PT 18.719 TT 559.90 TT/TTI 1.07945 CZ 616.24
CORR. FLOW 71.870 CORR. RPM 5122.4

Table II. Design Blade Element Parameters for QCSEE UTW Fan (Continued).

STATION 1.90000 Z 180.250000 CORE OGV EXIT ENGLISH UNITS

SL	PSI	RADIUS	% IMP	PHI	ALPHA	BETA	M-ABS	M-REL	C	W	CZ	U	CU	RU	SL
1	0.9021	20.2070	0.	-3.02	4.97	39.75	0.555	0.719	626.0	810.6	622.8	572.1	54.2	-517.9	1
2	0.9420	19.2823	37.9	-2.92	5.77	37.65	0.560	0.703	629.5	790.7	625.5	545.9	63.2	-482.6	2
3	0.9610	18.8234	56.8	-2.11	6.16	36.98	0.553	0.689	622.9	775.1	618.9	532.9	66.8	-466.1	3
4	0.9810	18.3114	77.8	-1.45	6.56	36.85	0.535	0.665	603.7	749.5	599.6	518.4	69.0	-449.4	4
5	1.0000	17.7700	100.0	-1.46	6.97	38.76	0.484	0.616	548.0	697.5	543.8	503.1	66.5	-436.6	5

SL	PSI	RADIUS	PI	TT	TT-REL	PS	TS	RHO	PT/PTI	TT/TTI	EFF	BLKAGE	SL
1	0.9021	20.2070	18.653	561.66	583.74	15.150	529.05	0.07719	1.2693	1.08285	0.8510	0.94000	1
2	0.9420	19.2823	18.578	559.50	578.55	15.019	526.52	0.07699	1.2641	1.07868	0.8803	0.94000	2
3	0.9610	18.8234	18.347	559.50	577.21	14.900	527.20	0.07628	1.2484	1.07868	0.8319	0.94000	3
4	0.9810	18.3114	17.941	559.40	575.82	14.760	529.06	0.07550	1.2206	1.07849	0.7473	0.94000	4
5	1.0000	17.7700	17.186	559.30	574.80	14.645	534.31	0.07398	1.1694	1.07829	0.5842	0.94000	5

SL	PSI	TPLC	RR-RLM	DEL-T	D	DF/G	CZ/CZ	SOLDTY	M-AVG	F-TAN	F-AXL	F-COEF	T-COEF	SL
1	0.9021	0.08884	0.9752		0.371	0.251	0.985	1.4411	20.2545	484.71	159.20			1
2	0.9420	0.05267	0.9853		0.352	0.271	0.990	1.5087	19.3195	447.62	165.87			2
3	0.9610	0.05590	0.9846		0.355	0.273	1.003	1.5436	18.8510	434.13	168.32			3
4	0.9810	0.09782	0.9735		0.374	0.265	1.002	1.5647	18.3269	415.62	153.81			4
5	1.0000	0.21766	0.9431		0.436	0.248	0.956	1.6445	17.7855	384.81	110.57			5

MASS AVERAGED VALUES

PT/PTI 1.2440 EFF 0.8101 PI 18.281 TT 559.90 TT/TTI 1.07945 CZ 610.07 RDW PT2/PT1 0.9766

CORR. FLOW 73.589 CORR. RPM 3122.4

Table II. Design Blade Element Parameters for QCSEE UTW Fan (Continued).

STATION 11.50000 Z 190.000000 BYPASS OGV INLET ENGLISH UNITS

SL	PSI	RADIUS	% IPP	PHI	ALPHA	BETA	M-ABS	M-REL	L	R	CZ	U	CU	RU	SL
1	0.	35.5000	0.	0.	31.07	46.68	0.620	0.775	705.6	880.9	604.4	1005.0	564.1	-640.9	1
2	0.1000	34.1873	9.0	0.31	30.18	44.78	0.628	0.765	711.4	866.3	614.9	967.8	557.6	-610.2	2
3	0.2500	32.1586	22.8	0.76	29.72	41.41	0.640	0.741	721.6	835.6	626.7	910.4	557.7	-552.7	3
4	0.4000	30.0202	37.4	1.23	30.45	37.07	0.653	0.705	734.0	793.0	632.1	849.9	571.9	-478.0	4
5	0.6900	25.3507	69.3	2.05	33.51	24.89	0.684	0.629	764.1	703.0	647.4	717.7	422.0	-295.7	5
6	0.8000	23.3093	83.3	1.78	34.71	18.89	0.696	0.605	776.0	674.3	637.1	659.9	441.7	-218.2	6
7	0.9021	21.1821	97.8	0.25	34.67	15.20	0.681	0.580	756.8	645.0	622.4	599.7	430.6	-169.1	7
8	0.9022	21.1800	97.8	0.24	4.19	37.01	0.652	0.814	726.9	907.9	724.9	599.6	53.0	-546.6	8
9	0.9184	20.8650	100.0	0.	4.44	36.50	0.650	0.806	724.4	898.5	722.2	590.6	56.1	-534.5	9

SL	PSI	RADIUS	PT	TT	TT-REL	PS	TS	RHO	PT/PTI	TT/TTI	EFF	BLKAGE	SL
1	0.	35.5000	20.104	579.60	602.75	15.507	538.18	0.07778	1.3680	1.11743	0.7975	0.95000	1
2	0.1000	34.1873	20.119	576.30	596.65	15.426	534.18	0.07794	1.3690	1.11107	0.8453	0.95000	2
3	0.2500	32.1586	20.148	572.90	587.67	15.299	529.56	0.07798	1.3710	1.10451	0.9027	0.95000	3
4	0.4000	30.0202	20.163	571.30	578.80	15.147	526.46	0.07766	1.3720	1.10143	0.9324	0.95000	4
5	0.6900	25.3507	20.045	569.10	561.56	14.659	520.43	0.07605	1.3640	1.09719	0.9542	0.95000	5
6	0.8000	23.3093	19.859	567.20	554.93	14.352	517.09	0.07492	1.3500	1.09352	0.9572	0.95000	6
7	0.9021	21.1821	19.128	561.66	548.62	14.023	513.99	0.07364	1.3016	1.08285	0.9440	0.95000	7
8	0.9022	21.1800	19.653	561.66	586.29	14.023	517.69	0.07311	1.2695	1.08285	0.8510	0.95000	8
9	0.9184	20.8650	19.623	560.78	584.30	14.022	517.11	0.07319	1.2672	1.08115	0.8626	0.95000	9

MASS AVERAGED VALUES

PT/PTI 1.3610 EFF 0.9124 PT 20.002 TT 571.03 TT/TTI 1.10090 CZ 630.13

CORR. FLOW 637.200 CORR. RPM 3091.8

Table II. Design Blade Element Parameters for QCSEE UTW Fan (Concluded).

STATION 11.90000 Z 200.000000 BYPASS OGV EXIT ENGLISH UNITS

SL	PSI	RADIUS	% IMP	PHI	ALPHA	BETA	M-ABS	M-REL	C	R	CZ	U	CU	RU	SL
1	0.	35.5000	0.	0.	0.	59.31	0.519	1.017	596.5	1166.7	596.5	1005.0	0.	-1005.0	1
2	0.1000	34.2075	8.8	-0.25	0.	57.62	0.537	1.002	614.1	1146.7	614.1	968.4	0.	-968.4	2
3	0.2500	32.2271	22.4	-0.21	0.	55.87	0.542	0.967	618.4	1102.2	618.4	912.3	0.	-912.3	3
4	0.4000	30.1381	36.6	-0.07	0.	54.06	0.543	0.926	618.5	1053.8	618.5	853.2	0.	-853.2	4
5	0.6900	25.5869	67.7	0.44	0.	49.98	0.535	0.832	608.4	946.0	608.4	724.4	0.	-724.4	5
6	0.8000	23.5917	81.4	0.95	0.	48.39	0.522	0.786	595.5	893.3	595.2	667.9	0.	-667.9	6
7	0.9021	21.3435	96.7	0.15	0.	50.58	0.436	0.686	496.7	782.1	496.6	604.2	0.	-604.2	7
8	0.9022	21.3407	96.7	0.13	0.	53.24	0.394	0.659	451.3	754.1	451.3	604.2	0.	-604.2	8
9	0.9184	20.8630	100.0	0.	0.	54.09	0.378	0.637	427.7	729.2	427.7	590.6	0.	-590.6	9

SL	PSI	RADIUS	PI	TI	TI-REL	PS	TS	RHO	PT/PTI	TT/TTI	EFF	BLKAGE	SL
1	0.	35.5000	19.601	579.60	863.66	16.315	549.99	0.08007	1.3538	1.11745	0.7304	0.98000	1
2	0.1000	34.2075	19.657	576.30	854.35	16.323	544.91	0.08085	1.3512	1.11107	0.8086	0.94000	2
3	0.2500	32.2271	19.967	572.90	842.18	16.347	541.07	0.08154	1.3586	1.10451	0.8756	0.94000	3
4	0.4000	30.1381	20.002	571.30	831.88	16.364	539.46	0.08188	1.3616	1.10143	0.9077	0.94000	4
5	0.6900	25.5869	19.985	569.10	812.78	16.349	538.29	0.08198	1.3517	1.09719	0.9252	0.94000	5
6	0.8000	23.5917	19.821	567.20	804.32	16.297	537.91	0.08178	1.3351	1.09352	0.9204	0.94000	6
7	0.9021	21.3435	18.516	561.66	592.05	16.253	541.13	0.08107	1.2599	1.08285	0.8236	0.94000	7
8	0.9022	21.3407	18.094	561.66	592.04	16.253	544.71	0.08054	1.2312	1.08285	0.7340	0.94000	8
9	0.9184	20.8630	17.898	560.78	589.81	16.253	545.55	0.08041	1.2178	1.08115	0.7136	0.94000	9

SL	PSI	TPLC	PR-FLOW	DFL-I	D	DP/Q	CZ/CZ	SLOPE	M-AVG	F-TAN	F-AXL	F-COEF T-COEF	SL
1	0.	0.10955	0.9750		0.366	0.176	0.987	1.2233	35.5000	784.87	165.01		1
2	0.1000	0.05574	0.9770		0.350	0.191	0.999	1.2974	34.1974	764.66	190.98		2
3	0.2500	0.03740	0.9910		0.317	0.216	0.987	1.4236	32.1929	732.65	194.99		3
4	0.4000	0.03218	0.9920		0.318	0.243	0.976	1.5750	30.0792	715.14	203.00		4
5	0.6900	0.03350	0.9910		0.342	0.314	0.955	1.9934	25.4898	677.18	223.94		5
6	0.8000	0.03978	0.9890		0.362	0.354	0.930	2.2278	23.4505	658.99	222.20		6
7	0.9021	0.11991	0.9880		0.454	0.437	0.798	2.5745	21.2628	505.24	151.81		7
8	0.9022	0.12085	0.9780		0.393	0.482	0.623	2.5761	21.2604	64.64	-24.09		8
9	0.9184	0.15765	0.9810		0.423	0.485	0.592	2.8676	20.8630	65.53	-37.04		9

MASS AVERAGED VALUES

PT/PTI 1.3445 EFF 0.8748 PI 19.759 TI 571.03 TT/TTI 1.10090 CZ 601.60 RUM PT2/PT1 0.9879

CORR. FLOW 645.028 CORR. RPM 3091.8

1.2.6 Rotor Blade Design

Detailed layout procedures employed in design of the fan blade generally parallels established design procedures. In the tip region of the blade, where the inlet relative flow is supersonic, the uncovered portion of the suction surface was set to ensure that the maximum flow passing capacity is consistent with the design flow requirement. Incidence angles in the tip region were selected according to transonic blade design practice which has yielded good overall performance for previous designs. In the hub region, where inlet flow is subsonic, incidence angles were selected from NASA cascade data correlations.

The blade trailing edge angle was established by the deviation angle which was obtained from Carter's Rule applied to the camber of an equivalent two-dimensional cascade with an additive empirical adjustment, X. This adjustment is derived from aerodynamic design and performance synthesis for this general type of rotor. The incidence and deviation angles and empirical adjustment angle employed in the design are shown in Figure 11.

Over the entire blade span, the minimum passage area, or throat, must be sufficient to pass the design flow including allowances for boundary layer, losses, and flow nonuniformities. In the transonic and supersonic region, the smallest throat area, consistent with permitting design flow to pass, is desirable since this minimizes overexpansions on the suction surface. A further consideration was to minimize disturbances to the flow along the forward portion of the suction surface to minimize forward propagating waves that might provide an additional noise source. Design experience guided the degree to which each of these desires was applied to individual section layouts. The percent throat margin, percentage by which the ratio of the effective throat area to the capture area exceeds the critical area ratio, is shown in Figure 12. The values employed are generally consistent with past experience. The blade shapes that result are generally similar to multiple circular arc sections in the tip region, with a small percentage of the overall camber occurring in the forward portion. In the hub region, the blade shapes are similar to double circular arc sections.

Figure 13 shows plane sections of the blade at several radial locations. Table III is a tabulation of the fan rotor blade coordinates (in inches) for the sections shown in this figure. The coordinate center is at the stacking axis. Figure 14 shows the resulting camber and stagger angle radial distributions. The radial thickness distributions employed, which were dictated primarily by aeromechanical considerations, are shown in Figure 15. The 0.13 thickness-to-chord ratio at the hub is larger than conventional practice because of the composite blade requirements and a small performance penalty will result The additional profile loss created by this thickness, however, is believed smaller than the system penalties associated with altering the configuration (such as reduction in the tip chord or a reduction in blade number) to reduce the hub thickness-to-chord ratio to 0.10, a value more representative of past experience.

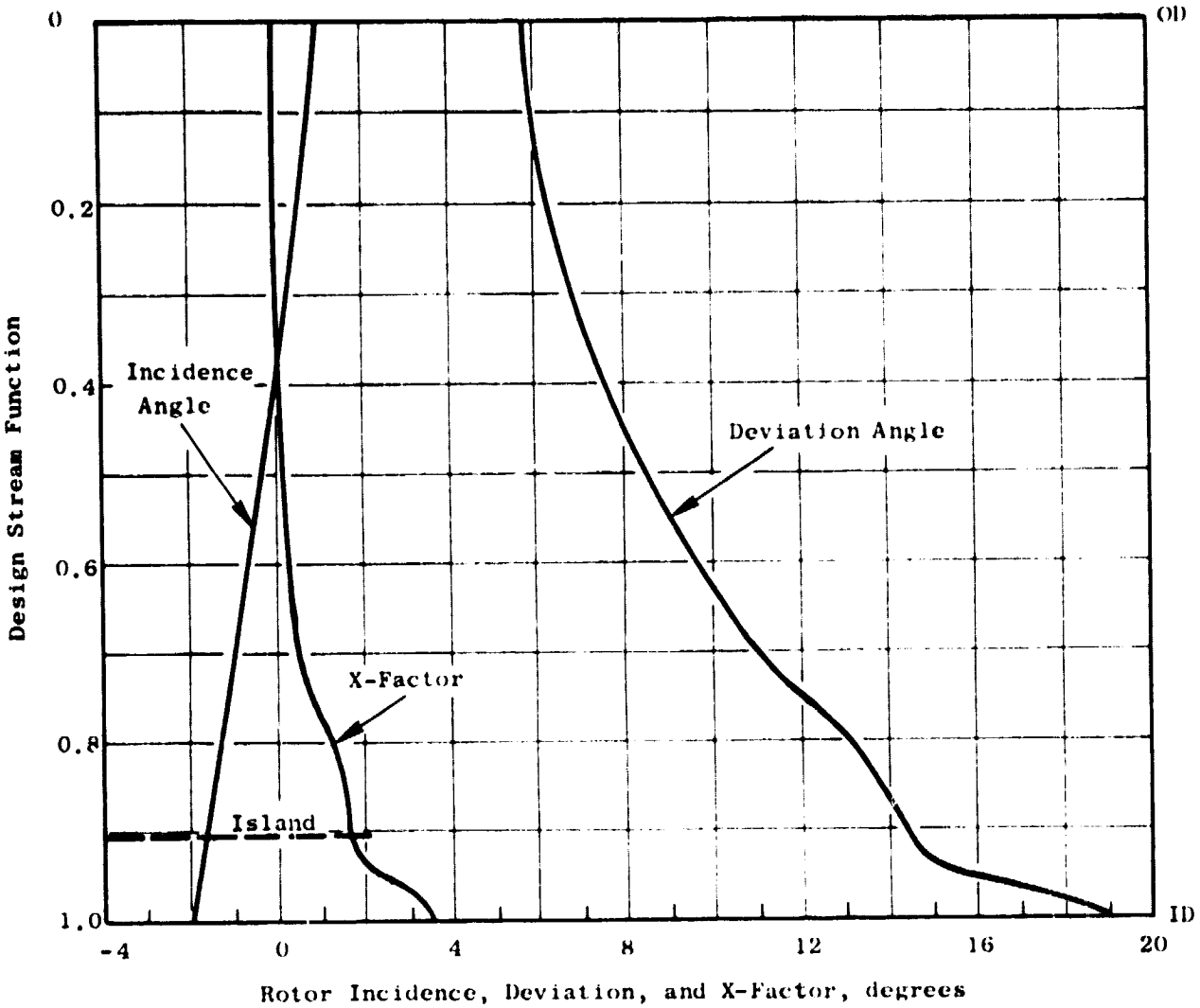

Figure 11. UTW Fan - Rotor Incidence, Deviation, and Empirical Adjustment Angles.

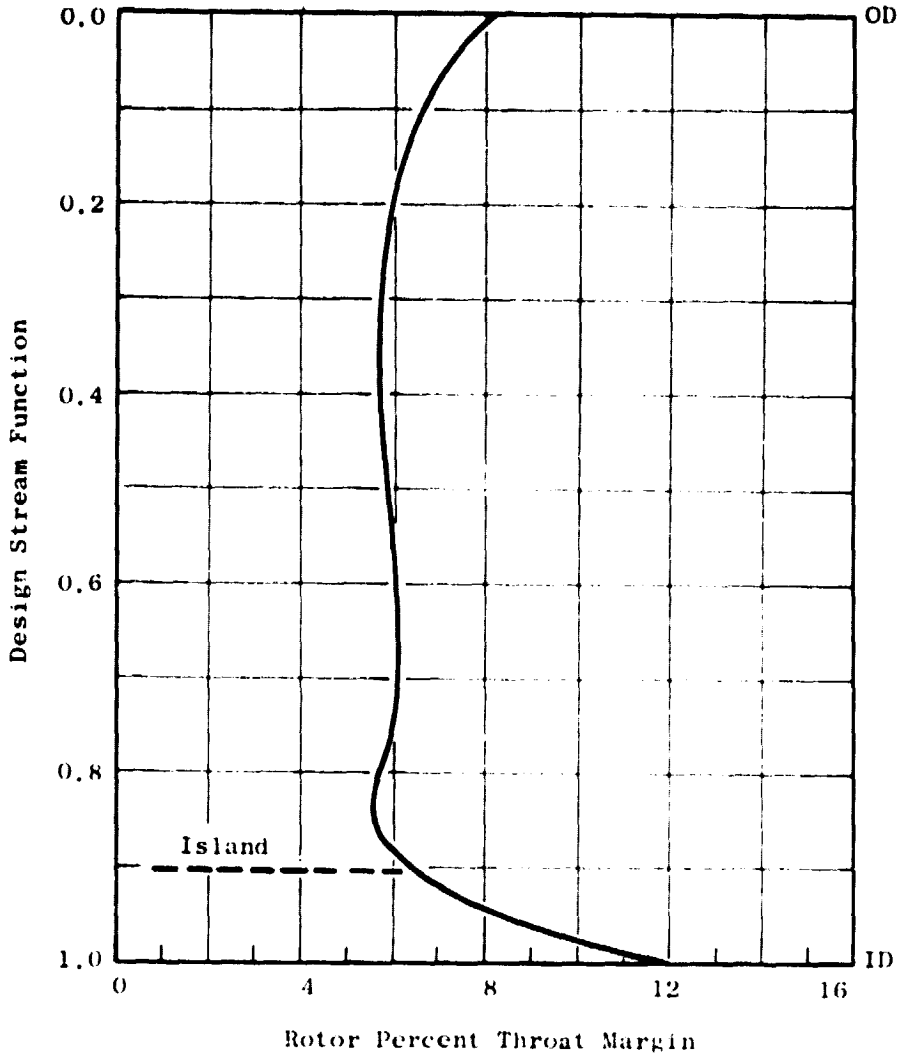

Figure 12. UTW Fan Rotor, Percent Throat Margin.

Section	Radius (cm)	(in.)
1	85.8	33.8
2	76.2	30.0
3	66.8	26.3
4	57.2	22.5
5	47.7	18.8

Tip L.E. Radius = 90.2 cm (35.5 in.)
Hub L.E. Radius = 40.1 cm (15.8 in.)

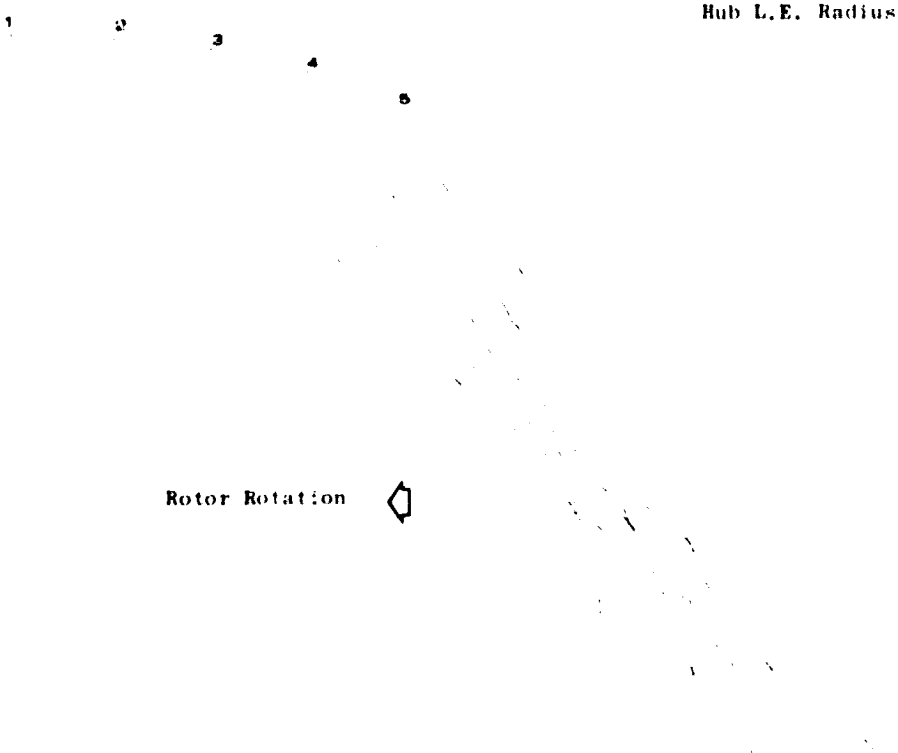

Figure 13. UTW Fan Rotor Blade Plane Sections.

Table III. UTW Fan Rotor Blade Coordinates.

SECTION 1 RADIUS 85.8 cm (33.8 in.)

Convex		Concave	
X (Axial)	Y	X (Axial)	Y
-3,57088	-4,59391	-3,57088	-4,59391
-3,58047	-4,57843	-3,55304	-4,59755
-3,58149	-4,55132	-3,52725	-4,58914
-3,57322	-4,51309	-3,49418	-4,56819
-3,55[illegible]68	-4,46442	-3,45477	-4,53407
-3,5[illegible]47	-4,40594	-3,40985	-4,48620
-3,46[illegible]72	-4,33791	-3,35965	-4,42440
-3,43173	-4,25976	-3,30327	-4,34931
-3,28197	-4,03998	-3,14552	-4,13796
-3,10837	-3,78879	-2,96199	-3,89548
-2,93466	-3,54118	-2,77855	-3,65661
-2,76085	-3,29697	-2,59523	-3,42110
-2,58691	-3,05594	-2,41203	-3,18870
-2,41283	-2,81788	-2,22897	-2,95911
-2,23861	-2,58255	-2,04606	-2,73207
-2,02933	-2,30343	-1,82678	-2,46255
-1,81981	-2,02749	-1,60773	-2,19574
-1,61005	-1,75422	-1,38893	-1,93102
-1,40004	-1,48309	-1,17038	-1,66776
-1,18976	-1,21357	-0,95209	-1,40535
-0,97919	-0,94512	-0,73410	-1,14321
-0,76830	-0,67730	-0,51643	-0,88090
-0,55706	-0,40974	-0,29910	-0,61801
-0,34544	-0,14216	-0,08216	-0,35428
-0,13341	0,12568	0,13438	-0,08948
0,07905	0,39390	0,35048	0,17649
0,29200	0,66258	0,56610	0,44367
0,50541	0,93165	0,78125	0,71187
0,71939	1,20090	0,99583	0,98088
0,93446	1,46953	1,20933	1,25060
1,15118	1,73661	1,42117	1,52080
1,36959	2,00127	1,63132	1,79057
1,58962	2,26258	1,83985	2,05873
1,81122	2,51919	2,04682	2,32380
2,03423	2,76958	2,25237	2,58435
2,25847	3,01244	2,45670	2,83912
2,48369	3,24657	2,66004	3,08697
2,70963	3,47109	2,86266	3,32710
2,93604	3,68531	3,06482	3,55877
3,16264	3,88877	3,26679	3,78150
3,35143	4,04988	3,43513	3,95992
3,50232	4,17313	3,56998	4,09777
3,53436	4,18426	3,58462	4,13010
3,57185	4,16733	3,57185	4,16733

Table III. UTW Fan Rotor Blade Coordinates (Continued).

SECTION 2 RADIUS 76.2 cm (30.0 in.)

Convex		Concave	
X (Axial)	Y	X (Axial)	Y
-3.53096	-3.78711	-3.53096	-3.78711
-3.53951	-3.77219	-3.51429	-3.79124
-3.53964	-3.74671	-3.48973	-3.78440
-3.53068	-3.71117	-3.45787	-3.76615
-3.51173	-3.66625	-3.41950	-3.73590
-3.48194	-3.61259	-3.37527	-3.69315
-3.44093	-3.55049	-3.32533	-3.63779
-3.38936	-3.47944	-3.26875	-3.57053
-3.23593	-3.27533	-3.10711	-3.37975
-3.06179	-3.05086	-2.92182	-3.16812
-2.88750	-2.83311	-2.73667	-2.96328
-2.71310	-2.62119	-2.55163	-2.76416
-2.53857	-2.41421	-2.36672	-2.56974
-2.36391	-2.21141	-2.18195	-2.37919
-2.18911	-2.01213	-1.99731	-2.19170
-1.97915	-1.77680	-1.77595	-1.96984
-1.76893	-1.54478	-1.55484	-1.75039
-1.55840	-1.31538	-1.33404	-1.53261
-1.34752	-1.08803	-1.11360	-1.31584
-1.13622	-0.86234	-0.89358	-1.09966
-0.92445	-0.63802	-0.67403	-0.88369
-0.71217	-0.41484	-0.45498	-0.66769
-0.49933	-0.19267	-0.23650	-0.45148
-0.28588	0.02855	-0.01862	-0.23502
-0.07178	0.24883	0.19860	-0.01830
0.14300	0.46807	0.41515	0.19855
0.35854	0.68608	0.63093	0.41533
0.57513	0.90231	0.84567	0.63193
0.79303	1.11612	1.05909	0.84814
1.01230	1.32693	1.27115	1.06331
1.23284	1.53411	1.48193	1.27675
1.45459	1.73698	1.69151	1.48777
1.67745	1.93487	1.89997	1.69568
1.90130	2.12710	2.10745	1.89976
2.12599	2.31301	2.31408	2.09936
2.35136	2.49202	2.52003	2.29388
2.57722	2.66361	2.72549	2.48276
2.80339	2.82735	2.93065	2.66553
3.02965	2.98287	3.13571	2.84173
3.25581	3.12995	3.34088	3.01103
3.44407	3.24594	3.51206	3.14659
3.59086	3.33233	3.64598	3.24884
3.62375	3.33641	3.66485	3.27823
3.65778	3.31641	3.65778	3.31641

Table III. UTW Fan Rotor Blade Coordinates (Continued).

SECTION 3 RADIUS 66.9 cm (26.3 in.)

Convex		Concave	
X (Axial)	Y	X (Axial)	Y
-3.44902	-3.03130	-3.44902	-3.03130
-3.45631	-3.01728	-3.43399	-3.03624
-3.45564	-2.99433	-3.41140	-3.03192
-3.44652	-2.96289	-3.38170	-3.01797
-3.42827	-2.92354	-3.34544	-2.99392
-3.40027	-2.87680	-3.30309	-2.95936
-3.36226	-2.82288	-3.25468	-2.91428
-3.31482	-2.76130	-3.19940	-2.85937
-3.15984	-2.56706	-3.02637	-2.68941
-2.99245	-2.36411	-2.83784	-2.51105
-2.82463	-2.16755	-2.64974	-2.33963
-2.65638	-1.97693	-2.46207	-2.17435
-2.48767	-1.79173	-2.27486	-2.01442
-2.31848	-1.61151	-2.08814	-1.85914
-2.14878	-1.43584	-1.90191	-1.70781
-1.94447	-1.23052	-1.67912	-1.53056
-1.73937	-1.03059	-1.45712	-1.35712
-1.53340	-0.83559	-1.23598	-1.18674
-1.32651	-0.64513	-1.01577	-1.01875
-1.11859	-0.45896	-0.79658	-0.85271
-0.90958	-0.27691	-0.57850	-0.68827
-0.69938	-0.09890	-0.36159	-0.52522
-0.48796	0.07507	-0.14590	-0.36339
-0.27532	0.24498	0.06856	-0.20265
-0.06144	0.41083	0.28178	-0.04291
0.15371	0.57254	0.49373	0.11595
0.37024	0.73003	0.70431	0.27396
0.58823	0.88309	0.91342	0.43096
0.80777	1.03142	1.12098	0.58671
1.02884	1.17467	1.32702	0.74066
1.25131	1.31237	1.53166	0.89227
1.47503	1.44402	1.73504	1.04101
1.69984	1.56905	1.93733	1.18636
1.92553	1.68698	2.13875	1.32781
2.15181	1.79732	2.33957	1.46492
2.37838	1.89976	2.54010	1.59735
2.60492	1.99412	2.74067	1.72484
2.83111	2.08047	2.94158	1.84731
3.05681	2.15904	3.14299	1.96460
3.28185	2.22986	3.34505	2.07641
3.46864	2.28300	3.51417	2.16531
3.61268	2.32088	3.64570	2.23165
3.64345	2.31843	3.66807	2.25485
3.66937	2.29101	3.66937	2.29101

Table III. UTW Fan Rotor Blade Coordinates (Continued).

SECTION 4 RADIUS 57.2 cm (22.5 in.)

Convex		Concave	
X (Axial)	Y	X (Axial)	Y
-3.27656	-2.27702	-3.27656	-2.27702
-3.28322	-2.26279	-3.26204	-2.28303
-3.28186	-2.24050	-3.23980	-2.28070
-3.27207	-2.21053	-3.21017	-2.26971
-3.25332	-2.17341	-3.17355	-2.24967
-3.22513	-2.12958	-3.13024	-2.22029
-3.18733	-2.07922	-3.08018	-2.18164
-3.14041	-2.02184	-3.02260	-2.13446
-3.00531	-1.86253	-2.86579	-2.00785
-2.84845	-1.68435	-2.68165	-1.86527
-2.69081	-1.51211	-2.49829	-1.72907
-2.53231	-1.34548	-2.31578	-1.59863
-2.37289	-1.18419	-2.13420	-1.47341
-2.21244	-1.02809	-1.95364	-1.35305
-2.05092	-0.87713	-1.77416	-1.23720
-1.85563	-0.70271	-1.56025	-1.10369
-1.65868	-0.53560	-1.34800	-0.97568
-1.46005	-0.37578	-1.13742	-0.85268
-1.25975	-0.22324	-0.92852	-0.73420
-1.05776	-0.07797	-0.72130	-0.61984
-0.85414	0.06003	-0.51571	-0.50917
-0.64895	0.19075	-0.31170	-0.40182
-0.44225	0.31420	-0.10920	-0.29746
-0.23413	0.43043	0.09188	-0.19578
-0.02466	0.53944	0.29162	-0.09654
0.18612	0.64122	0.49005	0.00047
0.39814	0.73569	0.68723	0.09543
0.61134	0.82282	0.88324	0.18838
0.82557	0.90254	1.07821	0.27929
1.04070	0.97480	1.27229	0.36809
1.25652	1.03950	1.46567	0.45467
1.47281	1.09659	1.65858	0.53892
1.68933	1.14604	1.85126	0.62070
1.90583	1.18789	2.04397	0.69984
2.12215	1.22220	2.23685	0.77609
2.33818	1.24891	2.43003	0.84904
2.55368	1.26786	2.62373	0.91817
2.76842	1.27875	2.81820	0.98277
2.98190	1.28127	3.01392	1.04212
3.19369	1.27534	3.21134	1.09559
3.36866	1.26400	3.37737	1.13521
3.50345	1.25130	3.50742	1.16266
3.52868	1.24005	3.53283	1.17756
3.54352	1.20850	3.54352	1.20850

Table III. UTW Fan Rotor Blade Coordinates (Concluded).

SECTION 5 RADIUS 44.7 cm (18.8 in.)

Convex		Concave	
X (Axial)	Y	X (Axial)	Y
-2.99111	-1.53332	-2.99111	-1.53332
-2.99661	-1.51937	-2.97778	-1.54019
-2.99415	-1.49848	-2.95672	-1.53986
-2.98342	-1.47101	-2.92817	-1.53206
-2.96398	-1.43741	-2.89242	-1.51649
-2.93547	-1.39809	-2.84966	-1.49292
-2.89777	-1.35321	-2.79978	-1.46149
-2.85128	-1.30229	-2.74206	-1.42298
-2.74618	-1.19129	-2.62085	-1.34350
-2.60488	-1.04793	-2.45456	-1.23970
-2.46249	-0.91015	-2.28934	-1.14224
-2.31901	-0.77783	-2.12523	-1.05062
-2.17438	-0.65084	-1.96226	-0.96435
-2.02861	-0.52907	-1.80043	-0.88293
-1.88167	-0.41240	-1.63979	-0.80592
-1.70357	-0.27903	-1.44876	-0.71897
-1.52347	-0.15302	-1.25975	-0.63765
-1.34115	-0.03456	-1.07296	-0.56178
-1.15662	0.07596	-0.88837	-0.49114
-0.97013	0.17822	-0.70574	-0.42527
-0.78186	0.27207	-0.52490	-0.36372
-0.59214	0.35744	-0.34551	-0.30593
-0.40109	0.43439	-0.16744	-0.25140
-0.20852	0.50299	0.00911	-0.19998
-0.01449	0.56305	0.18419	-0.15156
0.18120	0.61427	0.35762	-0.10623
0.37827	0.65609	0.52966	-0.06403
0.57603	0.68809	0.70102	-0.02487
0.77398	0.71018	0.87218	0.01129
0.97134	0.72250	1.04394	0.04463
1.16778	0.72543	1.21662	0.07529
1.36313	0.71937	1.39038	0.10335
1.55717	0.70473	1.56546	0.12878
1.74974	0.68192	1.74201	0.15152
1.94060	0.65140	1.92026	0.17148
2.12950	0.61378	2.10047	0.18861
2.31654	0.56974	2.28255	0.20292
2.50190	0.51979	2.46631	0.21426
2.68565	0.46433	2.65167	0.22235
2.86787	0.40358	2.83857	0.22666
3.01856	0.34896	2.99548	0.22686
3.13513	0.30368	3.10630	0.22470
3.15489	0.28737	3.13939	0.22758
3.16082	0.25675	3.16082	0.25675

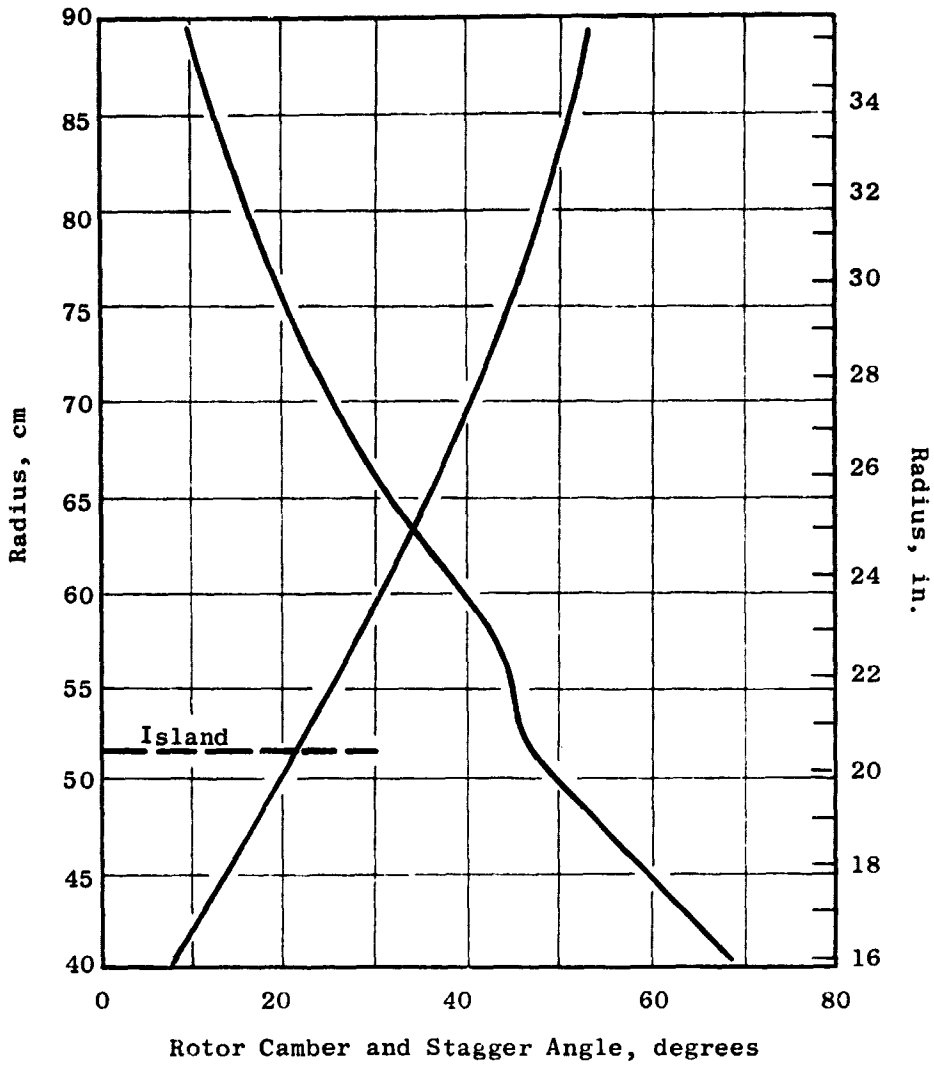

Figure 14. UTW Fan Rotor Camber and Stagger Angle Radial Distribution.

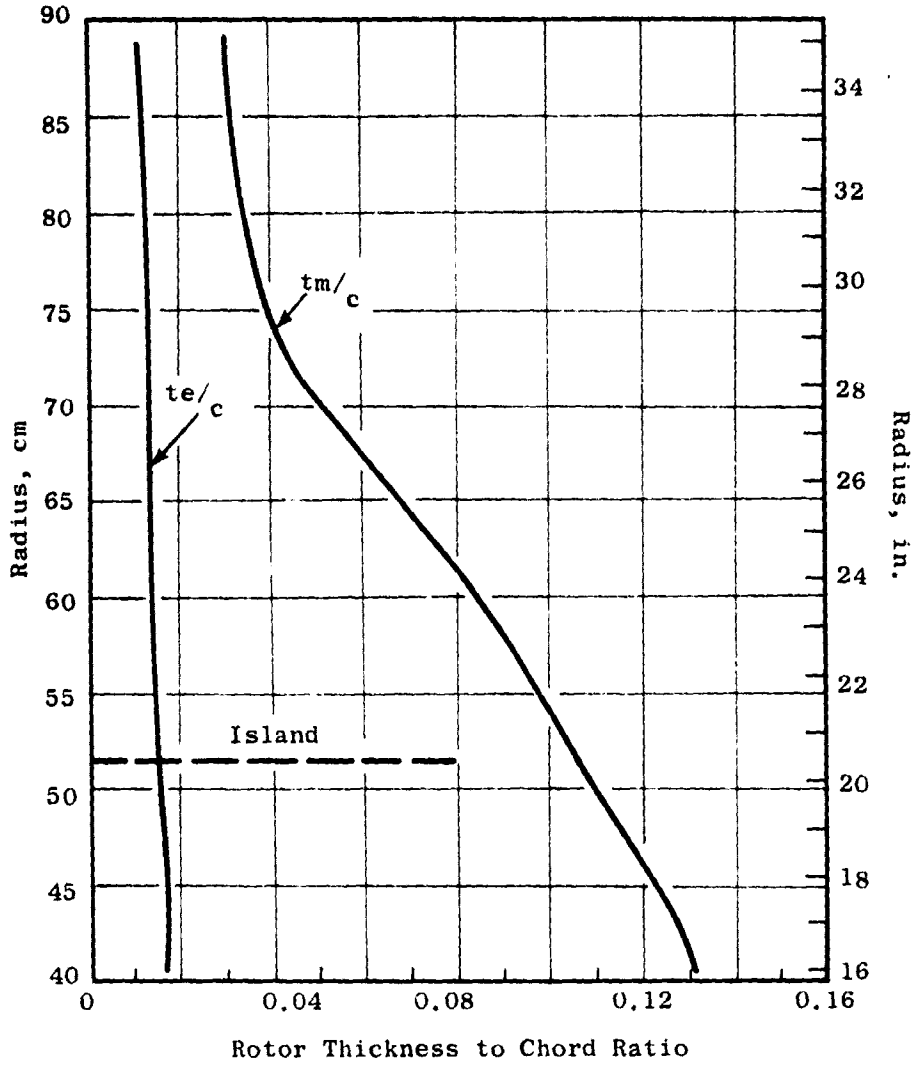

Figure 15. UTW Fan Rotor Thickness Distributions.

1.2.7 Core OGV Design

A moderately low aspect ratio of 1.3 was selected for the core portion OGV to provide a rugged mechanical system. This selection was in recognition of the potentially severe aeromechanical environment (i.e., large rotor wakes) of the core OGV because of its small size in relationship to that of the rotor blade. A solidity at the ID of 1.65 was selected to yield reasonable levels of diffusion factor, Figure 10. The number of vanes which result is 96. Radial distribution of total pressure loss coefficient, diffusion factor, Mach number, and air angle are presented in Figure 10.

The profiles for the core portion OGV are a modified NASA 65-series thickness distribution on a circular-arc meanline. The incidence angle over the outer portion of the span was selected from a correlation of NASA low-speed cascade data. Locally, in the ID region, the incidence angle was reduced 0.07 radian (4°). This local reduction in incidence was in recognition of traverse data results on other high-bypass fan configurations which show core stator inlet air angles several degrees higher than the axisymmetric calculated values. The deviation angle was obtained from Carter's Rule as was described for the rotor blade, but no empirical adjustment was made. The resulting incidence and deviation angles and throat margin are shown in Figure 16. The throat area for the selected geometry was checked to ensure sufficient margin to pass the design flow. The minimum margin relative to the critical contraction ratio was 6%, which is sufficient to avoid choke. Resulting parameters for the core OGV are presented in Figure 17. Figure 18 is a cylindrical section of the core OGV at the pitch line radius. A tabulation of the coordinates for this core OGV is given in Table IV.

1.2.8 Transition Duct Strut Design

The transition duct flowpath is shown in Figure 19. The ratio of duct exit to duct inlet flow area is 1.02. There are six struts in the transition duct which are aerodynamically configured to remove the 0.105 radian (6° of swirl left in the air by the core OGV's and to house the structural spokes of the composite wheels (see Figure 2). In addition, at engine station 196.5 (Figure 2), the 6 and 12 o'clock strut positions must house radial accessory drive shafts. The number of struts and axial position of the strut trailing edge were selected identical with the F101 engine to minimize unknowns in the operation of the core engine system. The axial positions and thickness requirements of the composite wheel spokes were dictated by mechanical considerations. The axial location of the strut leading edge at the OD was determined by its proximity to the splitter leading edge. At the OD flowpath, the strut leading edge is 17.8 mm (0.7 in.) forward of the wheel spoke. A relatively blunt strut leading edge results from the 26.7 mm (1.05 in.) wheel spoke thickness requirement. The wheel spoke is radial. The axial lean of the strut leading edge provides relief from the LE bluntness at lower radii and makes the LE approximately normal to the incoming flow. Since the inlet Mach number in the OD region is less than 0.5 and since the boundary layer along the outer wall initiates at the splitter LE, no significant aerodynamic penalty was assessed because of the bluntness. A NASA 65-series thickness distribution was selected for the basic profile thickness which was modified

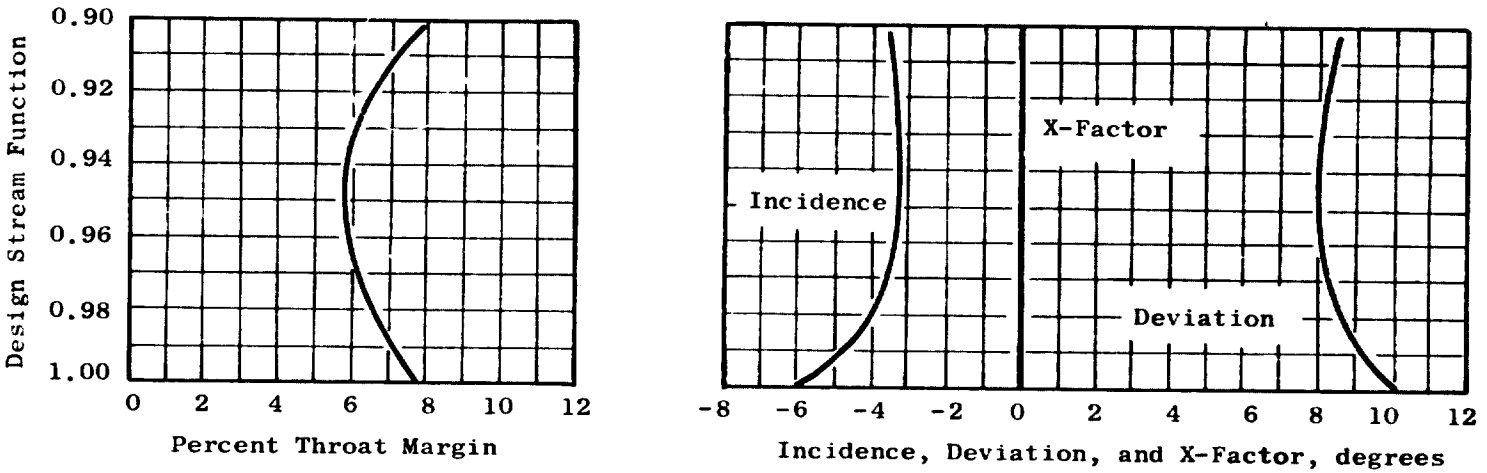

Figure 16. UTW Fan Core OGV.

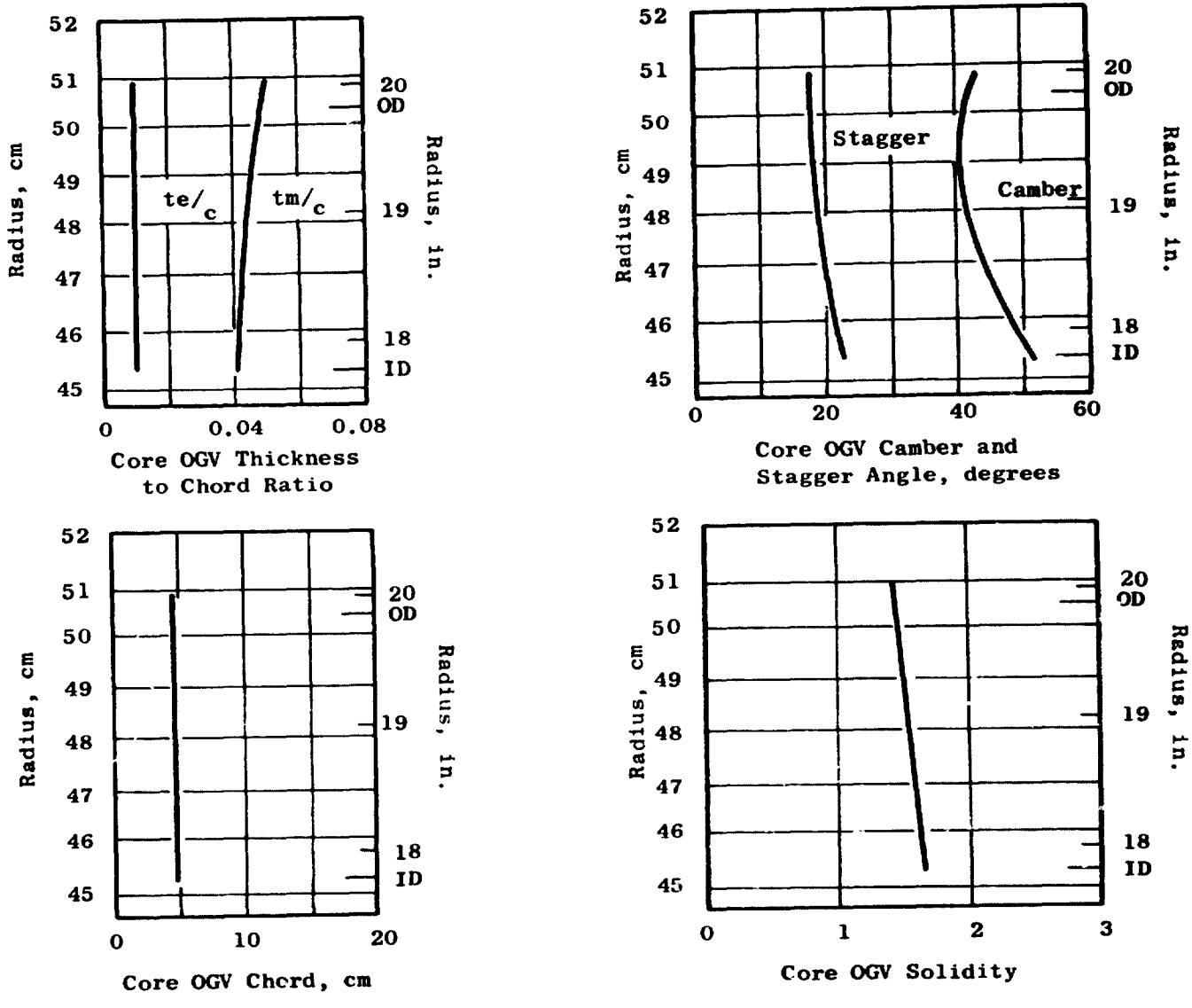

Figure 17. UTW Fan, Core OGV Geometry.

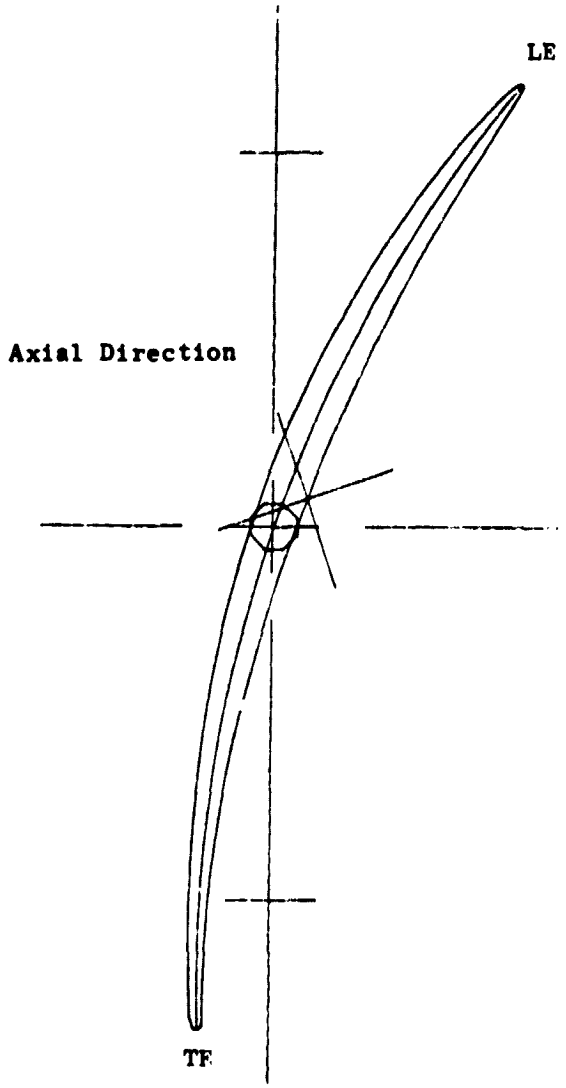

Figure 18. Cylindrical Section of UTW Fan-Core OGV at the Pitch Line Radius.

Table IV. UTW Fan Core OGV Coordinates at the Pitch Line Radius.

Convex		Concave	
X (Axial)	Y	X (Axial)	Y
-0.842769	0.477539	-0.842769	0.477539
-0.842102	0.478085	-0.843193	0.476788
-0.841193	0.478426	-0.843371	0.475831
-0.840041	0.478562	-0.843303	0.474671
-0.838648	0.478489	-0.842988	0.473308
-0.837016	0.478207	-0.842422	0.471747
-0.835148	0.477713	-0.841604	0.469990
-0.833043	0.477005	-0.840531	0.468041
-0.830706	0.476081	-0.839199	0.465902
-0.825930	0.473879	-0.836147	0.461586
-0.816825	0.468976	-0.829578	0.453512
-0.795126	0.455609	-0.811971	0.434780
-0.752668	0.428386	-0.775318	0.399261
-0.710699	0.401338	-0.737517	0.365474
-0.668893	0.374802	-0.698908	0.333049
-0.585404	0.323526	-0.619675	0.271892
-0.501676	0.274929	-0.538221	0.215193
-0.417507	0.229049	-0.454815	0.162726
-0.332770	0.185866	-0.369635	0.114358
-0.247368	0.145345	-0.282819	0.070005
-0.161246	0.107397	-0.194455	0.029661
-0.074357	0.071905	-0.104611	-0.006617
0.013395	0.038873	-0.013395	-0.038873
0.102065	0.008204	0.079131	-0.067022
0.191787	-0.019959	0.172840	-0.091196
0.282669	-0.045471	0.267634	-0.111499
0.374803	-0.068200	0.363446	-0.128002
0.468270	-0.087992	0.460225	-0.140766
0.563146	-0.104640	0.557937	-0.149878
0.659491	-0.117933	0.656574	-0.155395
0.757358	-0.127551	0.756149	-0.157452
0.856774	-0.133069	0.856712	-0.156245
0.876843	-0.133602	0.876951	-0.155667
0.896972	-0.133921	0.897236	-0.154995
0.917161	-0.134016	0.917569	-0.154238
0.937408	-0.133872	0.937951	-0.153407
0.948266	-0.133695	0.948850	-0.152936
0.954694	-0.136013	0.955078	-0.150279
0.958048	-0.142994	0.958048	-0.142994

for the special considerations required in this design. The strut thickness is the same for all radii aft of the forward wheel spoke LE (Figure 19) to facilitate fabrication. A cylindrical cut cross section showing the nominal strut geometry at three radii is shown in Figure 20. The thickness distribution for the 6 and 12 o'clock struts was further modified for the envelope of the radial drive shaft. Cylindrical cut cross sections of these struts are also shown in Figure 20. The leading edge 40% chord of these further modified sections is identical to that of the nominal strut geometry, and aft of forward wheel spoke LE, the strut thickness is the same for all radii. The core engine has demonstrated operation in the presence of a similar thick strut in the F101 application without duress.

1.2.9 Vane-Frame (Fan Bypass OGV) Design

The vane-frame performs the dual function of an outlet guide vane for the bypass flow and a frame support for the engine components and nacelle. It is a common piece of hardware for both the UTW and OTW engine fans. It is integrated with the pylon which houses the radial drive shaft at engine station 196.5 (see Figure 2), houses the engine mount at approximately engine station 210, provides an interface between the propulsion system with the aircraft system, and houses the forward thrust links. The vane-frame furthermore acts as an inlet guide vane for the UTW fan when in the reverse mode of operation.

A conventional OGV system turns the incoming flow to axial. The housing requirements of the pylon dictate a geometry which requires the OGV's to underturn approximately 0.174 radian (10°) on one side and to overturn approximately 0.174 radian (10°) on the other side. The vanes must be tailored to downstream vector diagrams which conform to the natural flow field around the pylon to avoid creating velocity distortions in the upstream flow. Ideally, each vane would be individually tailored. However, to avoid excessive costs, five vane geometry groups were selected as adequate.

The Mach number and air angle at inlet to the vane-frame (fan bypass OGV) are shown in Figure 21 for both the UTW and OTW fans. In the outer portion of the bypass duct annulus, the larger air angle in the UTW environment results in a less negative incidence angle for it than for the OTW environment. The Mach number in the outer portion of the annulus is also higher in the UTW environment. When selecting incidence angles, a higher Mach number environment naturally leads to the desire to select a less negative incidence angle. The amount by which the incidence angle would naturally be increased due to the higher Mach number UTW environment is approximately equal to the increase in the inlet air angle of the UTW environment. In the inner portion of the annulus, the inlet Mach number and air angle are higher for the OTW environment. The natural increase in incidence angle desired because of the higher Mach number is approximately the same as the increase in the inlet air angle. As a result of these considerations, no significant aerodynamic performance penalty is assessed to using common hardware for both the UTW and OTW fans.

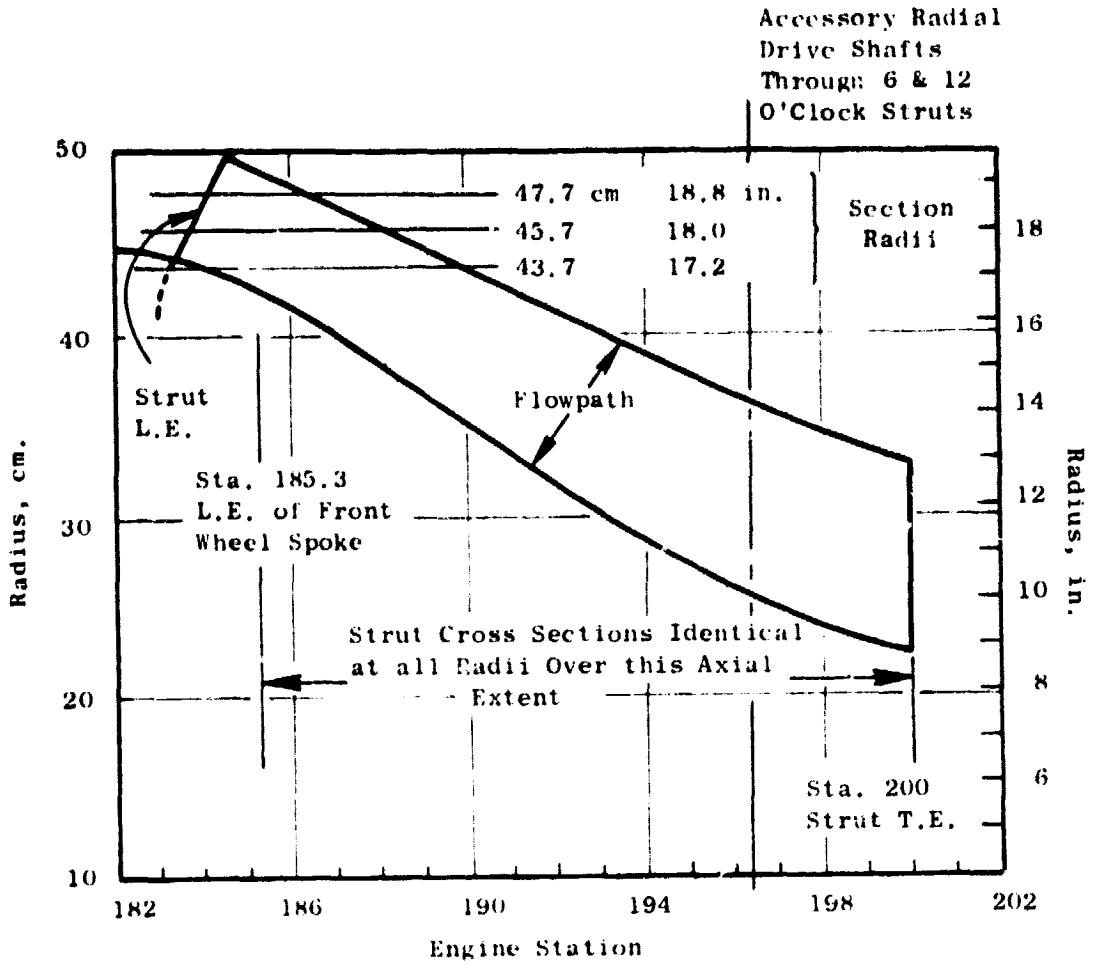

Figure 19. Transition Duct Flowpath.

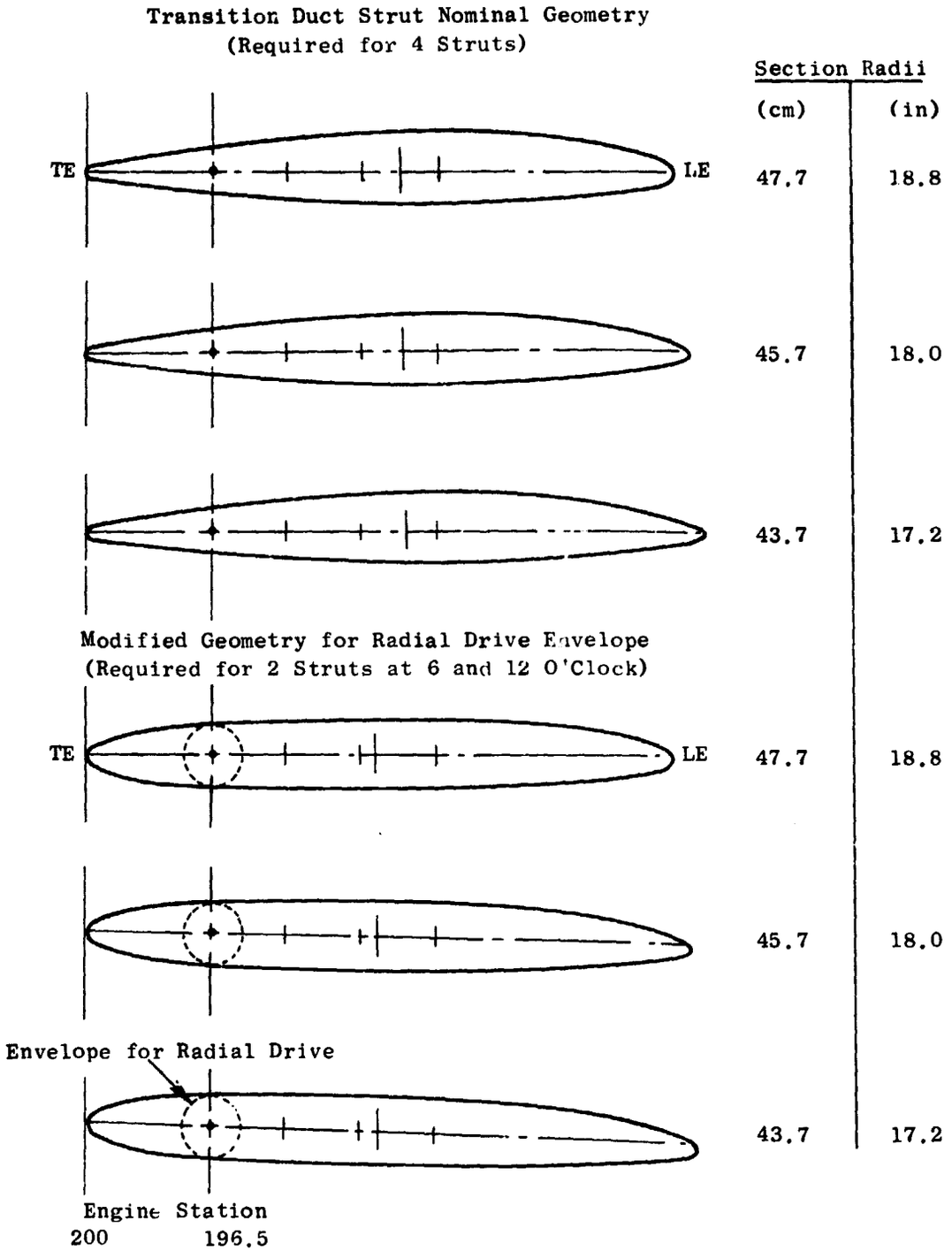

Figure 20. Transition Duct Strut Cylindrical Sections at Three Radii.

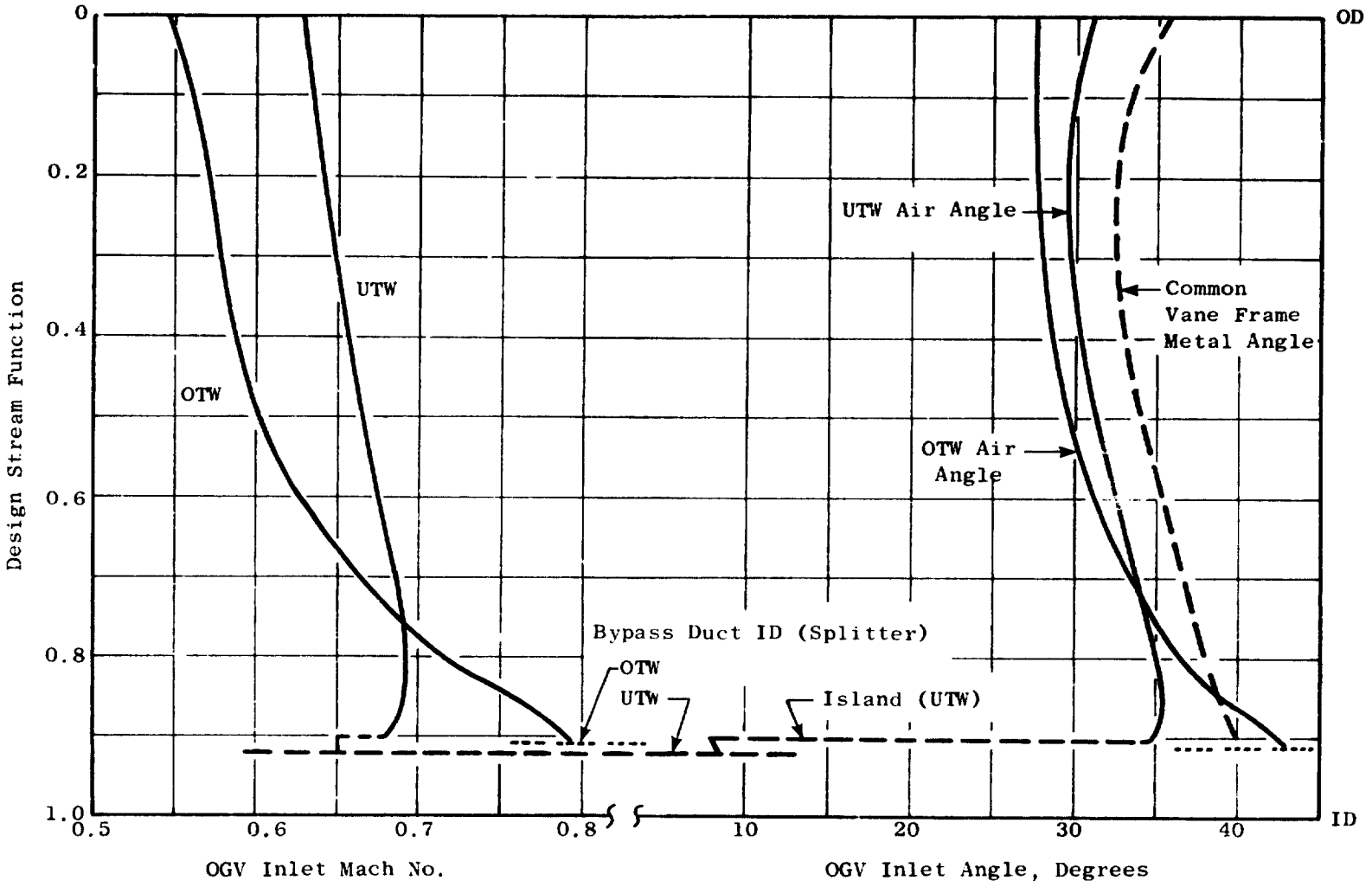

Figure 21. Vane-Frame (Fan Bypass OGV) Aerodynamic Environment.

Locally, near the bypass duct ID, there is a discontinuity in the aerodynamic environment of the UTW configuration. This discontinuity represents that portion of the flow which passes under the island but bypasses the splitter. The calculation ignored mixing across the vortex sheet. In the design of the vane geometry no special considerations were incorporated because of this discontinuity since it is believed that in a real fluid the mixing process will greatly diminish the vortex strength.

The vane chord at the OD was selected largely by the mechanical requirement of axial spacing between the composite frame spokes. At the ID, the vane leading edge was lengthened primarily to obtain an aerodynamically reasonable leading edge fairing on the pylon compatible with the envelope requirements of the radial drive shaft. The ID region is significantly more restrictive in this regard because of choking considerations, particularly for the OTW environment, with the reduced circumferential spacing between vanes. The solidity resulting from 33 vanes, an acoustic requirement, was acceptable from an aerodynamic loading viewpoint as shown in Figure 22. The two diffusion factor curves are a result of the two aerodynamic environments, UTW and OTW, to which the common vane frame geometry is exposed. The thickness is a modified NASA 65-series distribution. Maximum-thickness- and trailing-edge-thickness-to-chord ratios of 0.08 and 0.02, respectively, were selected at the OD. The same maximum thickness and trailing edge thickness were used at all other radii which results in maximum-thickness- and trailing-edge-thickness-to-chord ratios of 0.064 and 0.016, respectively, at the ID.

As a guide in the selection of the overall vector diagram requirements of the vane frame, a circumferential analysis of an approximate vane geometry, including the pylon, was performed. This analysis indicated, for uniform flow at vane inlet, that the vane discharge Mach number was approximately constant circumferentially and that the discharge air angle was nearly linear circumferentially between the pylon wall angles. Figure 23, an unwrapped cross section at the ID, shows the flowfield calculated by this analysis. The specific design criteria selected for the layout of the five-vane geometry groups was to change the average discharge vector diagram with zero swirl to vector diagrams with $\pm$ 5° of swirl and $\pm$ 10° of swirl.

The meanline shapes for each of the five-vane groups vary. For the vane group which overturns the flow by +10° the meanline is approximately a circular arc. As a result of passage area distribution and choking consideratons, the meanline shape employed in the forward 25% chord region of this vane group was retained for the other four groups.

The incidence angle for all vane groups was the same and was selected for the group with the highest camber. A correlation of NASA low-speed cascade data was the starting point for the incidence selection. Over the outer portion of the vane, where the inlet Mach number is lower, the incidence angles were slanted to the low side of the correlation. This was done in consideration of the reverse thrust mode of operation for the UTW fan. In this mode, the OGV's impart a swirl counter to the direction of rotor rotation. Additional vane leading edge camber tends to increase the counterswirl and therefore increase the pumping capacity of the fan in reverse. In the inner portion of the vane,

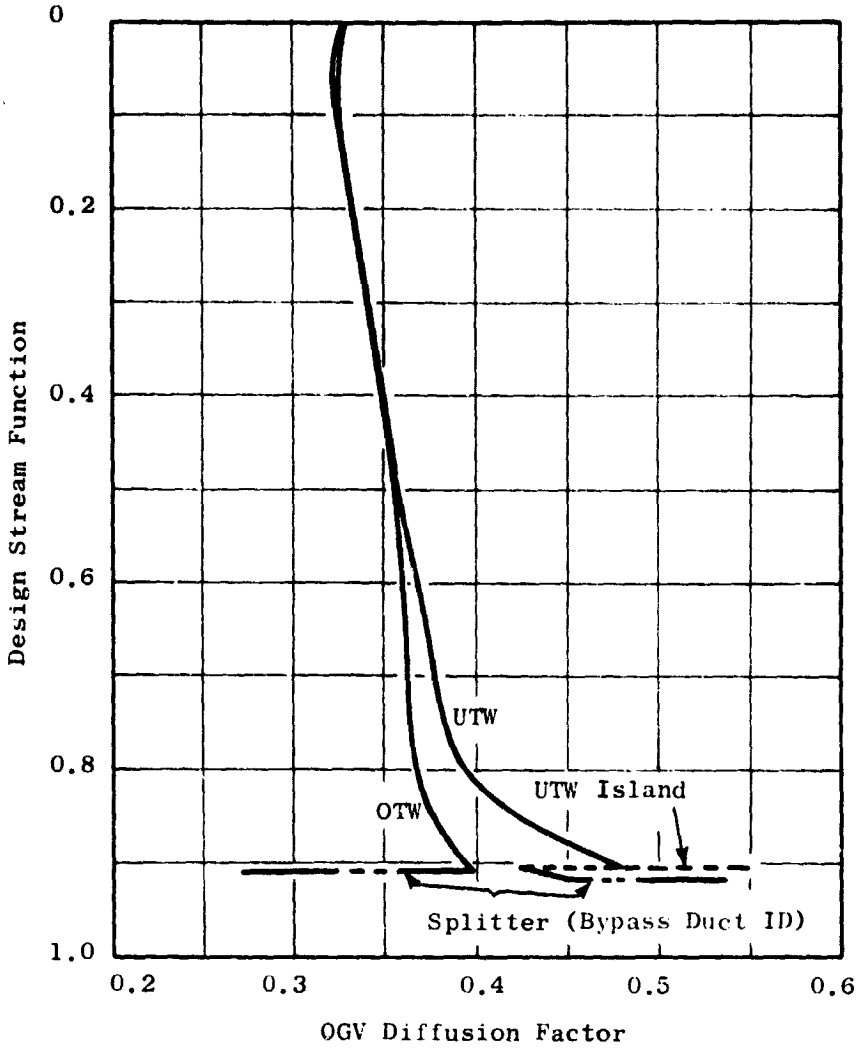

Figure 22. Vane-Frame (Fan Bypass OGV) Nominal Vane Configuration.

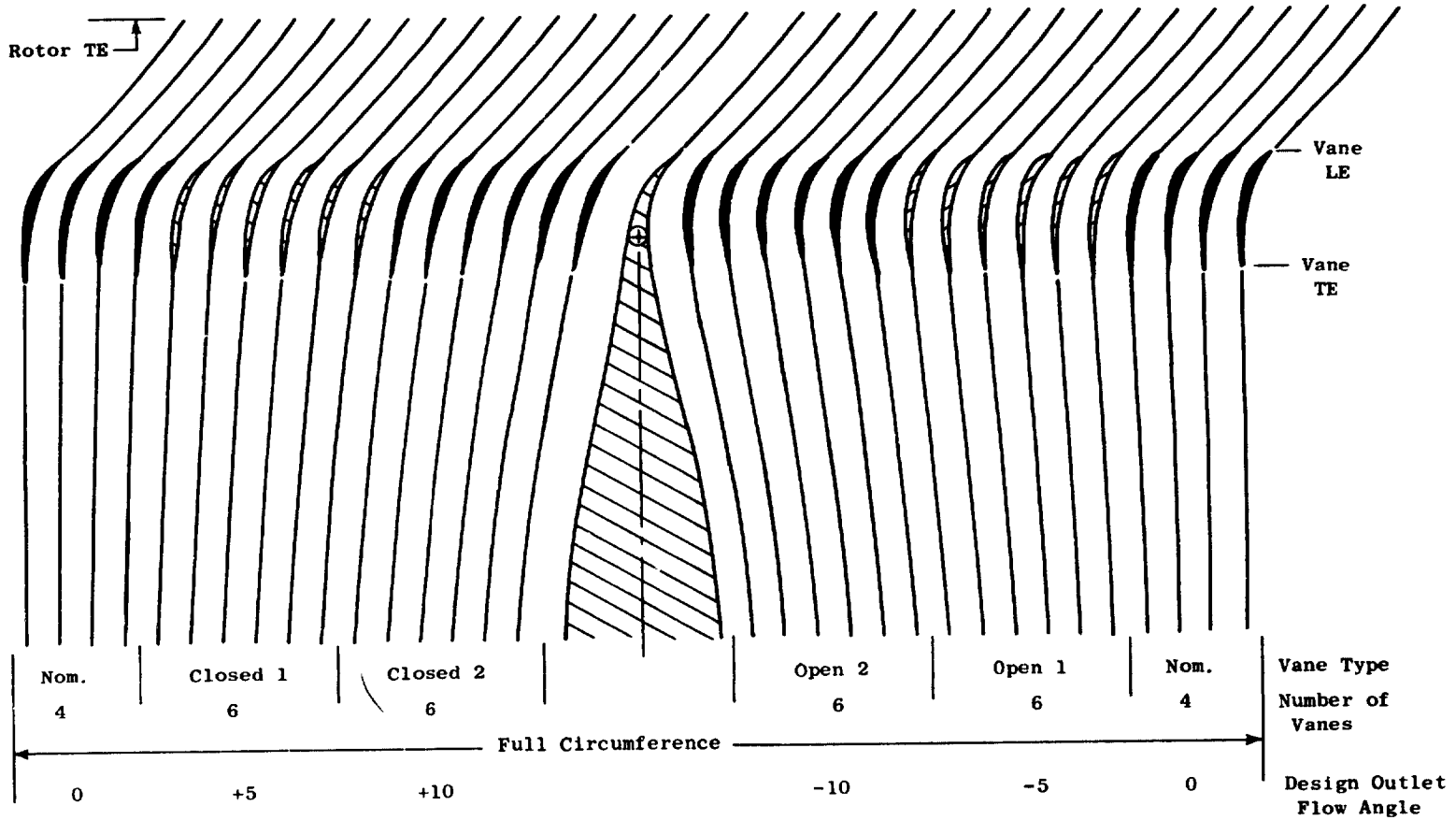

Figure 23. Vane-Frame (Fan Bypass OGV) Unwrapped Section at ID.

the incidence angles are higher than suggested by the correlation because of the higher inlet Mach number. Also, in the reverse mode of operation, this reduction in vane leading edge camber in the ID region reduces the swirl for that portion of the fluid which enters the core engine and tends to reduce its pressure drop.

The deviation angle for each of the five vane groups was calculated from Carter's Rule as described for the rotor. The portion of the meanline aft of the 25% chord point approximates a circular arc blending between the front circular arc and the required trailing edge angle. For the vane group which underturns the flow by 10°, the aft portion of the blade has little camber. Figure 24 shows an unwrapped cross section at the ID of two of the 10° over-cambered vanes and two of the 10° under-cambered vanes adjacent to the pylon. Note that the spacing between the pylon and the first under-cambered vane is 50% larger than average. This increased spacing was required to open the passage internal area, relative to the capture area, to retrieve the area blocked by the radial drive shaft envelope requirements.

Table V gives the detailed coordinate data for the two vane geometries and the pylon leading edge geometry shown in Figure 24. The coordinate data for the nominal vane geometry at three radial locations are also given in this table. The vane coordinate data are in inches.

Radial distributions of camber and stagger for the nominal and two extreme vane geometries are shown in Figure 25. Radial distributions of chord and solidity for the nominal vane are shown in Figure 26. The design held the leading and trailing edge axial projection common for all five groups which results in slightly different chord lengths for the other four vane types.

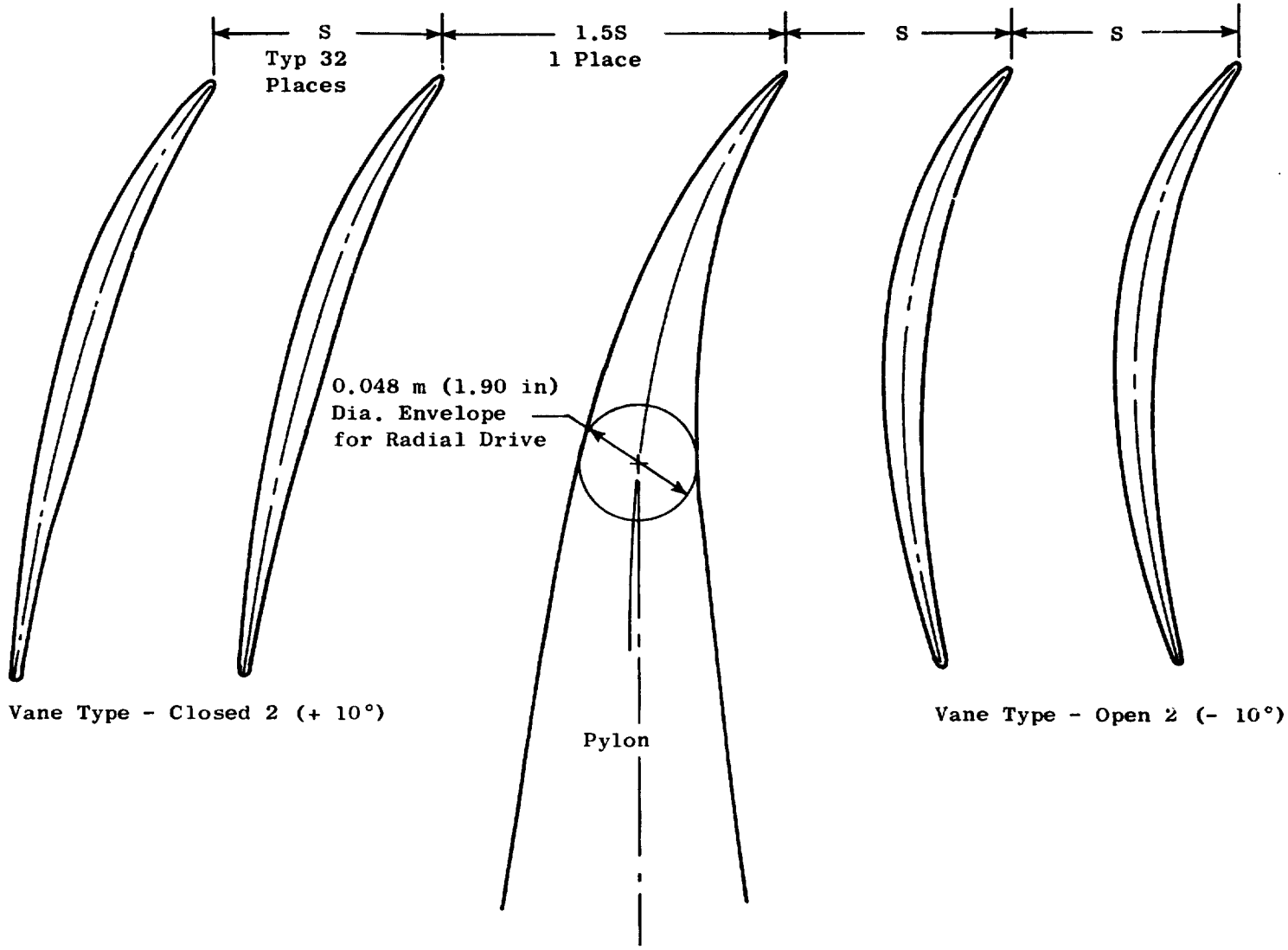

Figure 24. Vane-Frame (Fan Bypass OGV) Unwrapped Section at ID, 32 Vanes Plus Pylon LE Fairing.

Table V. Vane-Frame (Fan Bypass OGV) Coordinates.

Vane Type: Closed 2
Radius 53.0 cm (20.86 in.)

Convex		Concave	
X (Axial)	Y	X (Axial)	Y
-6.48210	2.34116	-6.48210	2.34116
-6.48759	2.32790	-6.47014	2.34917
-6.48654	2.30949	-6.45181	2.35181
-6.47875	2.28616	-6.42730	2.34886
-6.46396	2.25823	-6.39677	2.34011
-6.44206	2.22584	-6.36025	2.32555
-6.41331	2.18867	-6.31735	2.30561
-6.29919	2.05618	-6.16591	2.22947
-6.07119	1.83449	-5.89480	2.07990
-5.83097	1.63835	-5.63592	1.92961
-5.58939	1.45347	-5.37839	1.79199
-5.34632	1.27982	-5.12236	1.66526
-5.10018	1.11977	-4.86939	1.54502
-4.85192	0.97171	-4.61855	1.43098
-4.60258	0.83339	-4.36878	1.32361
-4.30233	0.67897	-4.07011	1.20263
-4.00106	0.53619	-3.77245	1.08890
-3.69886	0.40428	-3.47572	0.98129
-3.39590	0.28251	-3.17976	0.87882
-3.09242	0.16986	-2.88431	0.78108
-2.78889	0.06546	-2.58892	0.68742
-2.48547	-0.03115	-2.29341	0.59624
-2.18202	-0.12056	-1.99793	0.50613
-1.87857	-0.20389	-1.70246	0.41663
-1.57498	-0.28229	-1.40712	0.32765
-1.27110	-0.35637	-1.11208	0.23941
-0.96707	-0.42655	-0.81718	0.15212
-0.66307	-0.49346	-0.52225	0.06612
-0.35916	-0.55754	-0.22724	-0.01841
-0.05521	-0.61845	0.06774	-0.10206
0.24894	-0.67585	0.36251	-0.18531
0.55329	-0.73002	0.65709	-0.26774
0.85774	-0.78128	0.95157	-0.34873
1.16223	-0.82964	1.24600	-0.42780
1.46682	-0.87488	1.54034	-0.50454
1.77161	-0.91602	1.83448	-0.57877
2.07653	-0.95211	2.12848	-0.65013
2.38133	-0.98311	2.42260	-0.71727
2.68567	-1.00936	2.71719	-0.77845
2.98924	-1.03206	3.01255	-0.83151
3.24155	-1.04887	3.25934	-0.86832
3.41111	-1.05853	3.42574	-0.88974
3.46658	-1.04155	3.47884	-0.91753
3.50000	-0.98095	3.50000	-0.98095

Table V. Vane-Frame (Fan Bypass OGV) Coordinates (Continued).

Vane Type: Pylon Leading Edge
Radius 53.0 cm (20.86 in.)

Convex		Concave	
X (Axial)	Y	X (Axial)	Y
-6.48132	2.39154	-6.48132	2.39154
-6.48473	2.38081	-6.47148	2.39700
-6.48161	2.36491	-6.45525	2.39712
-6.47179	2.34406	-6.43279	2.39173
-6.45509	2.31849	-6.40420	2.38068
-6.43144	2.28828	-6.36944	2.36404
-6.40114	2.25305	-6.32808	2.34232
-6.28510	2.12434	-6.17848	2.26374
-6.06174	1.89820	-5.90277	2.12120
-5.82801	1.69438	-5.63744	1.98182
-5.58938	1.50620	-5.37700	1.85097
-5.35069	1.32592	-5.11662	1.73488
-5.11131	1.15379	-4.85694	1.63146
-4.86999	0.99135	-4.59920	1.53737
-4.62695	0.83784	-4.34317	1.45194
-4.33354	0.66380	-4.03770	1.36062
-4.03838	0.49997	-3.73397	1.28070
-3.74142	0.34566	-3.43206	1.21133
-3.44249	0.20051	-3.13211	1.15184
-3.14194	0.06430	-2.83378	1.10152
-2.84029	-0.06372	-2.53655	1.05974
-2.53811	-0.18441	-2.23985	1.02584
-2.23601	-0.29875	-1.94307	0.99894
-1.93375	-0.40770	-1.64646	0.97830
-1.63088	-0.51145	-1.35045	0.96310
-1.32713	-0.60978	-1.05531	0.95241
-1.02219	-0.70205	-0.76138	0.94519
-0.71617	-0.78789	-0.46851	0.94075
-0.40945	-0.86865	-0.17635	0.94005
-0.10190	-0.94573	0.11497	0.94418
0.20685	-1.01906	0.40510	0.95304
0.51627	-1.08827	0.69456	0.96621
0.82574	-1.15361	0.98398	0.98345
1.13505	-1.21546	1.27354	1.00450
1.44405	-1.27381	1.56343	1.02871
1.73876	-1.32623	2.14355	1.08453
2.03355	-1.37574	2.44720	1.11734
3.50000	-1.64800	3.50000	1.20800

Table V. Vane-Frame (Fan Bypass OGV) Coordinates (Continued).

Vane Type: Open 2
Radius 53.0 cm (20.86 in.)

Convex		Concave	
X (Axial)	Y	X (Axial)	Y
-6.48210	2.34116	-6.48210	2.34116
-6.48759	2.32791	-6.47013	2.34918
-6.48653	2.30950	-6.45180	2.35183
-6.47873	2.28619	-6.42726	2.34891
-6.46391	2.25830	-6.39669	2.34021
-6.44195	2.22597	-6.36008	2.32574
-6.41309	2.18893	-6.31705	2.30598
-6.29837	2.05743	-6.16673	2.23191
-6.06881	1.84013	-5.89719	2.08881
-5.82663	1.65165	-5.64026	1.94846
-5.58259	1.47746	-5.38519	1.82404
-5.33663	1.31730	-5.13205	1.71340
-5.08740	1.17343	-4.88217	1.61171
-4.83591	1.04408	-4.63456	1.51847
-4.58317	0.92682	-4.38819	1.43400
-4.27866	0.80069	-4.09378	1.34319
-3.97293	0.68941	-3.80058	1.26249
-3.66610	0.59230	-3.50849	1.19083
-3.35833	0.50871	-3.21733	1.12737
-3.04985	0.43788	-2.92688	1.07194
-2.74105	0.37917	-2.63676	1.02425
-2.43218	0.33258	-2.34670	0.98319
-2.12344	0.29797	-2.05652	0.94770
-1.81511	0.27447	-1.76592	0.91756
-1.50737	0.26103	-1.47473	0.89269
-1.20033	0.25681	-1.18284	0.87302
-0.89392	0.26100	-0.89033	0.85854
-0.58804	0.27293	-0.59728	0.84962
-0.28271	0.29217	-0.30369	0.84652
0.02205	0.31915	-0.00952	0.84873
0.32598	0.35420	0.28547	0.85578
0.62892	0.39664	0.58146	0.86776
0.93104	0.44568	0.87827	0.88487
1.23245	0.50099	1.17578	0.90731
1.53315	0.56243	1.47401	0.93516
1.83305	0.63035	1.77304	0.96799
2.13206	0.70496	2.07295	1.00552
2.43030	0.78549	2.37364	1.04842
2.72800	0.87086	2.67486	1.09772
3.02565	0.95941	2.97614	1.15510
3.27398	1.03479	3.22691	1.20994
3.44400	1.08772	3.39850	1.25063
3.49006	1.12517	3.45780	1.24339
3.50000	1.19138	3.50000	1.19138

Table V. Vane-Frame (Fan Bypass OGV) Coordinates (Continued).

Vane Type: Nominal
Radius 53.0 cm (20.86 in.)

Convex		Concave	
X (Axial)	Y	X (Axial)	Y
-6.48210	2.34116	-6.48210	2.34116
-6.48159	2.32791	-6.47013	2.34918
-6.48654	2.30949	-6.45181	2.35182
-6.47874	2.28617	-6.42729	2.34888
-6.46394	2.25825	-6.39675	2.34014
-6.44203	2.22588	-6.36020	2.32561
-6.41324	2.18874	-6.31726	2.30572
-6.29896	2.05654	-6.16614	2.23018
-6.07054	1.83608	-5.89545	2.08244
-5.82980	1.64205	-5.63708	1.93498
-5.58753	1.46015	-5.38025	1.80119
-5.34355	1.29036	-5.12513	1.67933
-5.09631	1.13518	-4.87326	1.56502
-4.84677	0.99309	-4.62370	1.45801
-4.59597	0.86190	-4.37539	1.35882
-4.29378	0.71764	-4.07866	1.24915
-3.99047	0.58679	-3.78304	1.14834
-3.68627	0.46852	-3.48832	1.05511
-3.38139	0.36194	-3.19426	0.96836
-3.07616	0.26589	-2.90057	0.88755
-2.77064	0.17937	-2.60697	0.81205
-2.46549	0.10210	-2.31339	0.74054
-2.16009	0.03377	-2.01986	0.67182
-1.85478	-0.02657	-1.72625	0.60556
-1.54964	-0.07997	-1.43246	0.54168
-1.24470	-0.12720	-1.13847	0.48014
-0.93983	-0.16894	-0.84442	0.42105
-0.63494	-0.20568	-0.55038	0.36497
-0.33012	-0.23761	-0.25628	0.31230
-0.02535	-0.26417	0.03788	0.26268
0.27916	-0.28484	0.33230	0.21567
0.58316	-0.30022	0.62722	0.17134
0.88725	-0.31091	0.92205	0.13018
1.19188	-0.31606	1.21636	0.09358
1.49640	-0.31452	1.51076	0.06272
1.80035	-0.30547	1.80573	0.03755
2.10352	-0.28852	2.10149	0.01793
2.40575	-0.26457	2.39819	0.00441
2.70721	-0.23490	2.69565	-0.00204
3.00816	-0.20101	2.99363	0.00047
3.25869	-0.17029	3.24220	0.01049
3.42752	-0.14778	3.40980	0.02082
3.47856	-0.12068	3.46729	0.00351
3.50000	-0.05474	3.50000	-0.05474

Table V. Vane-Frame (Fan Bypass OGV) Coordinates (Continued).

Vane Type: Nominal
Radius 69.8 cm (27.48 in.)

Convex		Concave	
X (Axial)	Y	X (Axial)	Y
-5.58734	1.85159	-5.58734	1.85159
-5.59204	1.83581	-5.57482	1.86239
-5.58888	1.81511	-5.55459	1.86805
-5.57767	1.78979	-5.52679	1.86834
-5.55820	1.76017	-5.49156	1.86305
-5.53036	1.72642	-5.44892	1.85215
-5.49435	1.68825	-5.39858	1.83610
-5.41795	1.61418	-5.30236	1.80216
-5.20924	1.44123	-5.05671	1.70308
-4.99074	1.28915	-4.82084	1.59775
-4.77087	1.14424	-4.58634	1.49967
-4.54950	1.00677	-4.35334	1.40820
-4.32535	0.87963	-4.12313	1.32006
-4.09911	0.76188	-3.89500	1.23567
-3.87166	0.65193	-3.66808	1.15607
-3.59755	0.52960	-3.39605	1.06657
-3.32237	0.41733	-3.12689	0.98287
-3.04629	0.31473	-2.85773	0.90412
-2.76943	0.22135	-2.58935	0.82965
-2.49196	0.13645	-2.32158	0.75933
-2.21403	0.05948	-2.05428	0.69304
-1.93557	-0.00932	-1.78749	0.62999
-1.65657	-0.06966	-1.52125	0.56948
-1.37718	-0.12194	-1.25540	0.51166
-1.09766	-0.16670	-0.98968	0.45683
-0.81820	-0.20440	-0.72390	0.40517
-0.53899	-0.23556	-0.45787	0.35687
-0.26019	-0.26089	-0.19163	0.31220
0.01826	-0.28092	0.07536	0.27132
0.29653	-0.29522	0.34234	0.23382
0.57458	-0.30326	0.60952	0.19928
0.85232	-0.30529	0.87702	0.16812
1.12961	-0.30174	1.14497	0.14089
1.40634	-0.29289	1.41349	0.11784
1.68247	-0.27890	1.68260	0.09902
1.95797	-0.25944	1.95234	0.08396
2.23282	-0.23433	2.22272	0.07231
2.50703	-0.20433	2.49376	0.06473
2.78065	-0.17056	2.76537	0.06289
3.05389	-0.13473	3.03738	0.06670
3.28146	-0.10422	3.26418	0.07653
3.42738	-0.08386	3.40977	0.08530
3.47882	-0.05633	3.46701	0.06804
3.50000	0.00941	3.50000	0.00941

Table V. Vane-Frame (Fan Bypass OGV) Coordinates (Concluded).

Vane Type: Nominal
Radius 90.1 cm (35.5 in.)

Convex		Concave	
X (Axial)	Y	X (Axial)	Y
-4.49480	1.64519	-4.49480	1.64519
-4.50141	1.62777	-4.48003	1.65611
-4.49961	1.60423	-4.45704	1.66064
-4.48913	1.57488	-4.42603	1.65851
-4.46969	1.54012	-4.38719	1.64946
-4.44110	1.50020	-4.34056	1.63344
-4.40352	1.45490	-4.28574	1.61098
-4.36001	1.40641	-4.22984	1.58666
-4.17865	1.23208	-4.01147	1.48459
-3.98730	1.08043	-3.80307	1.38218
-3.79412	0.93890	-3.59652	1.28894
-3.59889	0.80698	-3.39201	1.20396
-3.40085	0.68675	-3.19030	1.12394
-3.20110	0.57686	-2.99032	1.04840
-3.00038	0.47518	-2.79129	0.97765
-2.75845	0.36283	-2.55353	0.89860
-2.51543	0.26034	-2.31686	0.82511
-2.27133	0.16734	-2.08128	0.75648
-2.02632	0.08355	-1.84660	0.69213
-1.78065	0.00833	-1.61258	0.63195
-1.53453	-0.05889	-1.37902	0.57580
-1.28796	-0.11786	-1.14590	0.52287
-1.04094	-0.16853	-0.91323	0.47240
-0.79365	-0.21075	-0.68083	0.42448
-0.54628	-0.24579	-0.44852	0.37939
-0.29894	-0.27378	-0.21617	0.33741
-0.05184	-0.29518	0.01642	0.29879
0.19482	-0.31062	0.24945	0.26389
0.44100	-0.32059	0.48296	0.23289
0.68673	-0.32477	0.71691	0.20524
0.93213	-0.32276	0.95120	0.18045
1.17721	-0.31479	1.18580	0.15901
1.42173	-0.30120	1.42098	0.14150
1.66547	-0.28239	1.65692	0.12812
1.90844	-0.25865	1.89364	0.11880
2.15059	-0.22976	2.13118	0.11295
2.39198	-0.19569	2.36947	0.11011
2.63272	-0.15716	2.60842	0.11097
2.87313	-0.11508	2.84770	0.11677
3.11356	-0.07029	3.08696	0.13000
3.31347	-0.03164	3.28679	0.14794
3.43200	-0.00838	3.40618	0.16054
3.48205	0.02185	3.46416	0.14584
3.50000	0.08854	3.50000	0.08854

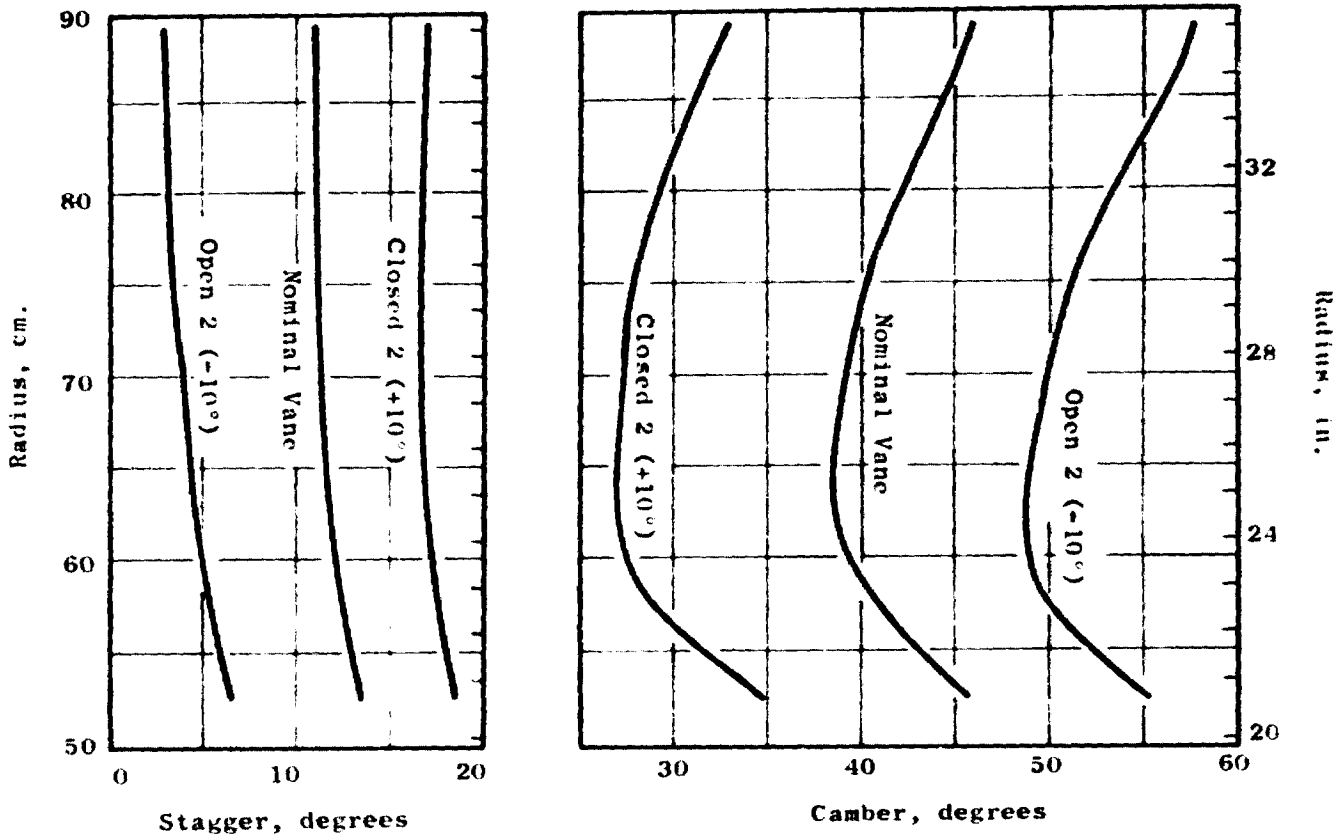

Figure 25. Vane-Frame (Fan Bypass OGV) Geometric Parameters.

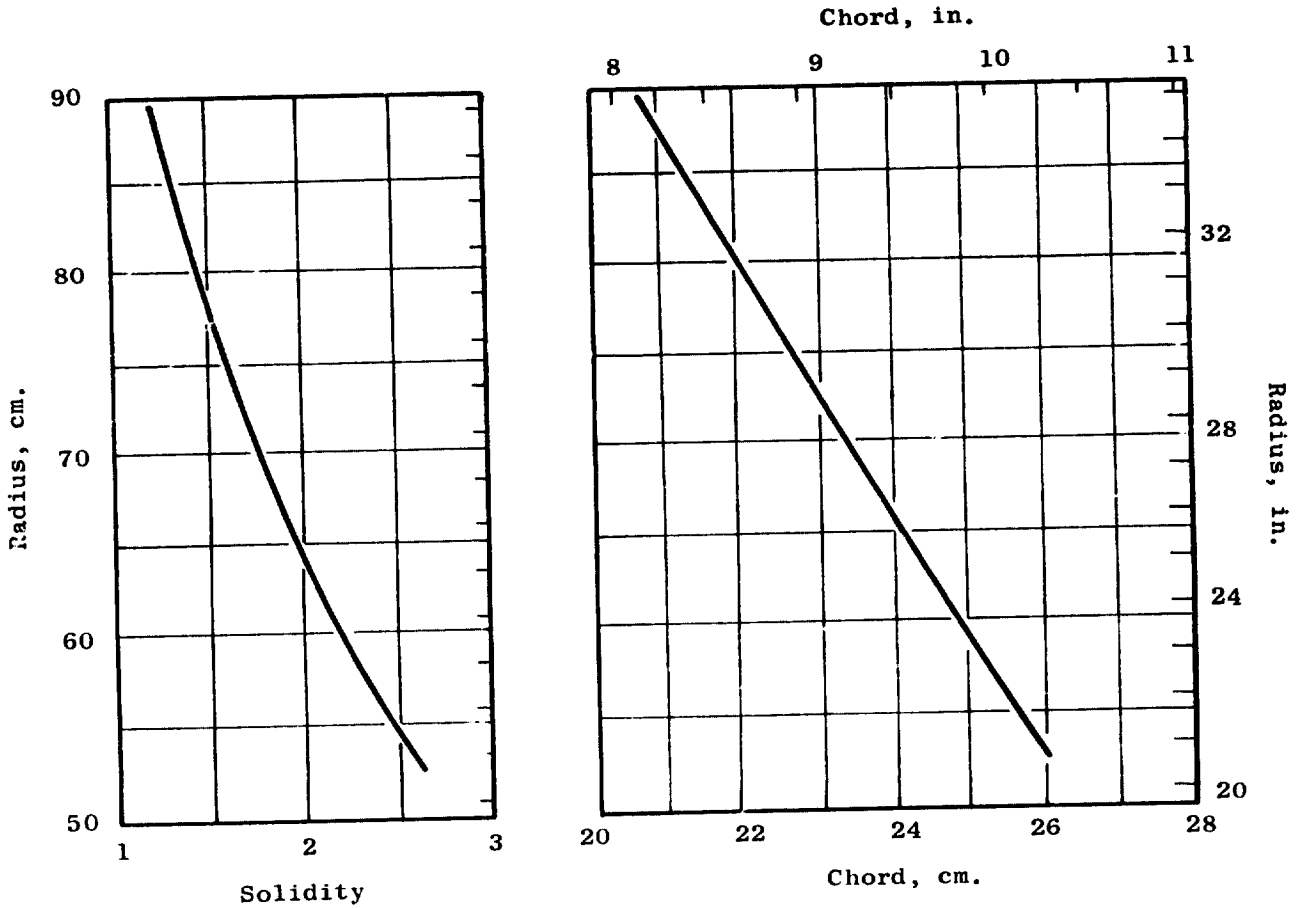

Figure 26. Vane-Frame (Fan Bypass OGV) Geometric Parameters.

SECTION 2.0

FAN MECHANICAL DESIGN

2.1 UTW FAN ROTOR SUMMARY

The UTW fan rotor has 18 composite blades mounted on a disk in a manner permitting changes in the pitch of the blades. This rotor is shown in Figure 27. The blades will be fabricated from a hybrid combination of Kevlar 49, graphite, boron, and S-Glass fibers in order to provide the desired combination of bird impact resistance and blade stiffness. The blades incorporate a metal foil leading edge to provide additional FOD and erosion protection. The solidity of the blades is slightly less than unity along the entire blade span to allow the blades to clear during actuation to reverse pitch through flat pitch. There are no mechanical restrictions on being able to reverse pitch the blades through either flat pitch or stall.

In a concept similar to that used on the CF6-50 fan, balance weights are accessible in the fan spinner, and field balance of the fan is possible without removing the spinner. Ease of maintenance has also been considered in the design of the other rotor components.

After removal of the spinner, the blades can be individually removed and replaced without disassembly of the blade trunnion. Access holes in the flange of the aft rotating flowpath permit removal of the fan rotor, blade actuator, and the reduction gear as a complete subassembly.

The centrifugal force of each blade and trunnion is carried by a single-row ball thrust bearing. This bearing has a full complement of balls to reduce the per-ball loadings. The race has a much higher conformance than is standard for thrust bearings because of its highly loaded, intermittently actuated environment. The bearing is grease lubricated, with a cup shield completely covering the upper race and most of the lower race, thus preventing the grease from leaking out under high radial "g" loads. This concept was successfully demonstrated on General Electric's reverse pitch fan. Grease tests have been completed that identified a grease for the QCSEE bearing which will not permit separation of the oil from the thickening base or extreme pressure additives after extended running in a centrifugal field higher than those planned for the UTW fan rotor. Fail-safe lubrication is accomplished by a tungsten disulfide coating applied to the balls and races. With this coating and under the loading planned, this bearing is capable of operating 9000 engine hours after loss of lubricant with only a slight increase in coefficient of friction and negligible wear.

Secondary and vibratory loads from the trunnion are resisted by dry thrust and journal bearings located in the OD of the fan disk.

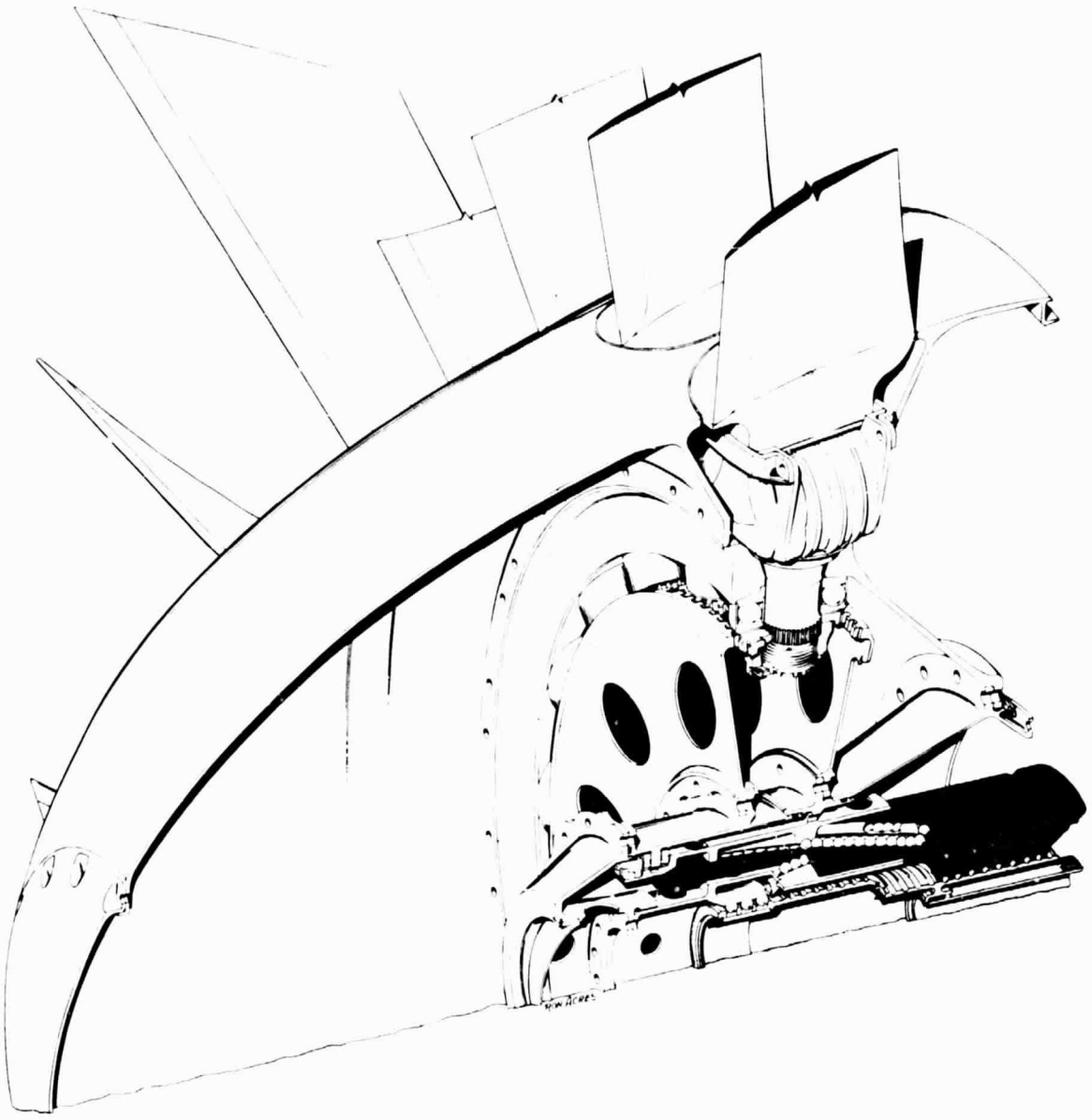

Figure 27. UTW Variable Pitch Fan.

2.2 COMPOSITE FAN BLADES

2.2.1 Design Considerations

Aerodynamic design of the UTW fan blade is presented in Section 2.0. Mechanical design considerations for the UTW fan blade were primarily a result of the requirement for variable-pitch operation through both the stall and flat pitch direction. The need for a composite blade was established early in the preliminary design phase for the following reasons.

- A practical metallic blade meeting aeromechanical requirements would require solidities of greater than 1.0 in the root which would restrict the variable-pitch operation of the blade to reverse pitch in only one direction.

- Even with a higher root solidity the metallic blade design and resulting disk and actuation system were extremely heavy and would have resulted in low reliability, high bearing loads, and high actuation loads.

Preliminary design of the composite blade was based primarily on the aeromechanical and bird impact requirements. Consideration was given to several hybrid materials and layup configurations which would provide the required blade stiffness and still maintain the capability to absorb the impact of a 1.8 kg (4 lb) bird without root failure. To reinforce the impact capability of the hybrid blade several dovetail designs were evaluated aimed at providing more root flexibility during impact.

2.2.2 Mechanical Design Requirements

The design requirements for the UTW composite fan blade were established to provide realistic long-life operation of a flight engine based on the typical mission shown in Table VI. These preliminary design requirements are listed as follows.

- Design Mechanical Speeds
  - 100% mechanical design - 3244 rpm
  - 100% SLS hot day takeoff - 3143 rpm
  - Maximum steady-state speed - 3326 rpm
  - Maximum design overspeed - 3614 rpm
  - Maximum burst speed - 141% of max. steady-state speed (4700 rpm)
- Design Life and Cycles
  - 36,000 hours
  - 48,000 cycles
  - 1000 ground checkout cycles, full power

Table VI. Flight Duty Cycle.						
Segment	Altitude		Mach No.	% Power	Time (Min)	% Time
	km	ft				
Start	0	0	0	-	0.5	1.11
Idle-Taxi	0	0	0	4-20	3.1	6.89
Takeoff	0	0	0-12	100	1.22	2.71
Climb	0-7.02	0-23K	0.3-0.5	Max. Cont	10.0	22.22
Cruise	6.41-7.63	21-25K	0.65-0.74	Max. Cr	14.0	31.11
Descent	7.02-0.3048	23-1K	0.7-0.4	F.I.	10.0	22.22
Approach	0.3048-0	1K-0	0.12	65	3.0	6.67
Reverse Thrust	0	0	0.12-0	Max. Rev	0.08	0.18
Idle-Taxi	0	0	0	4-20	3.1	6.89
					45.0	100

- Mechanical Requirements
  - Blades must operate through flat pitch and stall pitch without aeromechanical problems.
  - Blades shall be individually replaceable without major teardown.
  - Blade untwist will be factored into airfoil configuration.
  - Stresses shall be within Goodman Diagram with sufficient vibratory margin.
  - First flex frequency shall cross 2/rev in low speed range and have 15% margin over 1/rev at 115% speed.
  - Blade leading edge protection will be kept within aero airfoil limits.

Of these requirements, the first two are of prime importance. Successful operation of the experimental engine hinges to a great degree on having a rugged blade which can withstand reverse pitch operation and other inlet disturbances including crosswind testing.

2.2.3 Aerodynamic Blade Parameters

A summary of the aero blade parameters is presented in Table VII. The low root solidity of 0.98 is required for reverse pitch operation. Except for the large tip chord (high blade flare) the blade length, thickness, and twist dimensions are similar to previous composite blades which have undergone extensive development and proof testing.

2.2.4 Blade Configuration

The blade molded configuration consists of a solid composite airfoil and a straight bell-shaped composite dovetail. The dovetail is undercut at the leading edge and trailing edge to reduce local stresses and to permit better transitioning of the cambered airfoil section into the straight dovetail.

The airfoil definition is described by 15 radially spaced airfoil cross sections which are stacked on a common axis. The dovetail axial centerline is offset from the stacking axis by 0.254 cm (0.1 in.) to provide a smooth airfoil-to-dovetail transition. The molded blade drawing, as shown in Figure 28 provides a reduced leading edge thickness to allow a final coating of wire mesh/nickel plate for leading edge protection. The blade leading edge protection is shown on the finished blade drawing (see Figure 29).

2.2.5 Blade Layup/Material Selection

The material selection and ply arrangement for the UTW hybrid composite blade is based on previous development efforts conducted by General Electric and sponsored by NASA under contract NAS 3-16777. This work led to the

FOLDOUT FRAME 1

ORIGINAL PAGE IS
OF POOR QUALITY

AIRFOIL DATA TABLE

SHR MSP SECT E-E, H-H, K-K, M-M, P-P

SECTION	AIRFOIL CG LOCATION ALONG STACKING AXIS	TWIST ANGLE	THICKNESS			CHORD OVERALL	RADIUS LEADING & TRAILING EDGES	CAMBER ANGLE		DROP		UNDIMENSIONED DRAWING NO 40N3179-368
			LEADING	MAX	TRAILING			LEADING EDGE	TRAILING EDGE	LEADING EDGE	TRAILING EDGE	
		1 0° 90°	@ ±.005	@ ±.005	@ ±.005	±.040						
A-A	1.900			.730	.118		.050					SHEET 1
B-B	2.040			.738	.118							
C-C	2.580			.740	.118							
D-D	3.410			.748	.118							
E-E	4.535			.748	.121							
F-F	6.415			.730	.123							
G-G	8.889			.710	.125							SHEET 2
H-H	10.186			.686	.127							
J-J	12.048			.569	.118							
K-K	13.948			.488	.119							SHEET 3
L-L	15.796			.384	.119							
M-M	17.672			.363	.117							
N-N	19.549			.339	.113							SHEET 4
P-P	21.250			.988	.110							
R-R	21.429			.384	.110							
PA-PA	0.0	——	——	——	——	——	——	——	——	——	——	SHEET 5
T-T	+1.500	——	——	——	——	——	——	——	——	——	——	

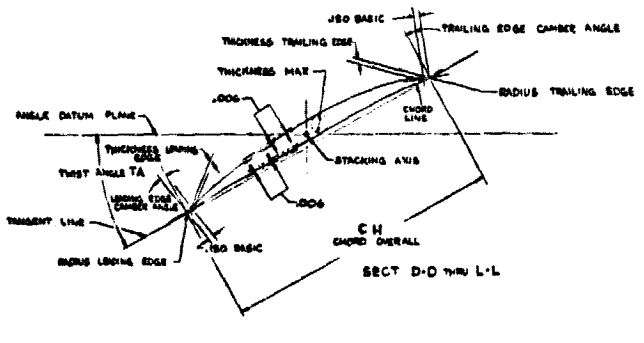

SECT D-D THRU L-L

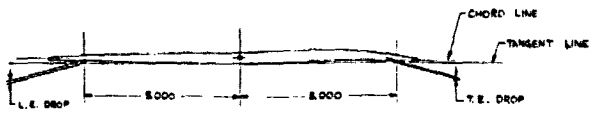

SECT M-M, N-N, P-P & R-R
DEFINITION OF TANGENT LINE OTHERWISE
SAME AS SECTS D-D THRU L-L

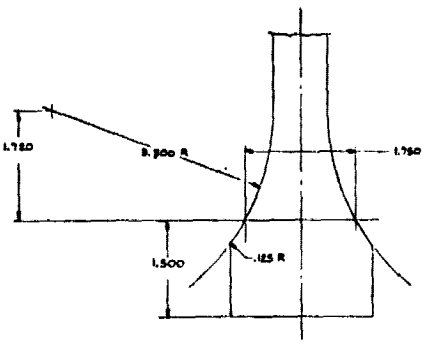

TYPICAL SECT THRU DOVETAIL
BASIC DIMENSIONS

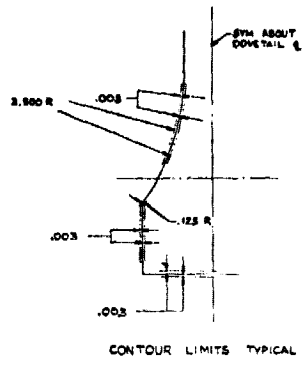

CONTOUR LIMITS TYPICAL

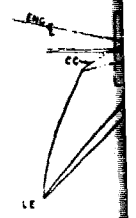

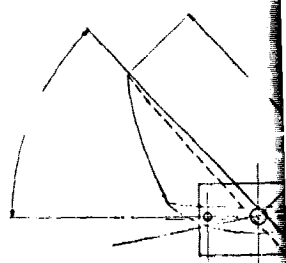

Figure 28. UTW Composite Fan Blade (Stage 1

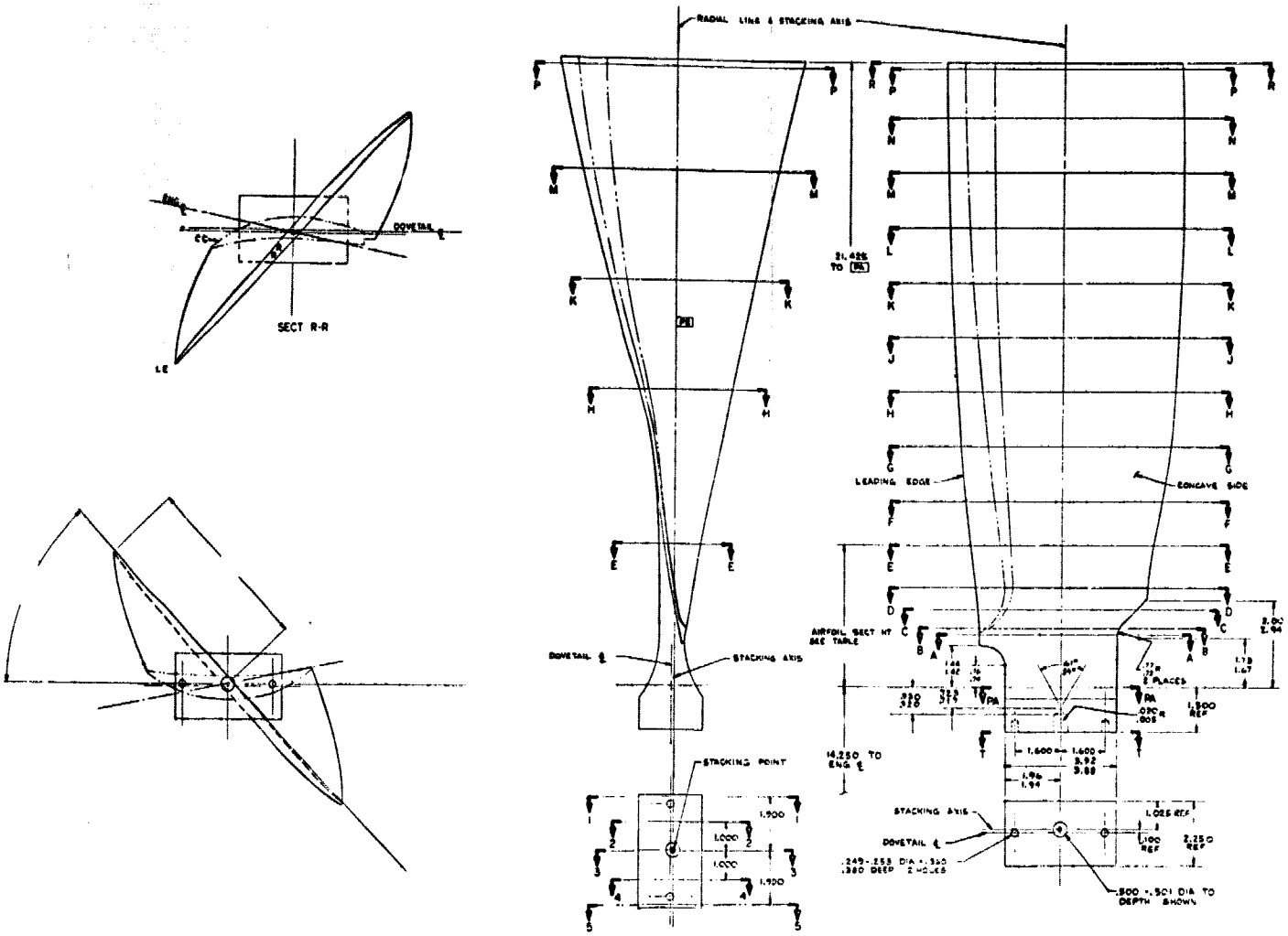

Fan Blade (Stage 1 Molded Blade Drawing).

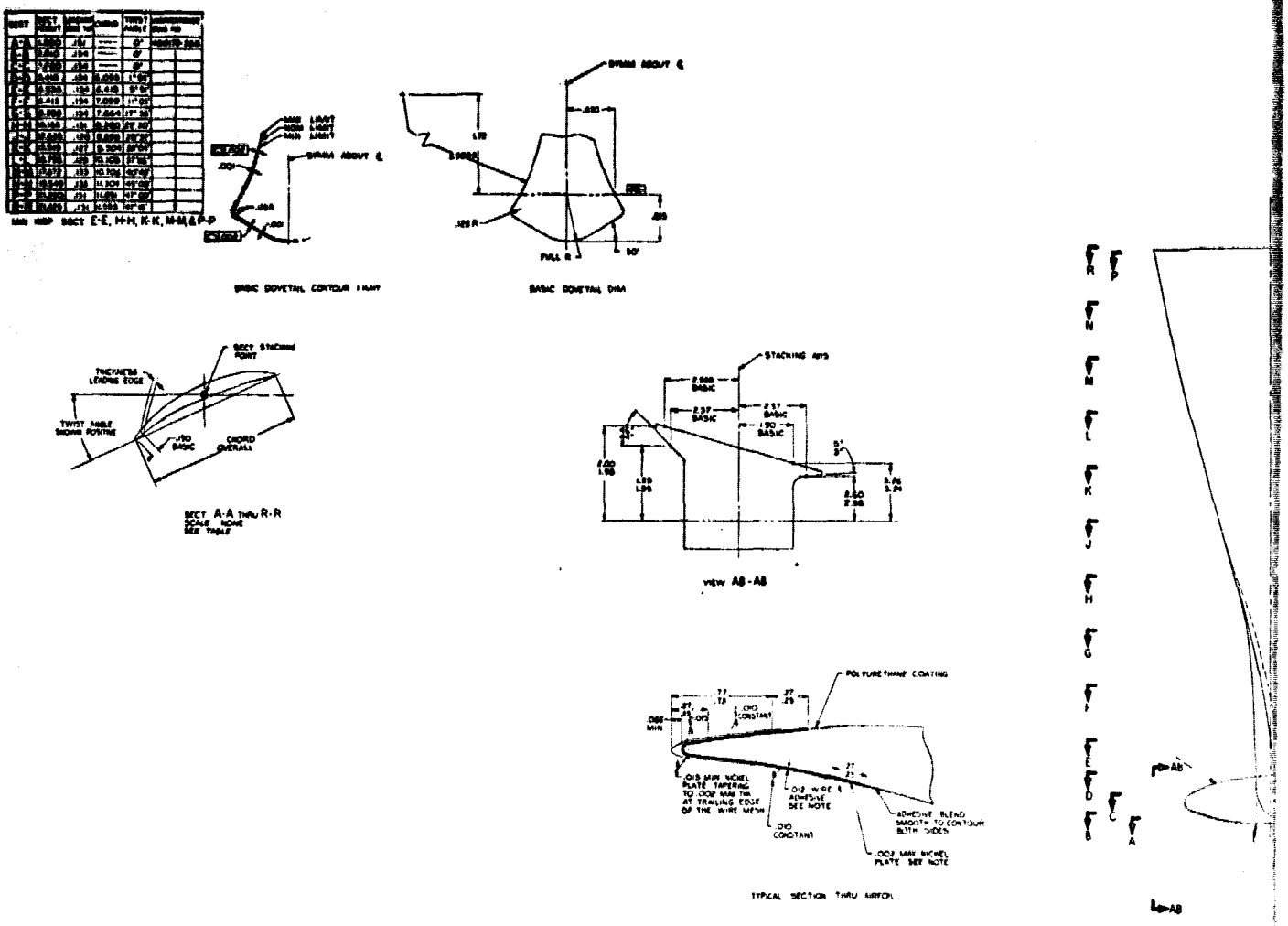

Figure 29. UTW Composite Fan Bl

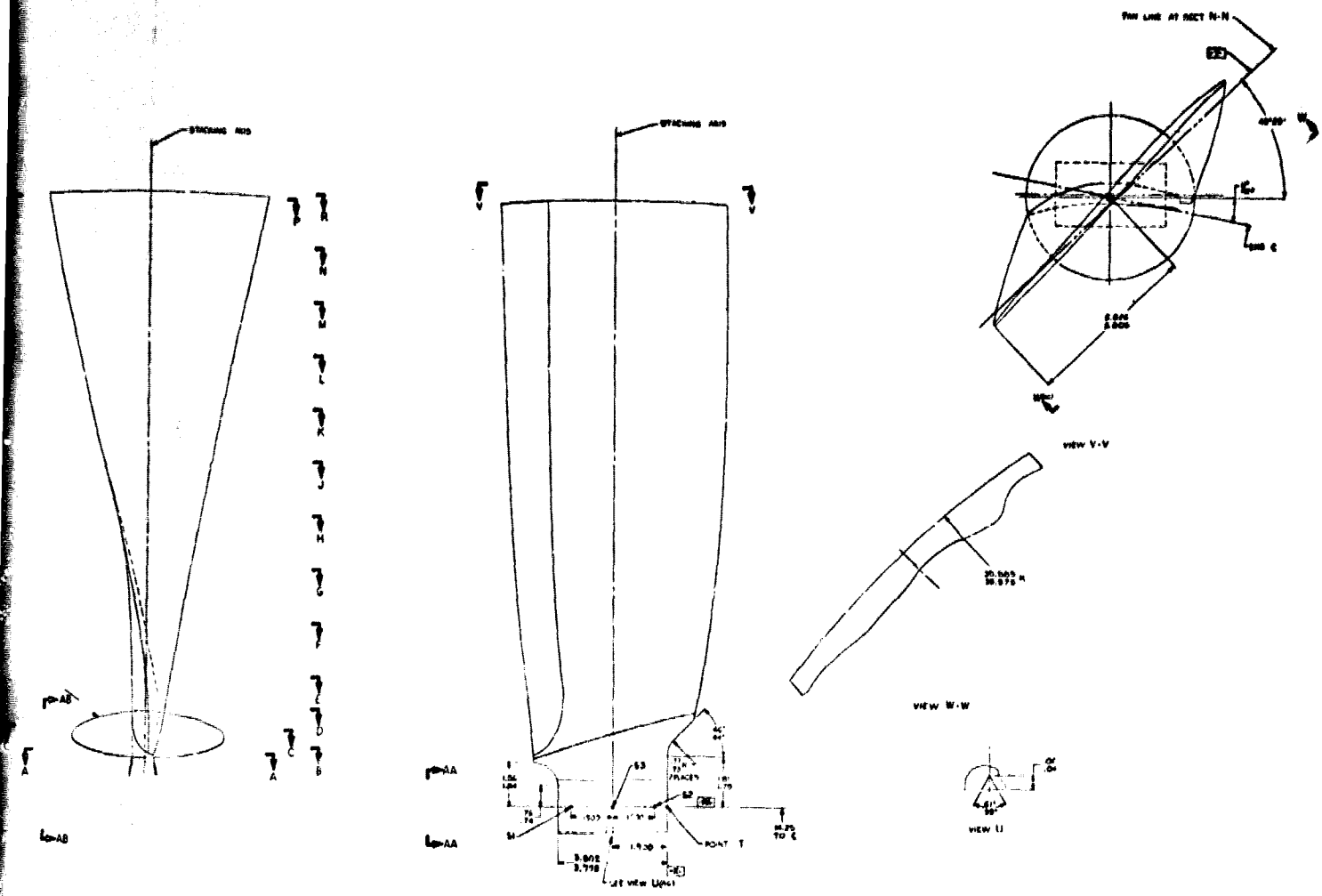

psite Fan Blade (Finished Blade Drawing).

Table VII. QCSEE UTW Composite Blade Preliminary Design Summary.

Aero Definition

Tip Speed	298 m/sec (978 ft/sec)
Tip Diameter	180 cm (71 in.)
Radius Ratio	0.452
Number of Blades	18
Bypass Pressure Ratio	1.27 Takeoff
Aspect Ratio	2.11
Tip Chord	30.3 cm (11.91 in.)
Root Chord	14.8 cm (5.82 in.)
T_M Root	1.92 cm (0.76 in.)
T_M Tip	0.91 cm (0.36 in.)
Root Camber	66.2°
Total Twist	45°
Solidity	
Tip	0.95
Root	0.98
Angle Change from Forward to Reverse	
Through Flat Pitch	85°
Through Stall	90°

selection of a combination of fibers in a single blade to provide the proper frequency response and bird impact characteristics to satisfy short-haul engine conditions. Figure 30 shows the general arrangement of the plies in the QCSEE UTW composite blade. The flex root surface plies in the lower region of the blade contain S-glass fibers. These plies being near the surface and having relatively low bending stiffness and high tensile strength provide higher strain-to-failure characteristics thereby allowing the blade to absorb large bird impact loading without the classic root failure that usually accompanies brittle composite materials. Torsional stiffening plies in the airfoil region of the blade are oriented at $\pm 45°$ to provide the shear modulus required for a high first torsion frequency. These plies will contain fibers of graphite and/or boron depending on the measured frequency characteristics and experimental FOD resistance to be obtained in the several preliminary blades. Plies of Kevlar 49 will be interspersed throughout the rest of the blade with the majority of them being in the longitudinal direction of the blade. Several of the Kevlar plies in the tip region of the blade will be oriented at 90° to the longitudinal axis to provide chordwise strength and stiffness to the blade for local impact improvement.

The resin system being used in this program is a product of the 3M Company and is designated as PR288. This is a resin system that has proven satisfactory for the needs of advanced composite blading. Some of its unique characteristics in the prepreg form are:

- Has consistent processing characteristics
- Can be prepregged with many different fibers including hybrids
- Uniform prepreg thickness and resin content.

Typical properties of the PR288/AU prepreg are shown in Table VIII. Material properties for several fiber composite prepregs are shown in Table IX. The basic ply layup arrangement and fiber orientation for the QCSEE preliminary blade is shown in Figure 31. The graphite/Kevlar system is preferred from the standpoint of bird impact and cost; however, it may be necessary to use some boron plies to achieve the desired first torsion frequency.

2.2.6 Blade Vibration Analysis

Blade "instability" or "limit cycle vibration" can be a problem on fans. It is characterized by a high amplitude vibration in a single mode (normally the first flexural or torsional mode) at a nonintegral per-rev frequency. It is not one of the classical airfoil flutter cases and is apparently confined to cascades. Because of the nonlinearity in the aerodynamics involved, it has resisted practical solutions by solely theoretical means. Accordingly, General Electric has adopted a semiempirical "reduced velocity" approach for limit cycle avoidance. Reduced velocity, V_R, gives a measure of a blade's stability against self excited vibration. This parameter is defined as

$$V_R = \frac{W}{bf_t}$$

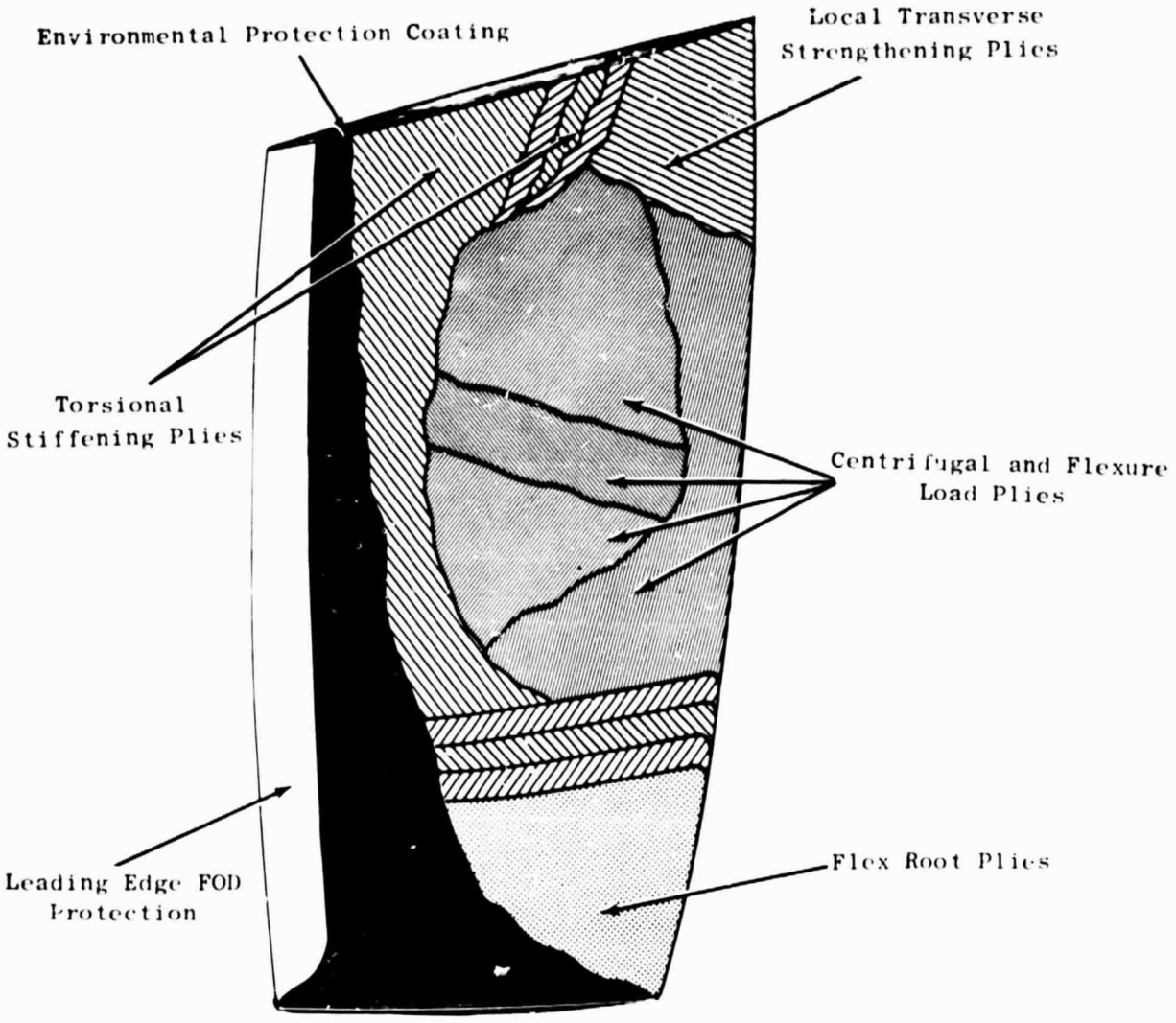

Figure 30. UTW Composite Fan Blade.

Table VIII. PR288/AU Prepreg Properties.

Property	PR288/AU
Supplier	3M
Process	Film - Cont. Tape
Cure Schedule	2.5 hrs at 129° C (265° F)
Postcure Schedule	4 hrs at 135° C (275° F)
Flex. Strength/Elast. Mod./Short Beam Shear	
Room Temp	193/11.9/8.0 kN/cm^2(280/17.2/11.6 ksi)
121° C(250° F)	138 /11.6/5.2 kN/cm^2(200/16.8/7.5 ksi)
Charpy Impact	21.2 J (15.0 ft-lb)
Fiber Volume, %	59.8
Sp. Gr., g/cc	1.58
Void Content, %	0.0
Cost per kg (lb)	$232 ($105)

Table IX. Composite Material Properties.

					Hybrids		
	PR288 AU	PR288 Boron	PR288 S-Glass	PR288 Kevlar 49	PR288 AU 20% S-Glass	PR288 AU 20% Kevlar 49	Kevlar 29 Epoxy
Fiber Volume, Percent	60	55	60	60	60	60	60
Elastic Modulus, $10^6 N/cm^2$ (10^6 psi) (0° Orientation)	11.9 (17.2)	20.0 (29.0)	5.9 (8.5)	7.6 (11.0)	10.6 (15.4)	11.0 (15.9)	3.7 (5.4)
Elastic Modulus, $10^6 N/cm^2$ (10^6 psi) (90° Orientation)	1.1 (1.6)	1.2 (1.8)	0.8 (1.1)	0.6 (0.8)	1.0 (1.5	1.0 (1.4)	0.6 (0.8)
Elastic Modulus, $10^6 N/cm^2$ (10^6 psi) (0/22/0/-22 Orientation)	9.5 (13.8)	11.7 (17.0)	4.7 (6.8)	5.9 (8.6)	8.6 (12.5)	8.9 (12.9)	3.2 (4.6)
Shear Modulus, $10^6 N/cm^2$ (10^6 psi) (0/22/0/-22)	1.1 (1.6)	1.9 (2.7)	0.6 (0.9)	0.6 (0.93)	1.0 (1.46)	1.0 (1.47)	0.6 (0.85)
Poisson's Ratio (0/22/0/-22)	0.65	0.97	0.39	0.90	0.60	0.70	---
Density, G/cm^3 (lb/in^3)	1.5 (0.056)	1.9 (0.070)	2.0 (0.072)	1.4 (0.050)	1.6 (0.059)	1.5 (0.055)	1.4 (0.050)
Tensile Strength, kN/cm^2 (ksi) (0°)	138 (200)	138 (200)	138+ (200+)	138 (200)	130 (189)	121 (176)	138 (200)
Tensile Strength, kN/cm^2 (ksi) (0/22/0/-22	95 (138)	95 (138)	95+ (138+)	95 (138)	89 (129)	83 (121)	95 (138)
Flex Strength, kN/cm^2 (ksi) (0°)	193 (280)	---	---	62 (90)	---	---	62 (90)
Flex Strength, kN/cm^2 (ksi) (0/22/0/-22)	168 (244)	---	172 (250)	59 (85)	---	---	59 (85)
Shear Strength, kN/cm^2 (ksi) (0°)	8.0 (11.6)	7.6 (11.0)	8.1 (11.8)	3.4-7(5-10)	7.2 (10.5)	6.8 (9.8)	3.4-7(5-10)
Charpy Impact, m-N (ft-lb) ($\pm$10°)	20 (15)	10 (7.5)	47 (35)	23 (17)	26 (19.4)	19 (14.0)	---

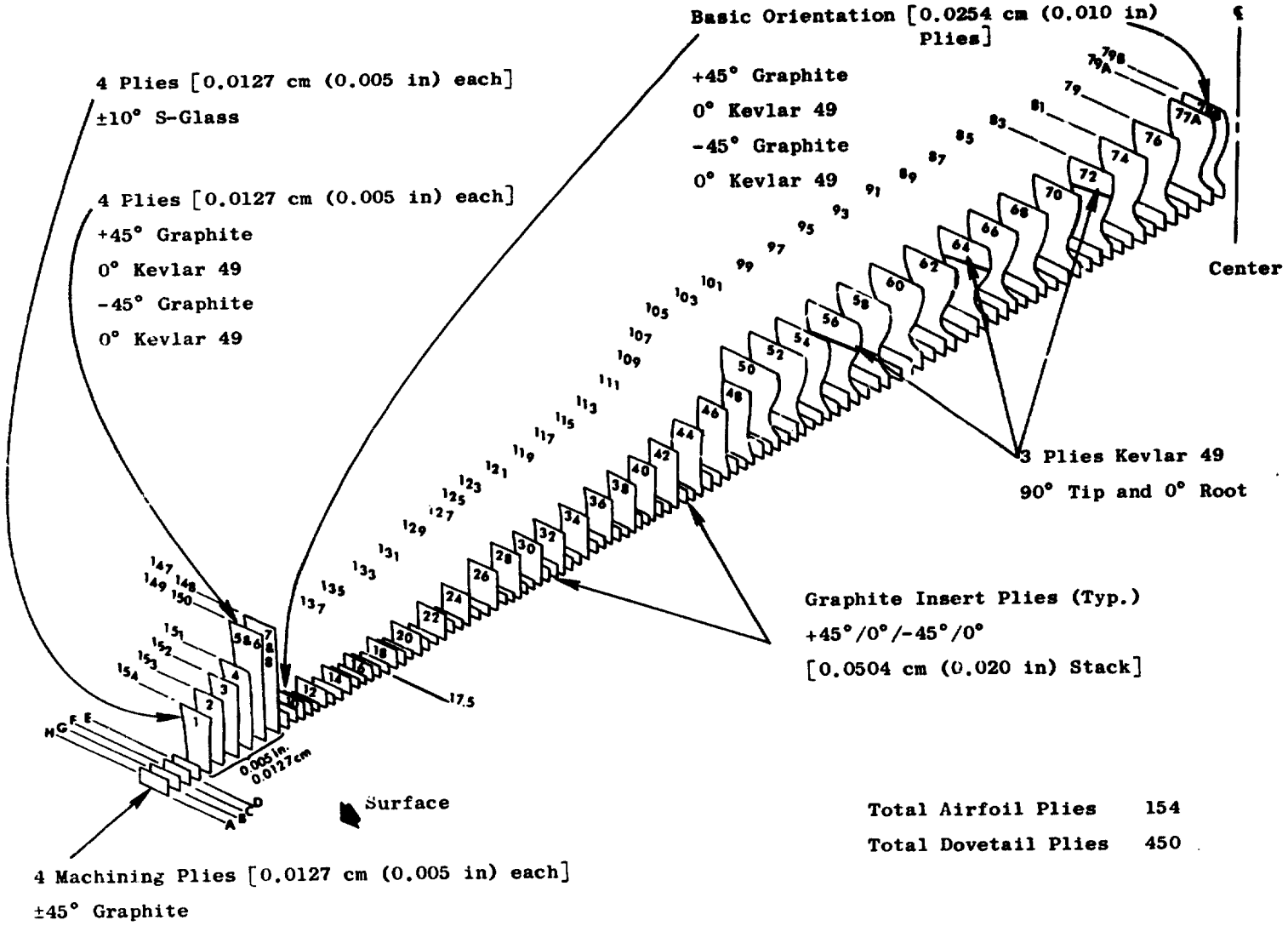

Total Airfoil Plies 154

Total Dovetail Plies 450

Figure 31. UTW Composite Fan Blade Fiber Orientation (Design Number 1).

where:

b = 1/2 chord at 5/6 span-m

W = average air velocity relative to the blade over the outer third of the span-m/sec

f_t = first torsional frequency at design rpm-rad/sec.

The basic criterion used for setting the design of the UTW composite blade was the requirement of having a reduced velocity parameter in the range of 1.3 to 1.4. This allowable range is based on previous testing of a variety of fan configurations in combination with the specific aerodynamic design of the UTW blade. Figure 32 shows the results of a 20- and 18-blade analysis for several fiber material candidates. The 18-blade design using the 50% graphite/50% Kevlar material was selected as providing the desired aeromechanical requirements and bird impact characteristics. The operating and stall characteristics of this blade are presented in Figure 33 in terms of reduced velocity versus incidence angle. This shows an acceptable blade design as compared with the anticipated QCSEE blade stability limit.

The Campbell diagram for the UTW blade is shown in Figure 34. The expected range of first flexural frequencies in the 2/rev crossover is shown to be between 54 and 67 speed. The margin over 1/rev at 100% speed is approximately 60%.

2.2.7 Airfoil Stress Analysis

A preliminary stress analysis of the UTW composite fan blade was performed using a homogeneous twisted blade computer program. This program is limited to accepting only effective longitudinal properties of the composite blade. It has been used successfully for preliminary design work in the past and offers an approximate state of stress for steady-state operating conditions. Correlation with detailed finite element analysis shows it to be a reaonable preliminary design tool. The resultant radial stresses for the steady-state operating condition including gas loads are shown in Figure 35. This shows the maximum stresses to be in the root leading edge and trailing edge areas having values of 1.38 and 1.66 kN/cm^2 (20 and 24 ksi), respectively. The average centrifugal stress at the root is 0.551 kN/cm^2 (8 ksi). The estimated room temperature stress range (Goodman diagram) for the radial direction of the proposed hybrid composite blade is shown in Figure 36. For the UTW composite blades, the anticipated maximum vibratory stress is 1.38 kN/cm^2 (20 ksi) single amplitude. For the steady-state condition shown, that of a hot day takeoff and maximum cruise, the combination of steady-state mean stress and expected maximum vibratory stress results in an acceptable blade life.

In addition to the airfoil stresses, the displacement and twist characteristics of the blade are presented in Figure 37. The maximum untwist is 2° without leading edge protection.

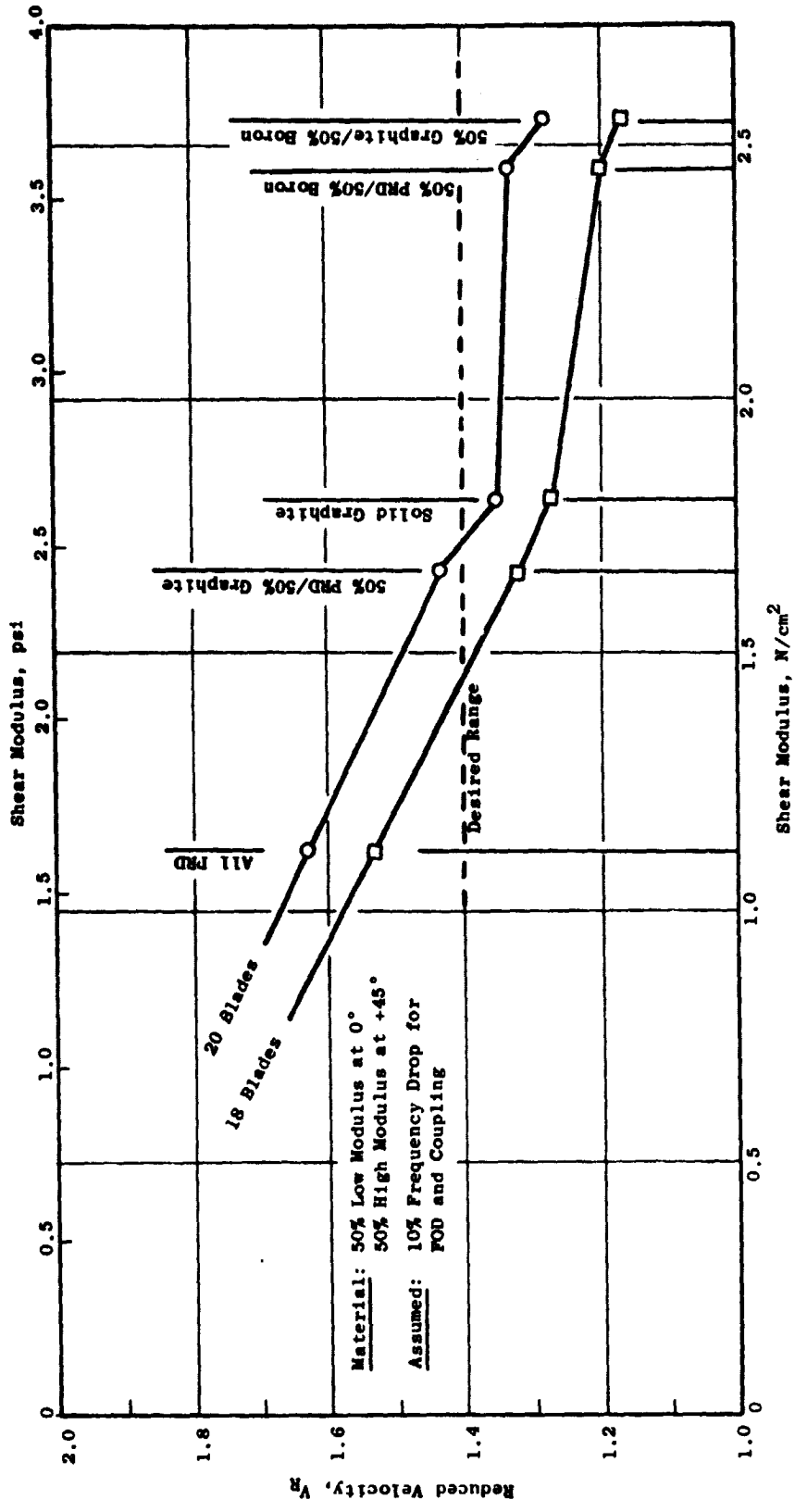

Figure 32. UTW Composite Fan Blade Vibration Characteristics.

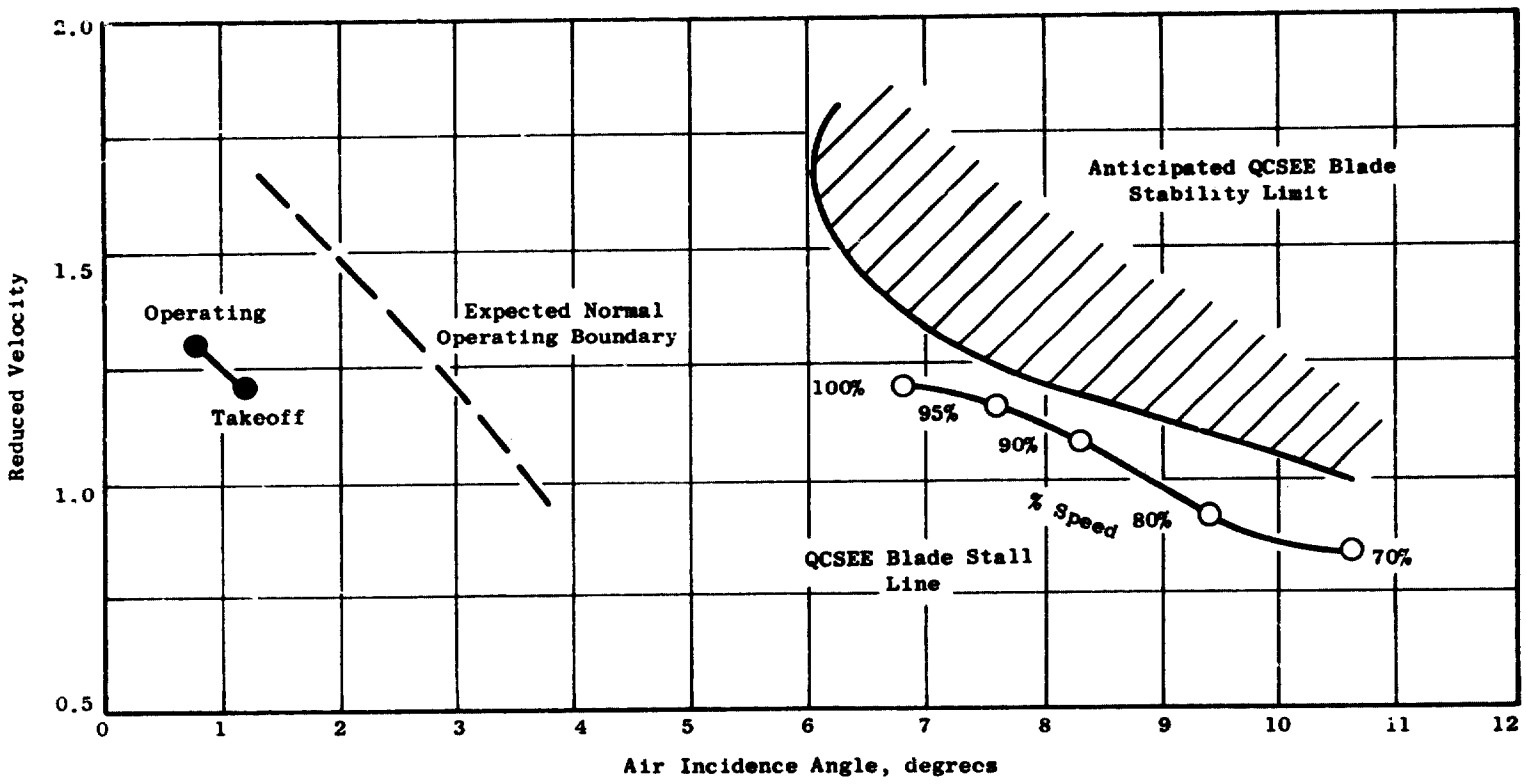

Figure 33. Limit Cycle Boundaries for UTW Composite Fan Blade.

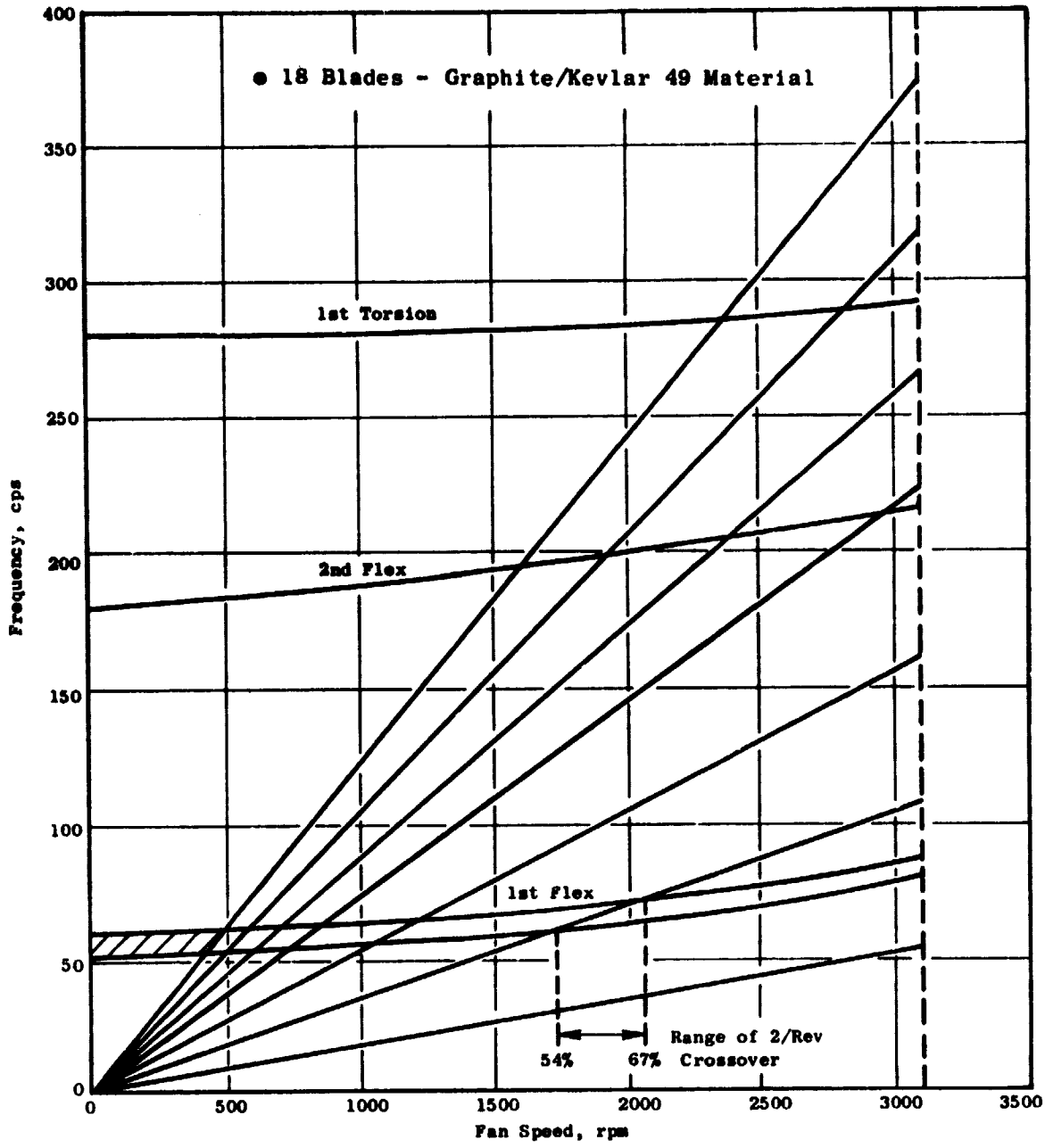

Figure 34. UTW Composite Fan Blade Campbell Diagram.

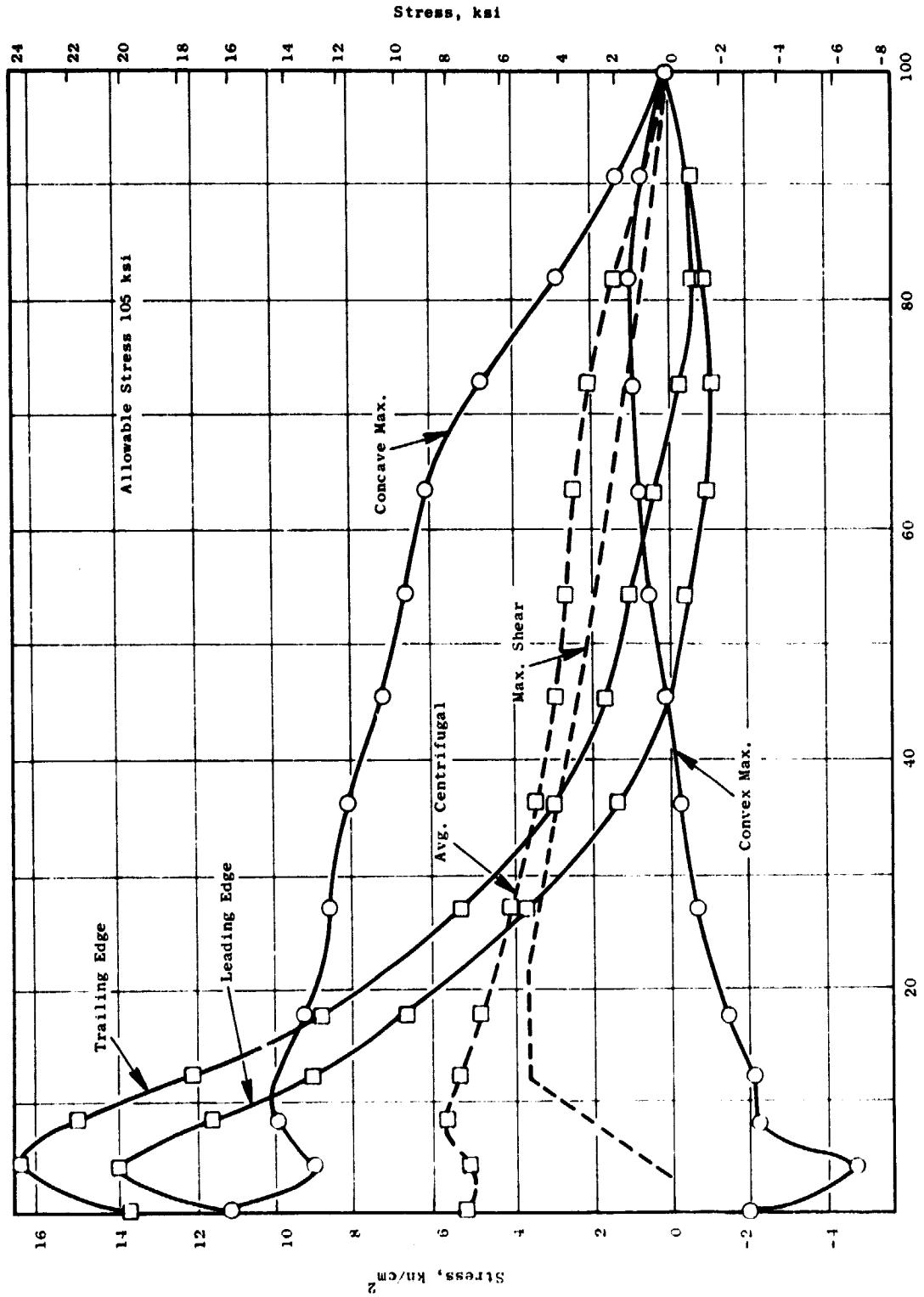

Figure 35. UTW Composite Fan Blade Resultant Radial Stress - 3157 rpm.

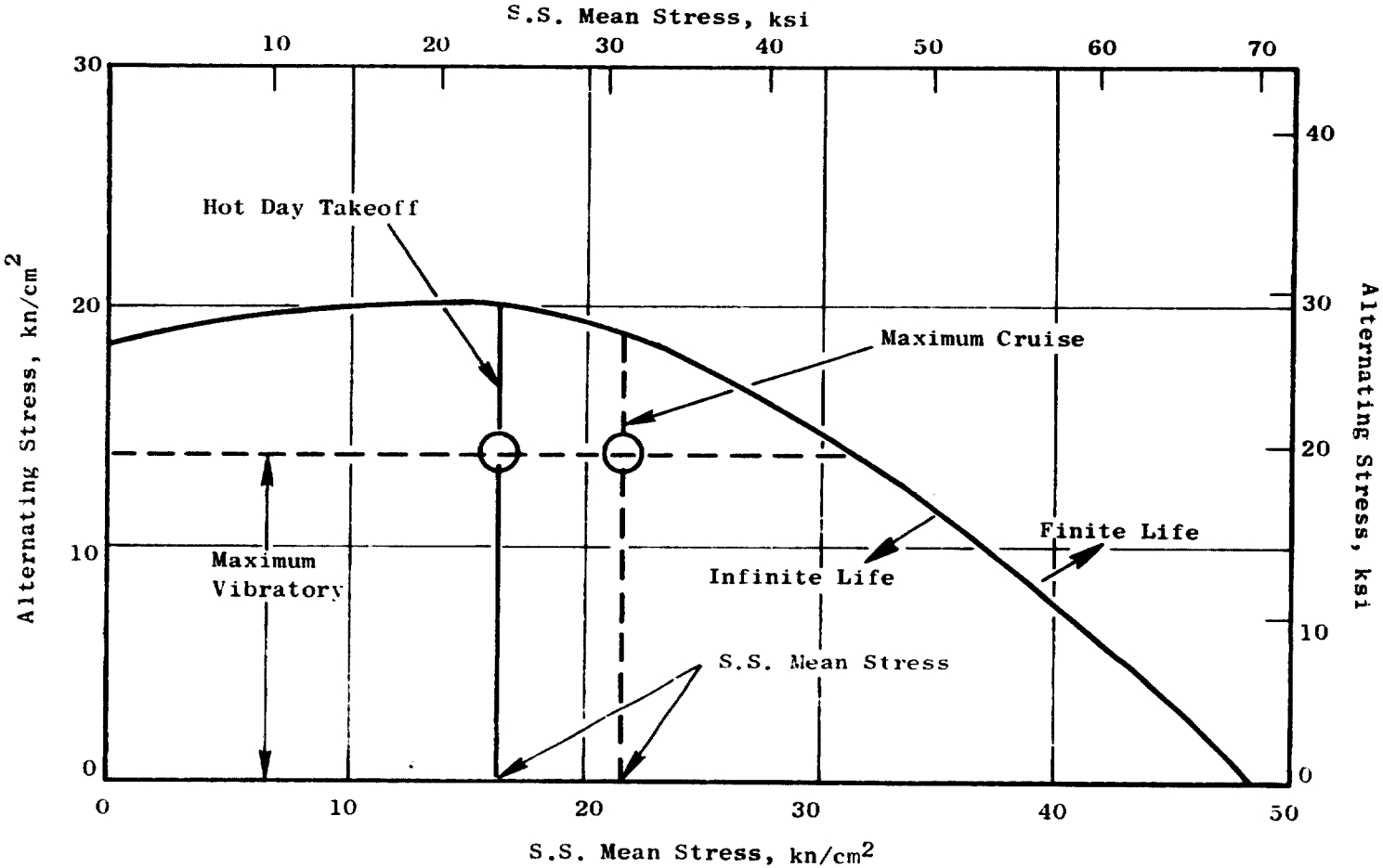

Figure 36. Blade Life (Goodman Diagram) for UTW Composite Fan Blade at Ambient Temperature.

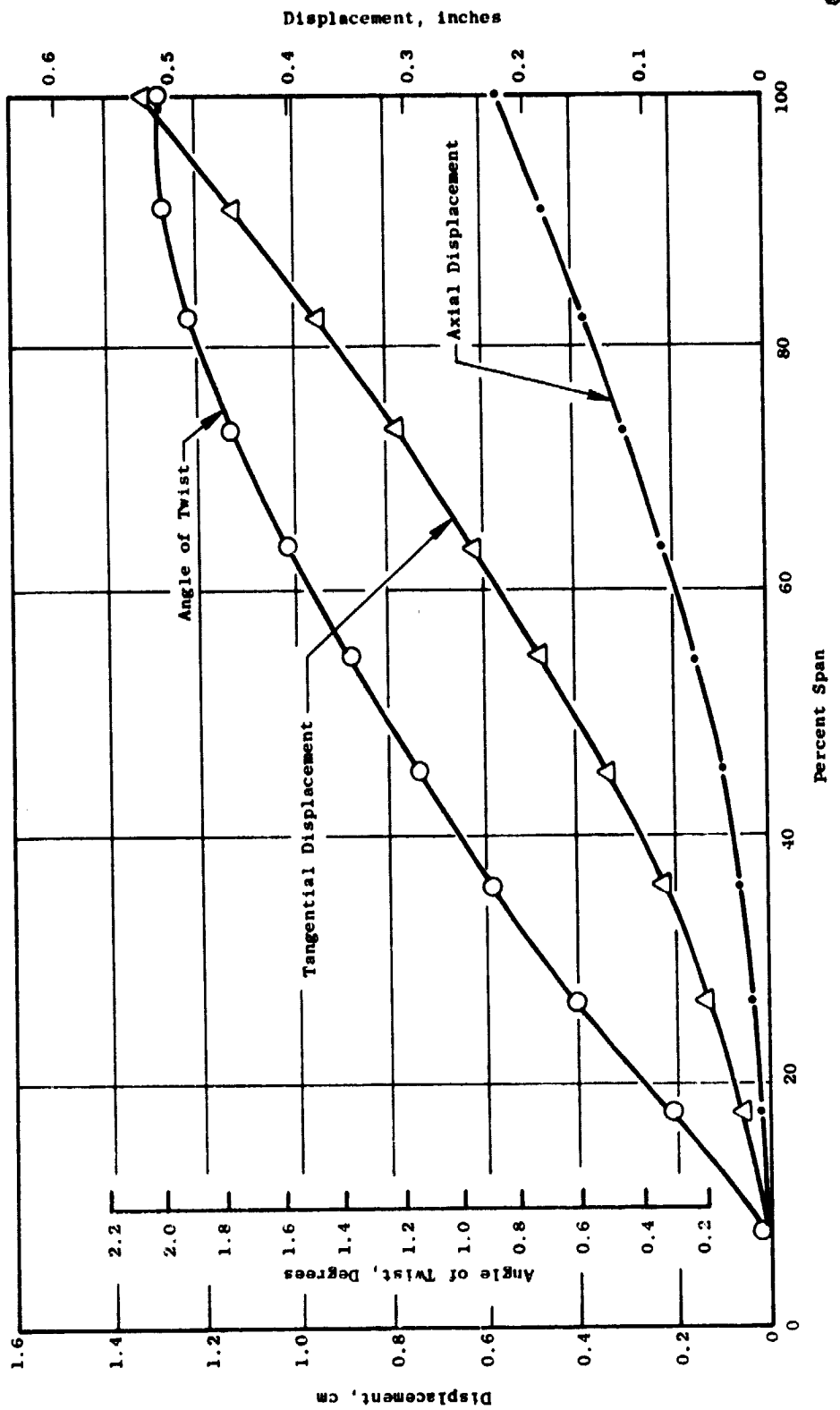

Figure 37. UTW Composite Fan Blade, Displacements and Twist - 3157 rpm.

The steady-state airfoil loads resulting from the twisted blade analysis are:

- 100% rpm centrifugal force: 118,000 N (26,500 lb)
- maximum centrifugal force: 155,000 N (35,000 lb)
- M_{tang} = 50,900 cm-N (4500 in-lb), M_{axial} = 61,000 cm-N (5400 in-lb) M_{twist} = 7900 cm-N (700 in-lb)

More detailed stress analysis using three-dimensional finite element techniques are planned during the final design phase.

2.2.8 Dovetail Design

The dovetail design for the UTW composite blade consists of a straight bell-shaped dovetail with an 8.9 cm (3.5 in.) radius. The bell-shaped dovetail design reflects many years of development efforts to achieve an efficient dovetail configuration having both high static pull strength and good fatigue strength. The dovetail crush normal and shear stresses were calculated and are shown on their respective stress range diagrams in Figures 38 and 39. The combination of mean stress and vibratory stress indicate there is considerable margin for infinite life under steady-state operating conditions.

2.3 FAN DISK

The fan disk is a single-piece-machined 6Al-4V titanium ring forging designed for a commercial life in excess of 36,000 hours. This disk is shown in Figure 40. Eighteen holes pierce the disk ring to provide for the blade support trunnion while retaining the blades. The excess disk material between the holes is removed where possible to reduce the dead disk weight and lower the stress concentration around these holes. An integral cone on the aft side of the disk connects the disk to the main bearing shaft through a bolted flange. The disk cone is contoured to alleviate LCF problems generated by the forward and aft cycles of thrust generated during engine operation. Flanges on the outside of the disk rim provide attachment planes for the spinner and aft flowpath adapter.

The inside of the disk rim is a turned modified spherical blade bearing seating surface for the blade retention bearing (Figure 41). This results in a low-cost, lightweight disk design with a uniformly stressed rim. The blade thrust bearings have mating spherical seats and are mounted as shown in Figure 41. The bearing seating surface is not machined perfectly spherical but is designed to become spherical under operating loads. An antifretting coating will be applied between the disk and the bearing, although at the pressure loadings expected beneath the bearing, fretting is not expected to be a problem.

The UTW fan disk design data are shown in Table X.

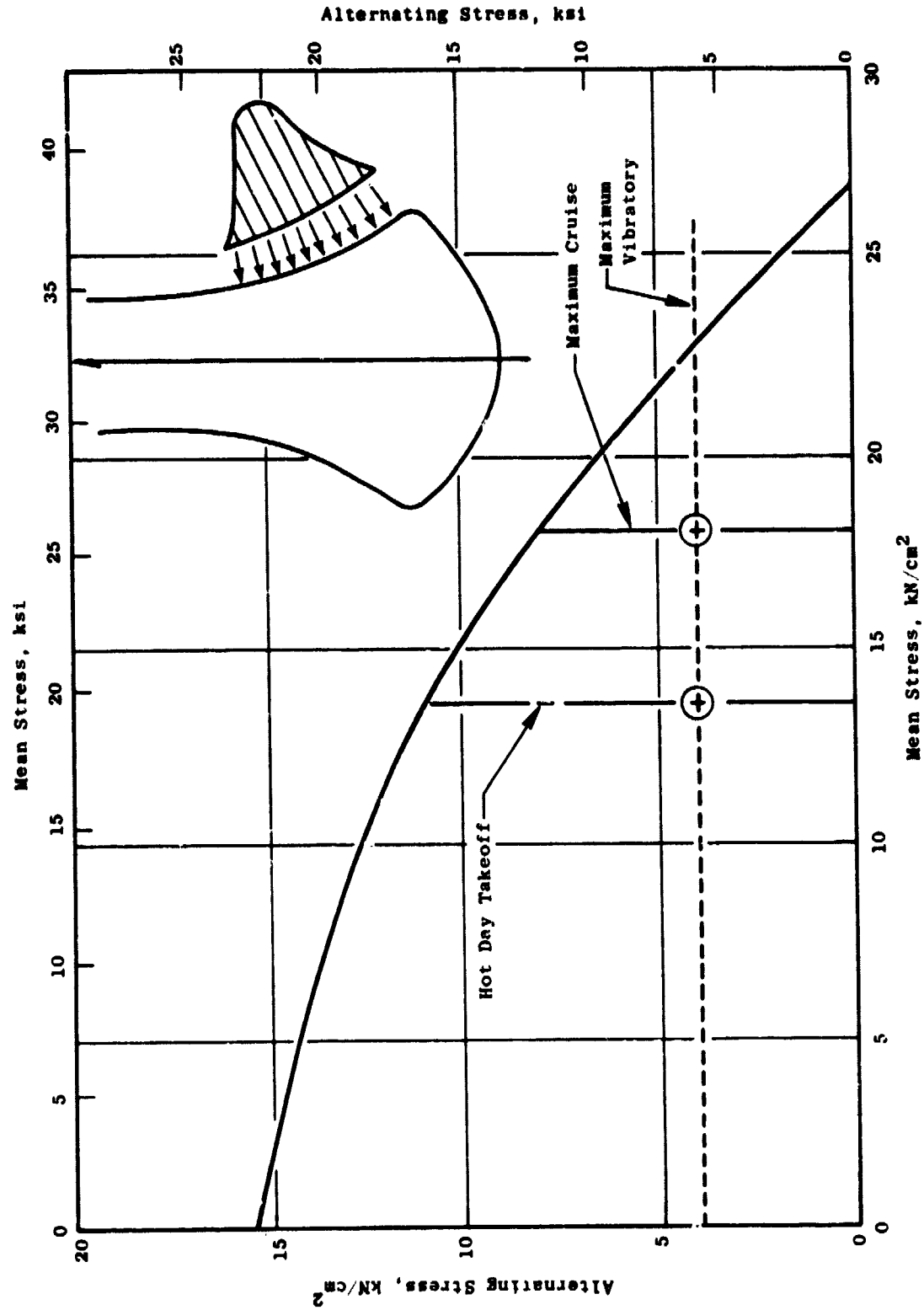

Figure 38. Allowable Stress Range Diagram - Dovetail Normal Stress for UTW Composite Fan Blade.

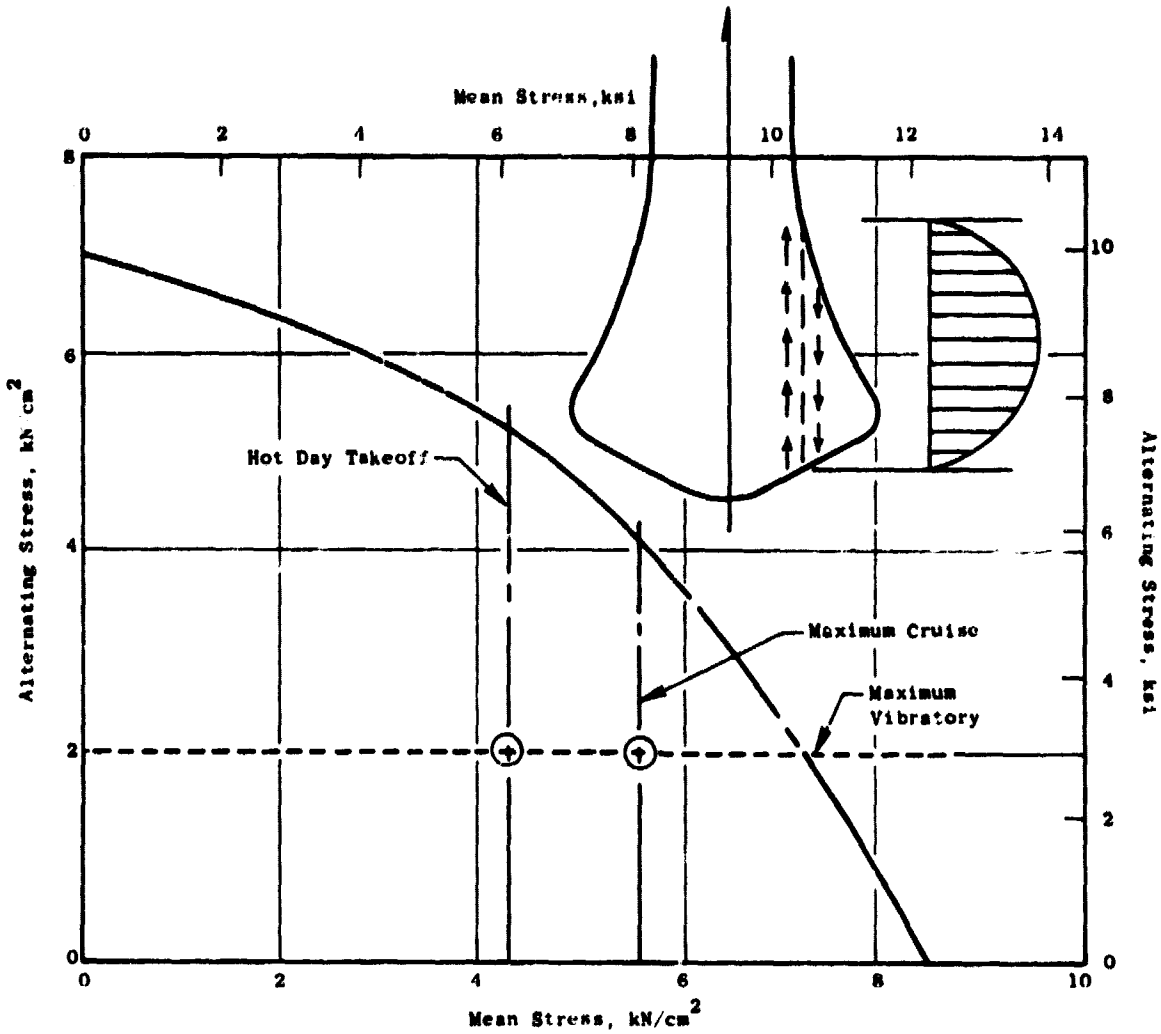

Figure 39. Allowable Stress Range Diagram - Dovetail Shear (PRD/Glass/Graphite Epoxy) for UTW Composite Fan Blade.

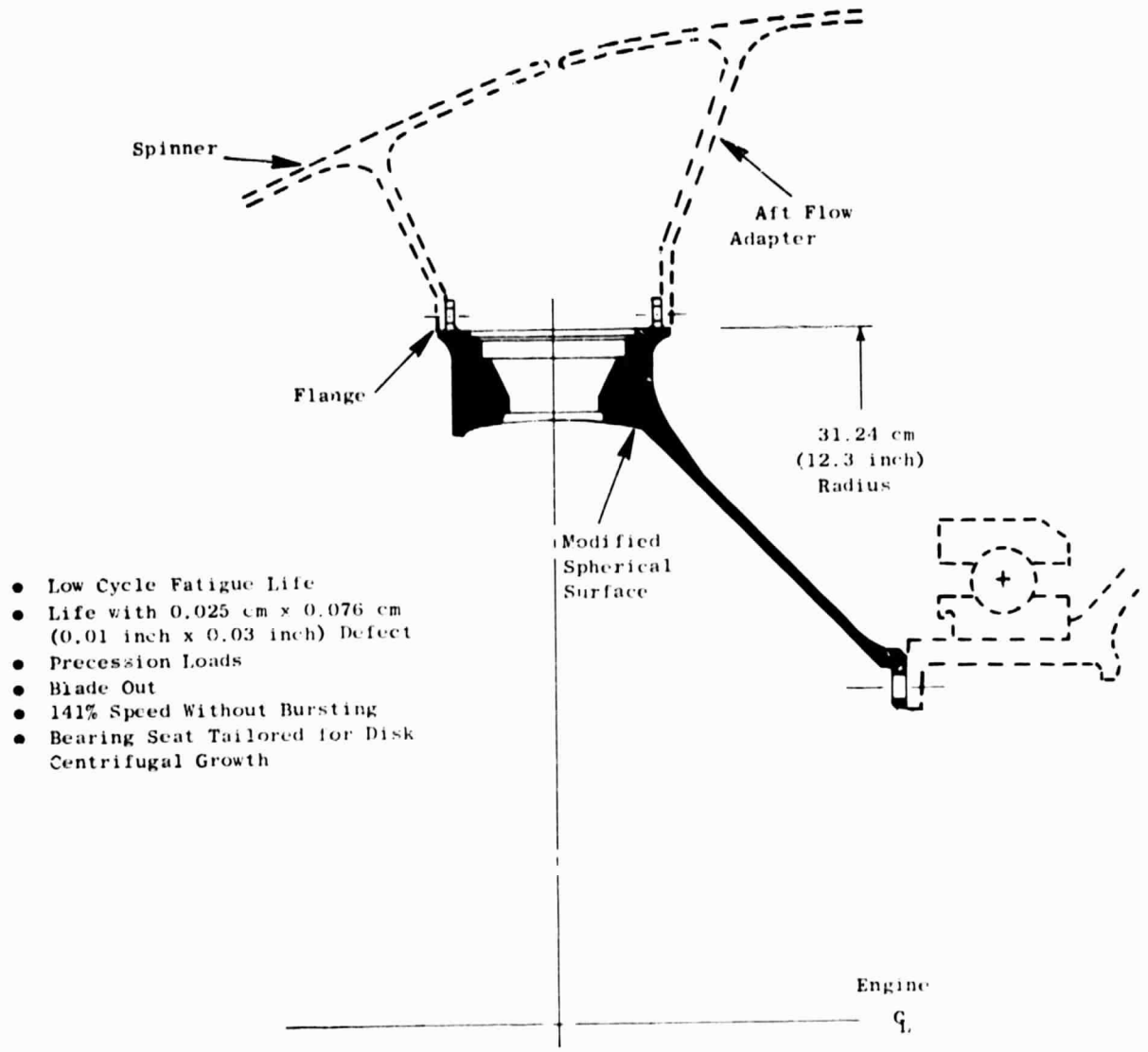

Figure 40. UTW Fan Rotor Disk.

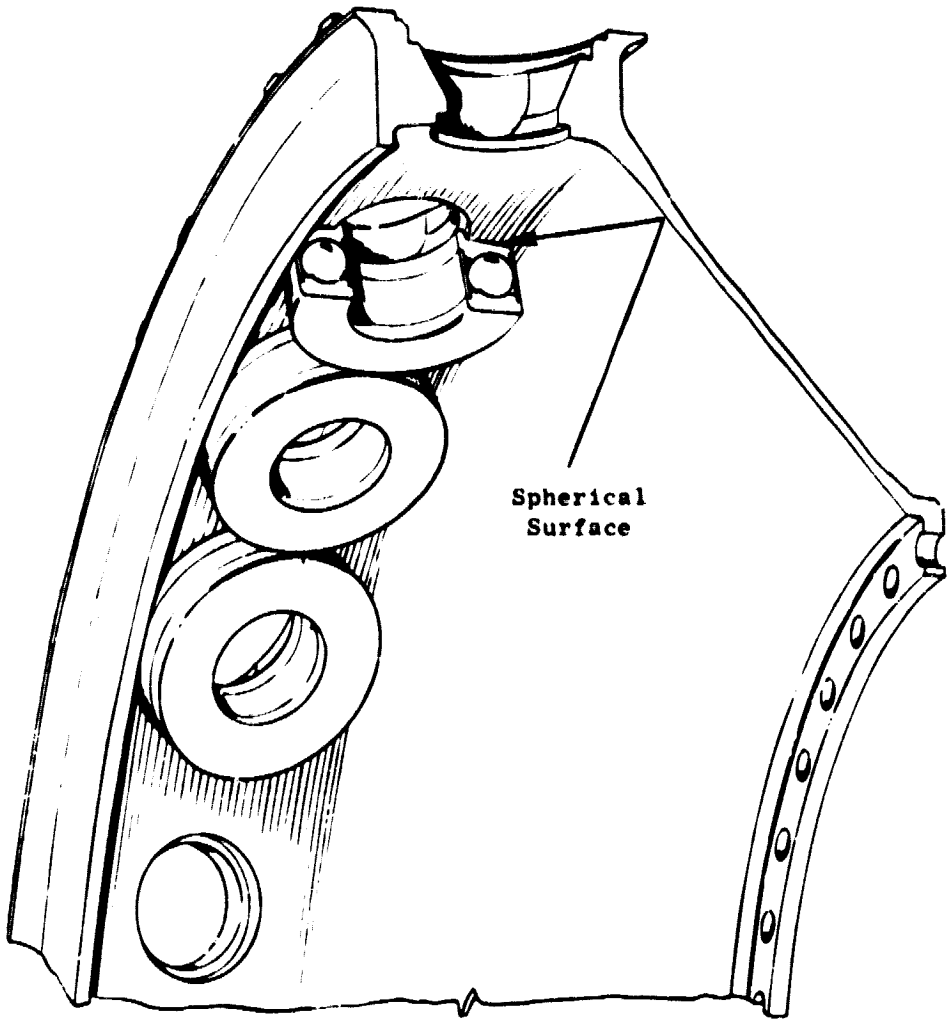

Figure 41. UTW Bearing and Disk Seat.

C-2

Table X. UTW Fan Disk Design Data.

Total Blade and Blade Attachment Load at 100% Mechanical Design Speed (3,244 rpm)	270,000 N/blade (60,777 lb/blade)
Total Live Rim Load at 100% Speed	5,043,691 N (1,133,867 lb)
Average Disk Rim Stress at Max. Duty Cycle Speed (3,326 rpm)	38.7×10^7 N/m^2 (56,085 psi)
Max. Disk Stress at Peak Location at Max. Duty Cycle Speed	42.1×10^7 N/m^2 (61,078 psi)
Overspeed Capability	4,865 rpm
LCF Life with 3σ Material Properties	> 48,000 Cycles
LCF Life with 0.025 x 0.076 cm (0.01 in. x 0.03 in.) Initial Defect	> 16,000 Cycles

2.4 BLADE SUPPORT BEARING

The blade support bearing has a full complement of balls to reduce the per-ball loading. Bearing race conformance is a relatively high 51% to extend the bearing fatigue life in its highly loaded environment. All surfaces on this bearing will be coated with a tungsten disulfide film. Tests on previous General Electric variable-pitch fan bearings have shown this coating provides enough lubrication to enable the bearing to safely operate for 9000 flight hours in the event of a loss-of-grease situation.

The QCSEE support bearing is shown in Figure 42. Shields attached to the outer race create a centrifugal "cup" which prevents the grease from leaking out in the high centrifugal field when the engine is running. Grease will not leak from the clearance gaps at the bottom of the shields when the engine is not operating due to the high viscosity of the grease, provided oil separation from the grease soaping agent does not occur. General Electric has conducted centrifuge tests on various greases and has identified one which has little tendency to separate even under prolonged periods of higher "g" loads than planned for the QCSEE bearing. The bearing test rig is shown in Figure 43.

Design criteria peculiar to variable-pitch blade support bearings had to be developed and applied to the design of this bearing. The unique design criteria used in designing the QCSEE UTW bearing are as follows:

1. The blade support bearing <u>system</u> B10 life should be 9000 flight hours. This requires an <u>individual</u> bearing B10 life of over 18 times the system B10 life. The need for this stringent requirement is based on the statistical problem of a multibearing system in a multiengine aircraft.

2. Blade bearings will not be dependent upon the grease lubricant to obtain 9000 hours between overhauls. This restriction ensures that failure will not occur due to loss of bearing grease. In addition to normal bearing design criteria, the following requirements must also be met, or by definition, failure is said to occur:

   a. An apparent coefficient of friction at the pitch diameter less than 0.01. This allows the blade actuator to be designed to a maximum capacity with assurance that it will not be overloaded because of worn bearings.

   b. Bearing wear less than the bearing preload [approximately 0.00508 cm (0.002 inch) total wear]. This definition provides a simple method for condition monitoring without rotor disassembly.

3. Ball or race fracture must not occur under the maximum possible bird impact loads. The actuation system of an 18-bladed fan is sufficiently powerful to cause secondary damage upon seizure of any one of the individual bearings. Ball fracture, a potential cause of such seizure, must be eliminated as a potential problem.

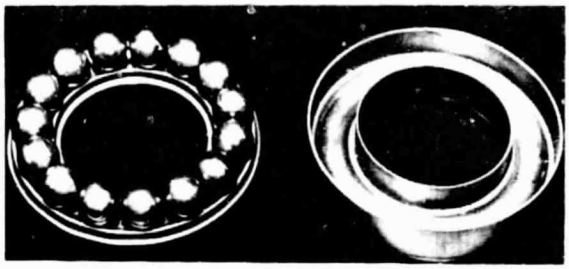

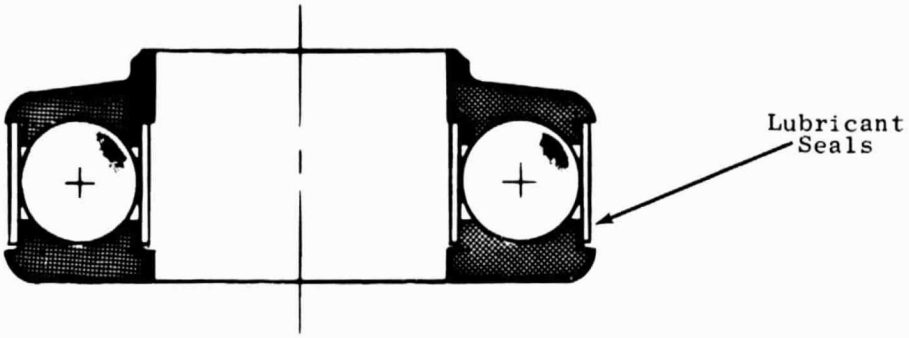

- Single Row Ball Thrust Bearing
- Full Complement of Balls (12)
- High Conformance (51%)
- Separable Races
- Lubricant Seals

Figure 42. UTW Fan Blade Thrust Bearing.

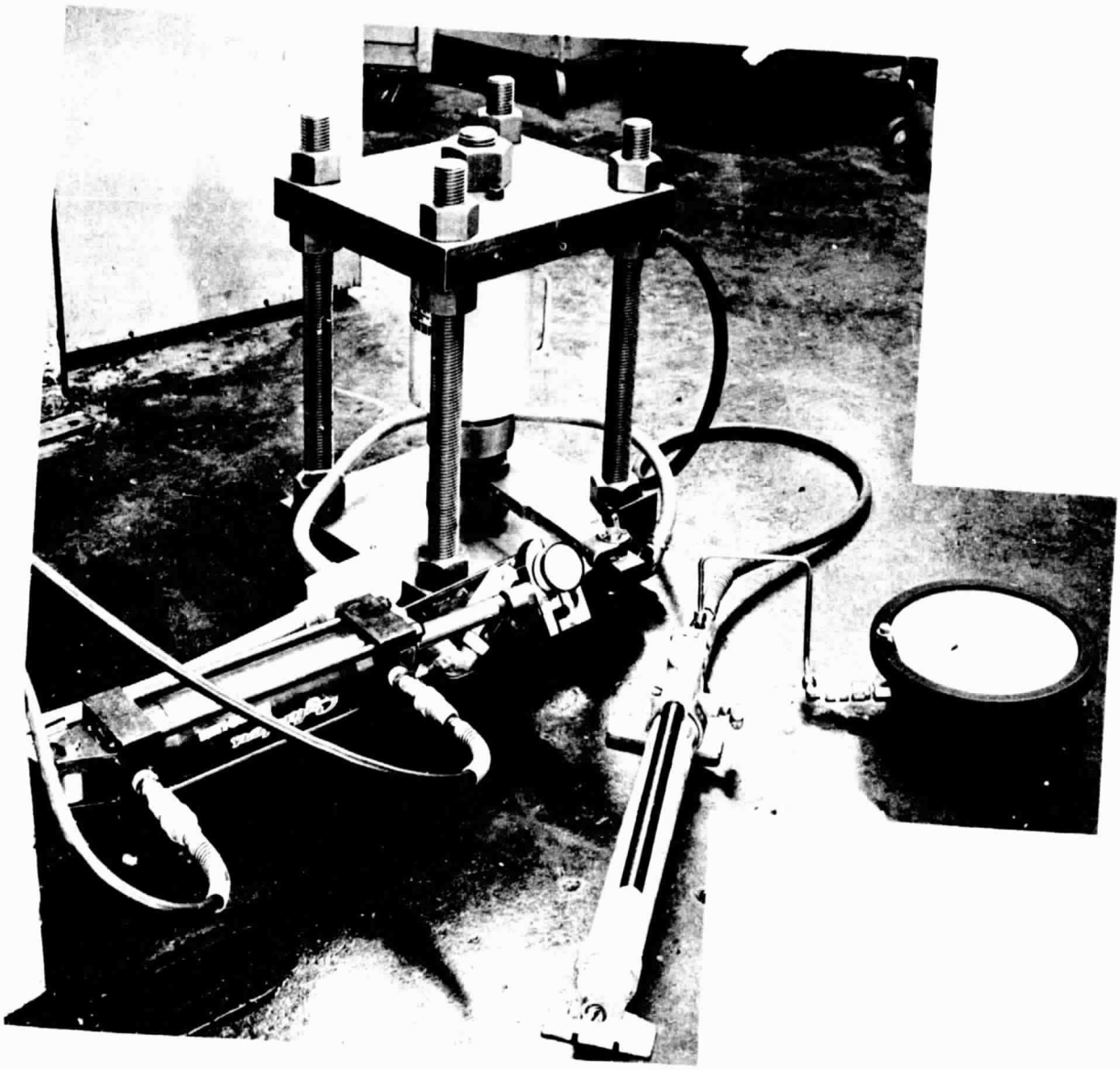

Figure 43. Bearing Test Rig.

4. Bearing life calculations are based on the mission/duty cycle as shown in Figure 44.

The top bearing race is a spherical surface which is designed in conjunction with the disk bearing seat to minimize transmission of warping stress to the race under operating conditions. This spherical mating surface will be coated with an antifretting coating to ensure that loss of LCF life of the fan disk will not occur. Bearing loads and life predictions are given in Table XI.

2.5 BLADE RETENTION TRUNNION

The blade retention trunnions mechanically tie the composite blades to the fan disk through the blade support bearing. They also provide an attachment point through which torque might be applied by the blade actuator to change the pitch of the blades.

Table XI. Bearing Load and Life Summary.

Average Bearing Load on Balls at 100% Mechanical Design Speed (3244 rpm)	262,392 N (58,988 lb)
Bearing Static Load Capacity	297,812 N (66,951 lb)
Bearing Elastic Deflection at 3244 rpm	0.0124 cm (0.0049 in.)
Individual Bearing B10 Life	128,190 Flight Hours

The entire blade support system is designed to withstand the maximum possible loads which can be transmitted into it by the blades without blade failure. This includes not only the trunnion but all of its mating components. This ensures that in the event of extensive foreign object damage only the small composite blade pieces will be broken off and secondary engine damage will be minimized.

The fan blades slide into the dovetail slots on top of the trunnion and are retained by shouldered strips. A relatively new material, MP159, is being considered for the strips because of its natural corrosion resistance and very high strength.

Restraint of the blade about the dovetail axis is provided by ester-based urethane rubber bumpers under the blade mount. This material has exceptional load absorption capabilities and is not affected by commonly used jet engine oils, fuels, or solvents.

The dovetail slot will be protected by an antifretting coating applied to the blade dovetails. Tests will be conducted to determine the best antifretting system. Two plasma sprayed coatings, one plated coating, and a chemical conversion coating are presetnly being considered for this wear coating.

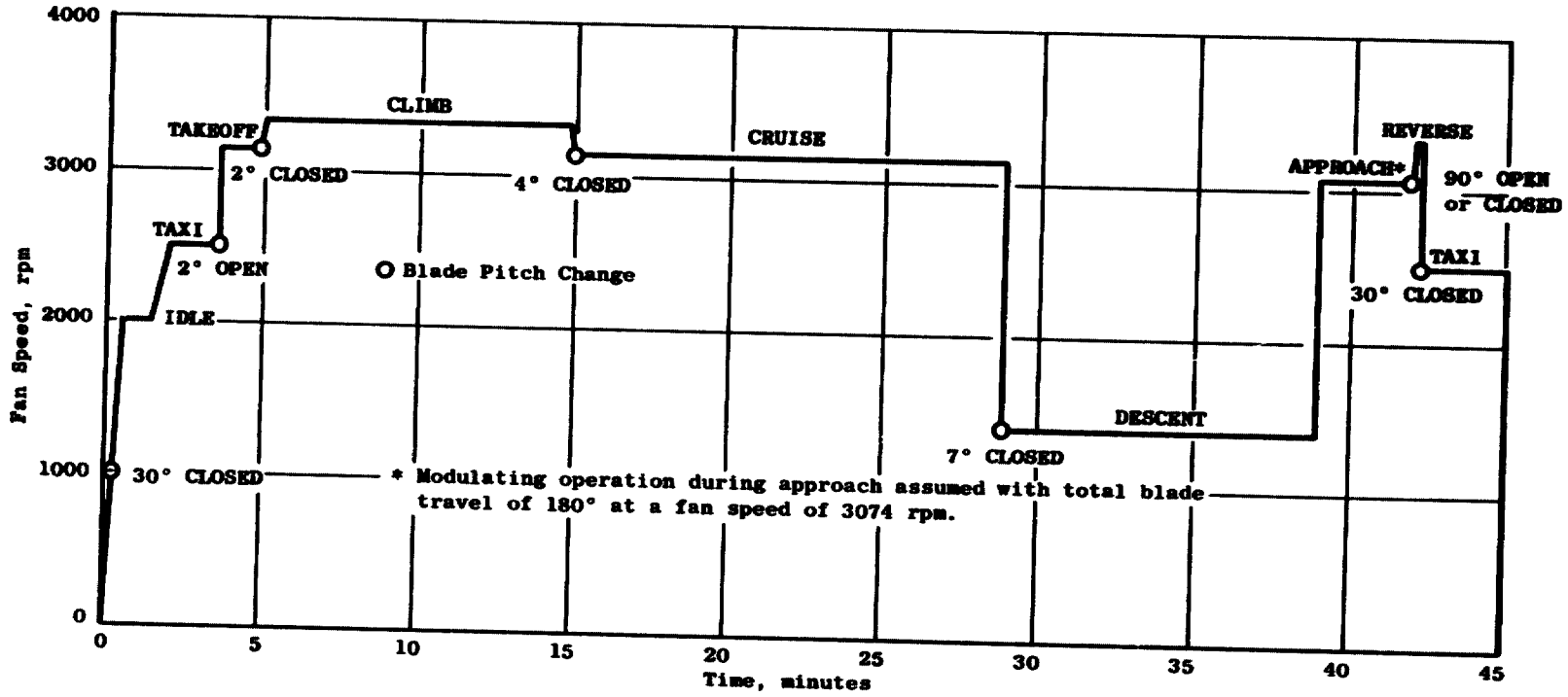

Figure 44. UTW Mission Duty Cycle.

The trunnion will be machined from single forgings of 6Al-4V titanium. This material was selected based on its natural corrosion resistance, low density, and high strength. This material also allows relatively large diameter threads to be rolled out on the trunnion end (per Mil-S-8879) for retention purposes by more conventional capacity thread rolling equipment. This rolling procedure has been used on the titanium trunnions of previous General Electric variable-pitch fans and produces above average properties in this critical region.

Each trunnion is held in the hole of the disk by a threaded steel retainer. This retainer can be torqued to preload the blade support bearing, and is locked by a redundant locking system. Either a pinion gear for the GE actuation system or a lever arm for the Hamilton Standard System is captured on the trunnion between the retainer and the blade support bearing [see Figures 45 (GE) and 46 (H.S.)]. Torque to change the blade pitch is carried through this device into mating splines just above the trunnion threads.

Outer sliding bearings support the top of the trunnion. The axial thrust washer is made of commercially available refractory matrix material containing molybdenum disulfide. Wear and load carrying characteristics of this material are excellent, and no measurable creep is expected under preload. This bearing serves as a weather seal under static conditions, but runs 0.0076 cm (0.003 in.) loose under normal engine speeds due to the elastic properties of the blade support bearing. The outer sleeve sliding bearing is a very high capacity bearing of Nomex and Teflon fibers. This bearing seats inside the disk and can easily tolerate the circumferential strain of the disk. The high capacity of this bearing, compared to conventional ball bearings, enables it to easily withstand anticipated vibratory and bird impact loads. Both outer bearings have resistance to all oils, fuels, and solvents which might normally come in contact with engine parts.

2.6 FAN SPINNER

The UTW fan has both a rotating forward spinner and flowpath adapter as shown in Figure 27. These parts attach to flanges on the fan disk. Both are scalloped where they meet to provide round holes for the blade platforms. Together they provide the inner flowpath for the fan. The spinners will be fabricated from 6061 Aluminum. This material has good section stiffness-to-weight and has the good welded properties needed for fabricating development hardware.

The forward spinner will also have a spinner cap for inspection and access to the interior of the fan assembly. After removal of the fan spinner, all of the rotating hardware and sump regions forward of the fan frame are easily accessible. Blades may be individually replaced and the blade actuator or the actuator and disk assembly may be removed as a package. This permits removal of the fan disk assembly, blade actuator, and main reduction gear as a complete module.

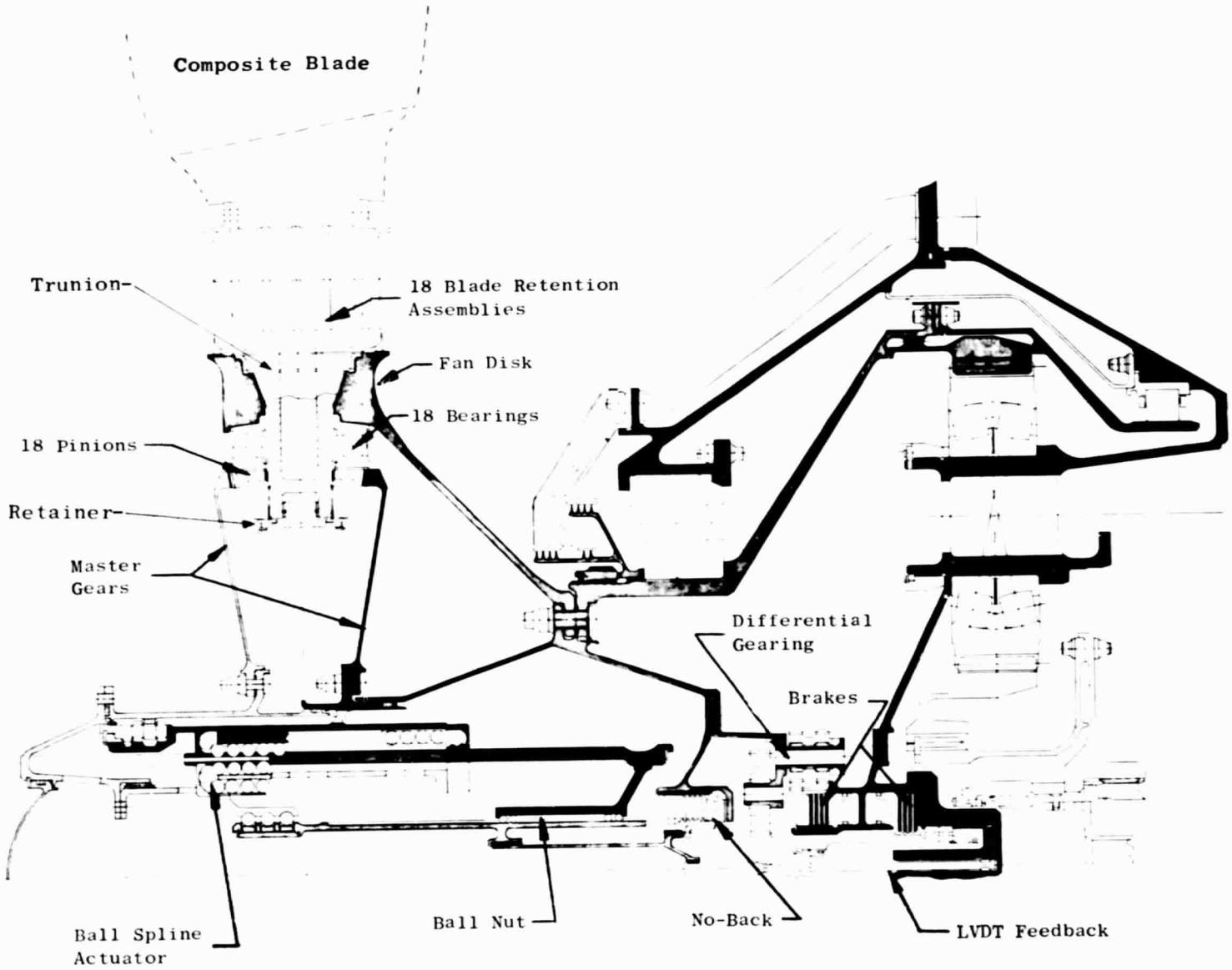

Figure 45. UTW Variable-Pitch Fan with GE Actuation System.

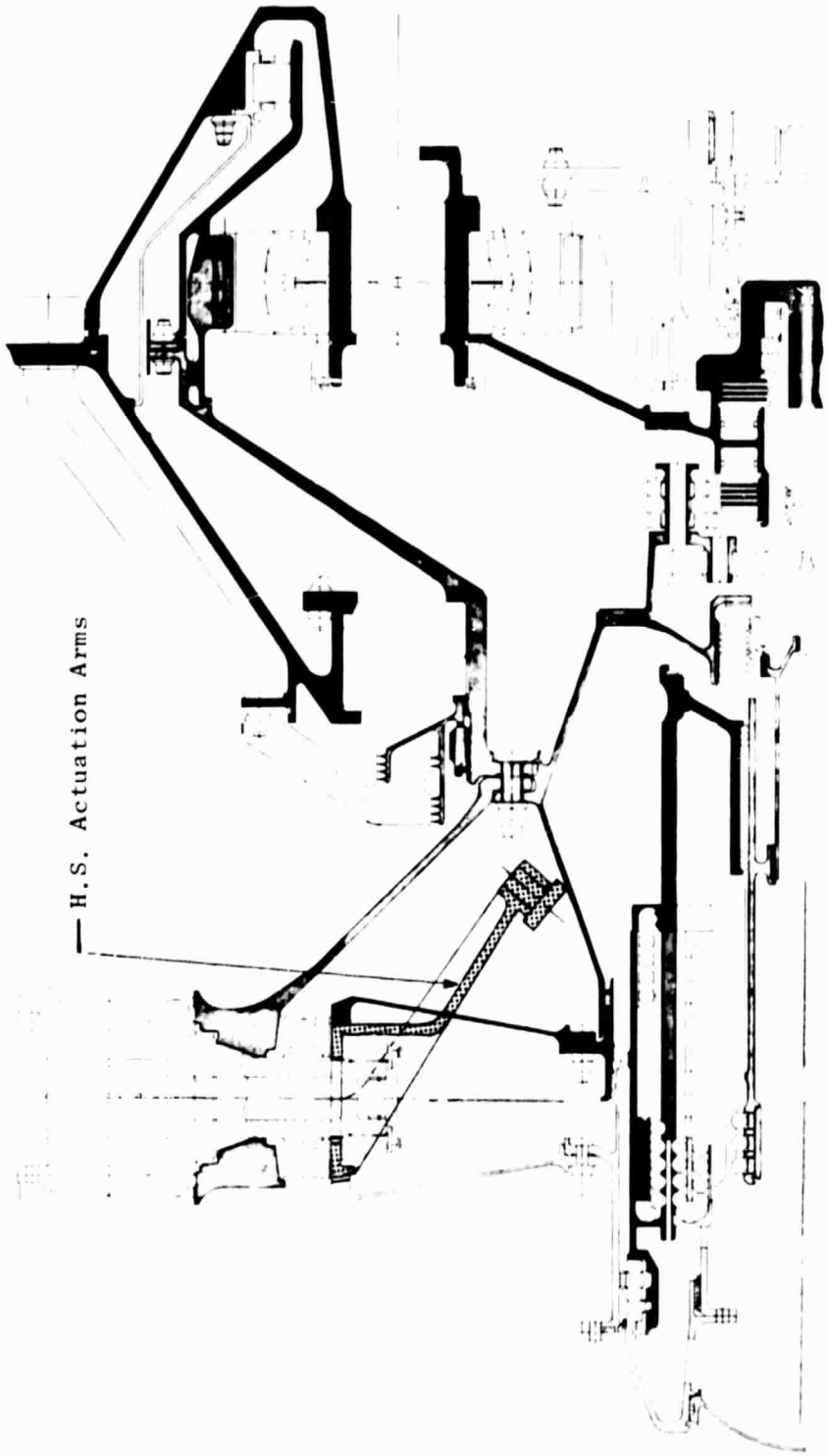

Figure 46. UTW Variable-Pitch Fan with Hamilton Standard Actuation Arms.

Radial fan balance screw bosses will be provided in the spinner. This will permit field balance of the engine without removal of the spinner. The concept has been developed and used successfully on General Electric's CF6-50 engine.

The aft flowpath adapter continues the inner flowpath back to the fan core OGV's. A flow discourager seal inhibits air recirculation at this point. There are access holes in the flange of the aft spinner which, with the forward spinner removed, permit access to the fan frame flange which retains the main reduction gear.